

South Dakota State University

# Open PRAIRIE: Open Public Research Access Institutional Repository and Information Exchange

---

Electronic Theses and Dissertations

---

2021

## Analysis of Metabolites and Therapeutics for Toxic Inhaled Agent Exposure

Abigail Bemah Donkor  
*South Dakota State University*

Follow this and additional works at: <https://openprairie.sdstate.edu/etd>



Part of the [Chemistry Commons](#), and the [Pharmacology, Toxicology and Environmental Health Commons](#)

---

### Recommended Citation

Donkor, Abigail Bemah, "Analysis of Metabolites and Therapeutics for Toxic Inhaled Agent Exposure" (2021). *Electronic Theses and Dissertations*. 5645.

<https://openprairie.sdstate.edu/etd/5645>

This Dissertation - Open Access is brought to you for free and open access by Open PRAIRIE: Open Public Research Access Institutional Repository and Information Exchange. It has been accepted for inclusion in Electronic Theses and Dissertations by an authorized administrator of Open PRAIRIE: Open Public Research Access Institutional Repository and Information Exchange. For more information, please contact [michael.biondo@sdstate.edu](mailto:michael.biondo@sdstate.edu).

ANALYSIS OF METABOLITES AND THERAPEUTICS FOR TOXIC INHALED  
AGENT EXPOSURE

BY

ABIGAIL BEMAH DONKOR

A dissertation submitted in partial fulfillment of the requirements for the

Doctor of Philosophy

Major in Chemistry

South Dakota State University

2021

## DISSERTATION ACCEPTANCE PAGE

Abigail Bemah Donkor

This dissertation is approved as a creditable and independent investigation by a candidate for the Doctor of Philosophy degree and is acceptable for meeting the dissertation requirements for this degree. Acceptance of this does not imply that the conclusions reached by the candidate are necessarily the conclusions of the major department.

Brian Logue  
Advisor

Date

Douglas Raynie  
Department Head

Date

Nicole Lounsbery, PhD  
Director, Graduate School

Date

This dissertation is dedicated to my father; John Yaw Donkor, my mother; Christiana Donkor, siblings (Celestina, Jeremiah, and John Junior) and my loving husband; Albert Aidoo. I am grateful for your encouragement and tremendous support during my PhD journey. This achievement would never have been possible without your unconditional support and prayers.

## ACKNOWLEDGEMENTS

I am eternally thankful to God almighty for his loving kindness, provision, divine health, faithfulness, and mercies throughout this academic journey. He has been my strong anchor and my source of encouragement. When things were gloomy and I felt I could not continue, He was by my side. I would not have come this far if not for the Lord. I am forever grateful. I also express my sincere gratitude to my advisor, Dr. Brian Alexander Logue for his mentorship, training, and guidance throughout my journey at SDSU. You have been a great teacher and coach and I will not forget the many nuggets of life you taught me. I thank my advisory committee members, Dr. Raynie Douglas, Dr. Fathi Halaweish and Dr. Christopher Schmidt for their practical feedback, reviews, and overall guidance throughout my doctoral studies. I am also grateful to Dr. Nesta Bortey-Sam, Dr. Obed Gyamfi, Dr. Frederick Ochieng and LARGE group for making my stay at SDSU a memorable one and Dr. Amanda Appel for teaching me most of the instrumentation I know today. My sincere appreciation goes to the funding institutions and the Department of Chemistry and Biochemistry for supporting me during my stay here.

I am very thankful to my church family; Holy Life Tabernacle, Brookings for their immense support and for being a home away from home during my stay in Brookings, South Dakota.

GLORY BE TO GOD

## TABLE OF CONTENTS

ABBREVIATIONS .....	viii
LIST OF FIGURES .....	xii
LIST OF TABLES .....	xiv
ABSTRACT.....	xv
Chapter 1. Introduction .....	1
1.1. Overall Significance.....	1
1.2. Project Objectives .....	1
1.3. Toxic Inhaled Agents.....	2
1.4. Sulfur Mustard .....	3
1.4.1. Exposure to sulfur mustard .....	3
1.4.2. Toxicity of sulfur mustard.....	4
1.4.3. Mechanism of action of sulfur mustard .....	5
1.4.4. Metabolism of sulfur mustard .....	6
1.4.5. Treatments and countermeasures for sulfur mustard poisoning.....	7
1.5. Methyl isocyanate .....	9
1.5.1. Exposure to Methyl isocyanate .....	9
1.5.2. Metabolism of Methyl isocyanate.....	10
1.5.3. Toxicity and Mechanism of Action of Methyl Isocyanate.....	11
1.6. 2-Mercaptoethane Sulfonate Sodium as a therapeutic for MIC and Sulfur Mustard exposure. .....	13
1.6.1. Uses of MESNA .....	13
1.6.2. Mechanism of action of MESNA.....	13
1.6.3. Metabolism and pharmacokinetics of MESNA .....	14
1.6.4. Toxicity of MESNA.....	15
Chapter 2. Identification and Analysis of a Methyl Isocyanate-Adduct for Exposure Verification .....	16
2.1. Introduction.....	16
2.2. Materials and Methods.....	20
2.2.1. <i>Materials</i> .....	20
2.2. <i>Synthesis of PMC and PMC-D<sub>5</sub></i> .....	21
2.2.2 <i>Biological samples</i> .....	22
2.2.3 <i>Sample preparation</i> .....	23
2.2.4 <i>HPLC-MS/MS analysis of PMC</i> .....	24

2.2.5 Calibration, quantification, and limit of detection.....	27
2.2.6 Recovery and matrix effect.....	28
2.2.7 Stability .....	28
2.3 Results and Discussion .....	29
2.3.1 Mechanism of MIC-tyrosine adduct formation .....	29
2.3.2 Phenyl methyl carbamate as a biomarker for MIC exposure. ....	32
2.3.3 Detection of serine as a by-product of base hydrolysis of MIC-tyrosine adducts .....	37
2.3.4 HPLC-MS/MS analysis of PMC.....	38
2.3.5 Accuracy and precision.....	39
2.3.6 Matrix effect and recovery .....	41
2.3.7 Stability of PMC and MIC-tyrosine adduct .....	41
2.3.8 Analysis of PMC from MIC-exposed animals and its correlation with MIC dose .....	42
2.4 Conclusion .....	43
2.5 Acknowledgements.....	44
Chapter 3. Analysis Of Sodium 2-Mercaptoethane Sulfonate in Rat Plasma Using High Performance Liquid Chromatography Tandem-Mass Spectrometry .....	45
3.1. Introduction.....	45
3.2. Materials and Methods.....	48
3.2.1 Materials .....	48
3.2.2. Biological Samples.....	48
3.2.3. Sample preparation for HPLC-MS/MS analysis .....	49
3.2.4. HPLC-MS/MS Analysis.....	49
3.2.5. Calibration, quantification, and limit of detection.....	52
3.2.6. Recovery, matrix effect, and selectivity.....	53
3.2.7. Stability .....	54
3.3. Results and Discussion .....	55
3.3.1. HPLC-MS/MS Analysis of MESNA.....	55
3.3.2. Linear range, calibration, and limit of detection.....	61
3.3.3. Accuracy and precision.....	63
3.3.4. Matrix effect, recovery, and stability .....	65
3.3.5. Analysis of MESNA in Treated Animals .....	68
3.4. Conclusion .....	68
3.5. Acknowledgements.....	68

Chapter 4. Investigation of the Interaction between Sulfur Mustard Analogue, 2-Chloroethyl Ethyl Sulfide and Methimazole for Possible Reaction Product Formation .....	69
4.1. Introduction.....	69
4.2 Materials and Methods.....	71
4.2.1 <i>Materials</i> .....	71
4.2.2 <i>Cell culture</i> .....	72
4.2.3 <i>MTT assay</i> .....	72
4.2.4 <i>Sample Preparation</i> .....	72
4.2.5 <i>HPLC-MS/MS analysis of ETTMI</i> .....	73
4.3. Results and Discussion .....	76
4.3.1 <i>Formation of 2-(2-(ethylthio)ethylthio)-1-methyl-1H-imidazole (ETTMI)</i> .....	76
4.3.2 <i>Confirmation of the formation of CEES-methimazole adduct.</i> .....	77
4.4 Conclusion .....	81
Chapter 5. Conclusions, Broader Impacts, And Future Work .....	82
5.1 Conclusions.....	82
5.2 Broader impacts .....	82
5.3. Future work.....	83
References.....	84



## ABBREVIATIONS

3-MPS: Sodium 3-mercapto-1-propane sulfonate

ATP: Adenosine triphosphate

CE: Collision energy

CEES: 2-Chloroethyl ethyl sulfide

CN: Cyanide

CXP: Collision cell exit potential

CYS: Cysteine

DMEM: Dulbecco's modified eagle media

DP: Declustering potential

ECD: Electrochemical detection

FDA: Food and drug administration

FLD: Fluorescence detection

FT: Freeze thaw

GSH: glutathione

HaCat: Human keratinocyte epithelial

Hb: Hemoglobin

HCY: Homocysteine

HPLC: High performance liquid chromatography

HPLC-MS/MS: High performance liquid chromatography

IS: Internal standard

IV: Intravenous

LLOQ: Lower limit of quantification

LOD: Limit of detection

MESNA: Sodium 2-mercaptoethane sulfonate

METH: Methimazole

MIC: Methyl isocyanate

MIH: Methyl isopropyl hydantoin

MRM: Multiple reaction monitoring

MS/MS: Tandem mass spectrometry

MSMTESE: 1-methylsulfinyl-2-[2- (methylthio)ethylsulfonyl]ethane

MTT: 3-(4,5-Dimethylthiazol-2-yl)-2,5-Diphenyltetrazolium Bromide

NAS: N-acetyl cysteine

NMI: N-methylimidazole

NOS: Nitric oxide synthase

OPA: O-phthaldialdehyde

PMC: Phenyl methyl carbamate

QC: Quality control

ROS: Reactive oxygen species

RSD: Relative standard deviation

RT: Room temperature

S/N: Signal-to-noise

SBMSE: 1,1' - sulfonylbis [2-(methylsulfinyl) ethane]

SBMTE: 1,1' -sulfonylbis[2- (methylthio) ethane]

SBSNAE: 1,1' -sulfonylbis[2-S- (N-acetylcysteiny) ethane]

SM: Sulfur mustard

SMG: S-(N-methylcarbamoyl) glutathione

SMO: Bis-  $\beta$ -chloroethyl sulfoxide

TDG: Thiodiglycol

TDGO: Thiodiglycol sulfoxide

TIAs: Toxic inhaled agents

TLV: Threshold limit value

ULOQ: Upper limit of quantification

ULOQ: Upper limit of quantification

## LIST OF FIGURES

Figure 1. 1 Formation of episulfonium ion as a result of intramolecular cyclization. ....	6
Figure 2. 1 Scheme for the synthesis of PMC from the reaction of phenol with MIC in acetonitrile (ACN) via Lossen rearrangement using N-methylimidazole (NMI) as a catalyst.(157) .....	21
Figure 2. 2 Reaction pathway for the formation of PMC from the reaction of tyrosine with MIC. Tyrosine is proposed to react with MIC to form an MIC-tyrosine adduct which undergoes base hydrolysis to produce phenyl methyl carbamate (PMC).....	30
Figure 2. 3 Proposed reaction mechanism for the formation of PMC. MIC-Tyrosine adduct undergoes an SN2 reaction in the presence of strong aqueous NaOH to cleave PMC at the CH-aromatic bond. R <sub>1</sub> = CHNH, R <sub>2</sub> = NHC=O and R <sub>3</sub> =CH <sub>3</sub> .....	31
Figure 2. 4 ESI (+) product ion mass spectra of PMC (A) and PMC-D5 (B) with identification of the abundant ions. Molecular ions of PMC and PMC-D5 [M+H] <sup>+</sup> correspond to 152.40 and 157.10, respectively. Insets, structures of PMC (A) and PMC-D5 (B) with abundant fragments indicated.....	34
Figure 2. 5 HPLC-MS/MS chromatograms of (A) PMC-spiked rat RBC (B) PMC from MIC-spiked rat RBC, (C) PMC from RBC of MIC-exposed rat, non-exposed and exposed are presented. ....	37
Figure 2. 6 Correlation of MIC dose to concentration of PMC from exposed rats.....	43
Figure 3. 1 ESI (-) product ion mass spectra of MESNA (A) and 3-MPS (B) with identification of the abundant ions. Molecular ions of MESNA and 3-MPS [M-H] <sup>-</sup> correspond to 140.40 and 154.70, respectively. Insets, structures of MESNA (A) and 3-MPS (B) with abundant fragments indicated.....	58
Figure 3. 2 Representative HPLC-MS/MS chromatograms of spiked (5 μM) and non-spiked MESNA and (B) 3-MPS (IS) in rat plasma. The chromatograms show signal response to the MRM transitions of MESNA (140.40 → 79.9 and 140.40 → 138.9 m/z) and 3-MPS (150 → 80.0 and 154.70 → 93.9 m/z).....	60
Figure 3. 3 HPLC-MS/MS chromatogram from the plasma of MESNA-treated rats and rat plasma obtained prior to MESNA treatment. The chromatograms represent signal response to MRM quantification transition of MESNA (140.40 → 79.9 m/z).....	67
Figure 4. 1 Reaction pathway for the formation of ETTMI from the reaction CEES with methimazole. CEES is proposed to react with methimazole to form 2-(2-(ethylthio)ethylthio)-1-methyl-1H-imidazole (ETTMI) which prevents the action of CEES on affected cells. ....	77
Figure 4. 2 ESI (+) product ion mass spectra of with identification of the ETTMI abundant ions. Molecular ion of ETTMI [M+H] <sup>+</sup> corresponds to 204.30. Insets, structure of ETTMI with abundant fragments indicated. ....	79

Figure 4. 3 HPLC–MS–MS chromatograms ETTMI from spiked media and from cell lysates is presented. ....	80
Figure 4. 4 A bar graph showing the comparison of ETTMI from PBS buffer, media and from cell lysates is presented.....	81

## LIST OF TABLES

Table 2. 1 Comparison of methods for analysis of MIC-protein adducts.....	19
Table 2. 2 MRM transitions, optimized collision energies (CEs), cell exit potentials (CXPs) and declustering potentials (DPs) for the detection of PMC and PMC-D5 by MS/MS analysis. ....	26
Table 2. 3 Intra and interassay accuracy and precision of PMC produced by base hydrolysis of MIC-tyrosine adduct. ....	40
Table 2. 4 Calibration equations and coefficients of determination (R <sup>2</sup> ) for calibration curves created over 3 days.....	40
Table 3. 1 Comparison of bioanalytical methods for analysis of MESNA.....	47
Table 3. 2 MRM transitions, optimized collision energies (CEs), cell exit potentials (CXPs) and declustering potentials (DPs) for the detection of MESNA and 3-MPS by MS/MS analysis. ....	51
Table 3. 3 Linear equations, coefficients of determination (R <sup>2</sup> ), and percent residual accuracy (PRA) for calibration curves created over 3 days. ....	62
Table 3. 4 The intra- and interassay accuracies and precisions of MESNA analysis from spiked rat plasma by HPLC-MS/MS. ....	64
Table 4. 1 MRM transitions, optimized collision energies (CEs), cell exit potentials (CXPs) and declustering potentials (DPs) for the detection of ETTMI by MS/MS analysis. ....	75

ABSTRACT

ANALYSIS OF METABOLITES AND THERAPEUTICS FOR TOXIC INHALED  
AGENT EXPOSURE

ABIGAIL BEMAH DONKOR

2021

The inhalation of toxic inhaled agents (TIAs) such as methyl isocyanate and cyanide can compromise an individual's general health due to their extremely toxic nature. Nonetheless, these gases are used extensively in the electronics, chemical, welding, electroplating industries, etc., increasing the risk of exposure to both civilians and industrial workers. It is therefore very crucial to develop analytical methods for TIA metabolites and therapeutic agents. Methyl isocyanate (MIC), an intermediate in the synthesis of carbamate pesticides is a toxic industrial chemical that causes irritation and damage to the eyes, respiratory tracts, and skin. Due to its reactivity with proteins, protein adducts can be used to confirm exposure, but this type of analysis is cumbersome, time consuming and expensive. Hence, we investigated the interaction between MIC and proteins to identify a novel marker, phenyl methyl carbamate (PMC) based on hydrolysis of tyrosine-MIC adducts. A simple base hydrolysis was used for sample preparation with sensitive HPLC-MS/MS analysis of this marker. The method produced excellent sensitivity for PMC with a detection limit of 0.02 mg/kg and calibration curve linearity extending from 0.06–1.51 mg/kg ( $R^2 = 0.998$  and overall %RA >90). The accuracy and precision ( $100 \pm 9\%$  and <10% relative standard deviation, respectively) of the method were outstanding. The validated method was successfully able to detect elevated levels of PMC from MIC-spiked hemoglobin and further used to detect significantly elevated PMC levels from hemoglobin isolated from MIC-exposed rats.



Sodium-2-mercaptoethane sulfonate (MESNA), has been suggested as a potential antidote for MIC exposure. It has previously proven to be effective in inactivating acrolein, the toxic metabolite of anti-tumor drugs (cyclophosphamide and ifosfamide). However, current methods available to analyze MESNA have limitations, including low sensitivity, poor selectivity, high degree of difficulty, and many time-consuming steps. Hence, we developed and validated a simple and selective HPLC-MS/MS method for the analysis of MESNA in plasma. The method showcases an excellent limit of detection of 20 nM with excellent linearity ( $R^2 = 0.999$  and overall %RA > 90), and a wide linear range (0.05–200  $\mu$ M). The method also produced very good accuracy and precision ( $100 \pm 10\%$  and <10% relative standard deviation, respectively). The validated method was successfully used to analyze MESNA from treated animals and will enhance pharmacological and therapeutic research on this promising antidote.

Lastly, sulfur mustard (SM) is a toxic bifunctional alkylating warfare agent, which causes severe damage to skin, eyes, and respiratory tract. However, there is no antidote for treating sulfur mustard poisoning and treatment is limited to either washing the affected area with soap and water or supportive care in cases of inhalation exposure. In recent research, methimazole (METH), an antithyroid drug has proven to be an effective nucleophilic scavenger to combat the toxic effects of sulfur mustard analog, 2-Chloroethyl ethyl sulfide (CEES) but there are no studies on the underlying mechanism of the scavenging ability of methimazole for CEES in preventing cell death. In this study, we investigated the interaction between methimazole and CEES for a possible formation of the novel compound, 2-(2-(ethylthio)ethylthio)-1-methyl-1H-imidazole (ETTMI). The production of ETTMI from the reaction of CEES with methimazole was proven by the

detection of ETTMI from CEES-methimazole cell lines. An HPLC-MS/MS method was developed to analyze ETTMI from HaCat cell lines and media. Using this method, we showed that ETTMI is produced from the interaction of CEES with methimazole and the formation of ETTMI could be one of the underlying pathways for the scavenging ability of methimazole for CEES.

## **Chapter 1. Introduction**

### **1.1. Overall Significance**

Toxic inhaled agents (TIAs) such as methyl isocyanate, sulfur mustard and cyanide are used widely in the electronics, chemical, welding, electroplating industries, etc. due to their great importance. The chemical and electroplating industries process large quantities of cyanide in the manufacture of solvents, fertilizers, fumigants, plastics, and the myriad of requirements of modern society. Methyl isocyanate is used in the polyurethane industries to produce synthetic rubber, adhesives, pesticides, and herbicide intermediates. Despite the advantages of these TIAs, they can pose serious risks to humans and the environment upon exposure. It is therefore crucial to develop analytical methods for TIA metabolites and therapeutic agents to confirm human exposure to TIAs, provide diagnosis and to develop effective therapeutic agents to combat their toxic effects.

### **1.2. Project Objectives**

This research work addresses three main objectives: 1) Identify a methyl isocyanate-adduct produced from the interaction of methyl isocyanate (MIC) with tyrosine and develop an analytical method for its analysis, 2) Develop a simple and rapid technique for the analysis of sodium 2-mercaptoethane sulfonate in plasma, and 3) Identify the reaction product formed from the reaction of sulfur mustard analog, CEES and methimazole. Chapter 2 describes the reaction of MIC with tyrosine to produce a novel MIC biomarker, phenyl methyl carbamate utilizing base hydrolysis. Chapter 3 details the analysis of sodium 2-mercaptoethane sulfonate in plasma using high-performance liquid chromatography tandem mass-spectrometry. Chapter 4 focuses on the formation of 2-(2-(ethylthio)ethylthio)-1-methyl-1H-imidazole(ETTMI) from the reaction of CEES with

methimazole and analysis of the compound from cell lines. Chapter 5 contains the conclusion, broader impacts and proposed future works.

### **1.3. Toxic Inhaled Agents**

Inhalation of gases, vapors and aerosols can cause a wide range of adverse health effects, varying from simple irritation to systemic disease. The large number of chemicals and complex mixtures present in the environment, such as oxidizing, electrophilic, acidic, or basic gases, is an area of growing concern for human health.<sup>(1, 2)</sup> Toxic inhaled agents (TIAs) are noxious gases and vapors that are harmful and often deadly when inhaled. Examples include cyanide, methyl isocyanate, sulfur mustard, methyl mercaptan, and hydrogen sulfide. Due to industrialization and vast growth in the human population, these TIAs are used extensively for several purposes.<sup>(2)</sup> Many TIAs are important reactants in metallurgy and in the organic synthesis of plastics, pharmaceuticals, semiconductors, and other materials. For example, large amounts of chlorine gas and other TIAs are used for bleaching and chemical synthesis, and large quantities of ammonia and nitric acid are used for fertilizer production.<sup>(3, 4)</sup> Also, cyanide is used in gold mining, electroplating, for the production of fertilizers, etc.<sup>(5)</sup> and methyl isocyanate is also used to produce pesticides, plastics, rubbers, and adhesive.<sup>(6)</sup>

Large volumes of TIAs are often transported and stored, sometimes near large population centers to maintain a supply for their use. Unfortunately, accidental leaks from industrial facilities and transportation vehicles do increase the risk of exposure to both civilians and industrial workers.<sup>(7-9)</sup> The Bhopal incident, where a total of 200,000 in a city of 800,000, in 1984<sup>(10)</sup> were exposed to the MIC is an example of a major industrial disaster caused by a leakage in an MIC tank stored by a carbide industry in India.<sup>(7, 11)</sup> Sulfur

mustard, chlorine gas, cyanide, etc., have also been used as chemical warfare agents by many military and terrorist groups to kill and injure civilian population.<sup>(12-15)</sup>

Exposure to TIAs can cause a spectrum of adverse health effects that range from subclinical to immediately lethal.<sup>(16)</sup> Most TIAs are reactive chemical gases (e.g. MIC) and vapors that can severely change the structures of the proteins, lipids, DNA, and other biomolecules, resulting in a loss of protein function, DNA mutations, and necrosis of airway epithelial cells.<sup>(17, 18)</sup> TIAs such as sulfur mustard also targets and depletes sulfhydryl-containing proteins, such as glutathione (GSH), which plays a major role in maintaining a redox homeostasis in the tissues. This depletion leads to oxidative stress and other oxidative cellular damage.<sup>(19)</sup> CN can compromise the oxygen carrying capacity of blood, as well as the ability of peripheral tissues to utilize oxygen in aerobic metabolism.<sup>(20-22)</sup> Trace level exposure to reactive TIAs induces irritation, sneezing, coughing, mucus secretion, tearing, and upper airway inflammation<sup>(23)</sup> and in severe prolonged exposure, causes severe lung damage. Long-term exposure also damages the delicate alveolar sacs by reacting with the lung tissues and may even lead to death in some cases.<sup>(24, 25)</sup>

## **1.4. Sulfur Mustard**

### **1.4.1. Exposure to sulfur mustard**

Sulfur mustard (bis-(2-chloroethyl) sulphide, SM) is a well-known chemical warfare agent. It is very oily and hydrophobic in nature. Hence, it easily penetrates membranes and fatty tissues in living systems and stays in soils and other environmental materials for weeks.<sup>(26, 27)</sup> Sulfur mustard gas was first synthesized in 1822 by Despretz and 1860 by Niemann and Guthrie during the studies of interactions between olefins and

sulfur halogen compounds.<sup>(28, 29)</sup> Both investigators noticed the typical vesicant properties of the agent.

The first use of SM was by the Germans during the Battle of Flanders, Belgium in 1917 during World War I.<sup>(30, 31)</sup> Since its first use, SM has been deployed in several combat situations, such as United Kingdom against the Red Army (1919), Spain in Morocco (1921-1927), Italy in Libya (1930), Soviet Union against Japan (1930), Italy against Abyssinia (1935- 1940), Poland against Germany, Germany against Soviet Union and Poland, Japan against China during Second World War, and Egypt against Yemen (1963-1967).<sup>(32, 33)</sup> During the Iran/Iraq conflict, SM caused more than 100,000 Iranian casualties.<sup>(34)</sup>

#### **1.4.2. Toxicity of sulfur mustard**

The usual routes of entry of SM are the skin, respiratory tract, and eyes, or through the gastrointestinal tract if SM-contaminated food is consumed.<sup>(35)</sup> The high lipophilicity of SM allows it to rapidly penetrate through the hair follicles and sweat glands of skin and mucous membranes.<sup>(36)</sup> It has been found that 80% of SM applied to human skin evaporates and the remaining 20% penetrate the skin.<sup>(26)</sup> Out of the 20% that penetrates only 10–20% are fixed to macromolecules in skin.<sup>(37)</sup> The remaining 80–90% are rapidly transported away by circulation and distributed among various tissues.<sup>(38)</sup> Consequently, SM can cause severe systemic intoxication along with its pronounced local damage.<sup>(39)</sup>

Exposure to SM could cause several effects. Medical effects of exposure in humans include ocular and dermal injury, respiratory tract damage, reproductive and developmental toxicity, gastrointestinal effects, hematological effects, and cancer.<sup>(40)</sup> The first contact to SM is mostly painless and only a garlic or sulfur odor can be noticed. Typically, a symptom-free period is observed for several hours.<sup>(41)</sup> The duration of this

period is inversely proportional to the absorbed dose of the agent with the maximum intensity of symptoms occurring after days.<sup>(41)</sup> Although the acute effects of SM exposure are usually delayed, occasional cases of nausea, vomiting, and eye irritation have been reported, and contact with very high doses may lead to convulsions and coma within this period.<sup>(42)</sup> Within 2–6 hours of exposure, typical signs are nausea, fatigue, headache, painful eye inflammation with photophobia, reddening of face and neck, soreness of throat, and increased respiratory rate. These symptoms become more severe during the subsequent 6–24-hour period, with skin inflammation and blistering.<sup>(32)</sup> The blistering becomes more marked after the 24 hours and there is productive coughing with pus. Anemia may become apparent after 4–5 days, indicating bone marrow dysfunction.<sup>(43, 44)</sup> In severe cases, death is probable after a delay of days or weeks and, in less severe cases, the burns heal slowly.<sup>(45)</sup>

#### **1.4.3. Mechanism of action of sulfur mustard**

The most presently accepted theory of the basis of toxic effects by the SM proposes that these are consequences of alkylation reactions with cell constituents, mainly with DNA, but also RNA, proteins, and lipid membranes.<sup>(46, 47)</sup> These reactions may result in physiological, metabolic, and genetic failure of cellular functions.

Each 2-chloroethyl side chain of the SM molecule undergoes intramolecular cyclization with the release of the chloride ion.<sup>(33)</sup> It has been suggested that the ethylene sulfonium cation intermediate opens to form the highly reactive carbonium ion which reacts immediately with nucleophiles, such as DNA, RNA, proteins, and other molecules.<sup>(40)</sup> Although the full mechanism behind sulfur mustard toxicity is still not known due to the number of pathways it can affect, the most characterized mechanism within living systems is the alkylation of DNA.<sup>(48)</sup> Almost all bases of DNA are susceptible

to alkylation, but the N7 position of guanine is particularly important as it is the most negative site within DNA bases.<sup>[82]</sup> DNA damage can activate poly (ADP-ribose) polymerase (PARP) and other repair enzymes. Over-activation or higher levels of PARP can lead to apoptotic or necrotic cell death.<sup>(49)</sup>

SM also reacts with glutathione. Depleted intracellular glutathione favors the production of endogenously produced oxygen species resulting in subsequent peroxidation of membrane lipids and other oxidative cellular damage.<sup>(48)</sup>

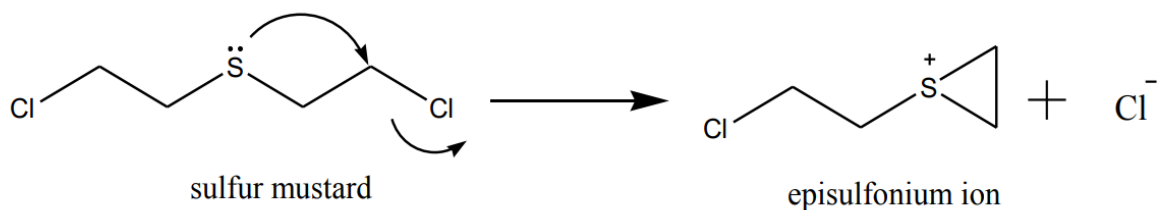


**Figure 1. 1** Formation of episulfonium ion as a result of intramolecular cyclization.

#### 1.4.4. Metabolism of sulfur mustard

As a bifunctional alkylating agent, SM reacts rapidly with various nucleophiles (e.g., water, glutathione, DNA, and proteins) under physiological conditions via the intermediate episulfonium ion. Based on these interactions, four major metabolic routes have been identified in animal models (e.g., rat and mouse).<sup>(50, 51)</sup> The first metabolism pathway involves the direct oxidation product of SM, bis- $\beta$ -chloroethyl sulfoxide (SMO), the directly hydrolyzed metabolite thiodiglycol (TDG), and its oxidation product thiodiglycol sulfoxide (TDGO).<sup>(52)</sup> The second pathway involves a reaction with abundant glutathione and further oxidation to the sulfone followed by  $\beta$ -lyase cleavage. This leads to the formation of 1,1'-sulfonylbis[2-S- (N-acetylcysteinyl) ethane] (SBSNAE), 1,1'-sulfonylbis[2-(methylthio) ethane] (SBMTE), 1-methylsulfinyl-2-[2-



(methylthio)ethylsulfonyl]ethane (MSMTESE) and 1,1-sulfonylbis [2-(methylsulfinyl) ethane] (SBMSE).<sup>(53)</sup> The third is the reaction on the critical nucleophilic sites in DNA to produce SM-DNA adducts.<sup>(54)</sup> The major sites of DNA alkylation by SM include N7, O6 positions of guanine, N3 position of adenine, and interstrand or intrastrand crosslinks at the N7 position of guanine. The last route involves reaction with various amino acid residues present in proteins to form major adducts like HETE-valine adduct of hemoglobin and an HETE-cysteine adduct of albumin.<sup>(49)</sup>

#### **1.4.5. Treatments and countermeasures for sulfur mustard poisoning**

There is no specific antidote against SM intoxication and also no pretreatment is available to avoid SM injuries. Several hypotheses have been proposed for SM toxicity and various treatments have been evaluated.<sup>(55)</sup> Countermeasures and treatments available are limited to symptom management and medical therapy. A more recent countermeasure is scavenger therapy with lots of ongoing research. Medical management involves rapid decontamination with large amounts of soap and water, followed by supportive care that may include fluids, respiratory support, analgesia, infection prevention, and basic burn dressings. Larger blisters (> 2 cm) may heal faster if lanced and debrided.<sup>(56)</sup> For SM victims with severe respiratory problems, endotracheal intubation should be considered.<sup>(57)</sup> For severe skin and eye damage, skin grafts and transplantation (i.e., corneal transplantation) may be necessary if chronic effects arise.<sup>(57)</sup>

##### *1.4.5.1. Proposed and tested therapies.*

A more researched area of therapeutics for SM poisoning includes biotherapy and transplantation. In biotherapy, biological products such as proteins and polysaccharides are

used to treat sulfur mustard exposure. Proteins like cytokines are used to induce proliferation and enhance wound healing and protease inhibitors to prevent sulfur mustard's vesicating effects.<sup>(58)</sup> Transplantation as a therapy also includes mesenchymal stem cell (MSC) transplantation to counteract pulmonary disorders, bone marrow transplantation to alleviate bone marrow suppression, and amniotic membrane (AM) transplantation to treat corneal damage.<sup>(59, 60)</sup> Nonetheless, many of these proposed therapies have several disadvantages like unwanted toxic effects, counterproductive biological impacts, and sometimes ineffectiveness in serious cases.

#### *1.4.5.2. Scavenger therapy*

In a scavenger therapy, a biologically safe compound is administered to react with sulfur mustard. The molecule should have high affinity for sulfur mustard (e.g., highly nucleophilic molecules). Hypothetically, this compound if given right away could help reduce the direct damage caused by sulfur mustard poisoning and in effect could provide a different route of sulfur mustard neutralization.<sup>(61)</sup> Keeping enough level of this scavenger in either locally affected tissues or systemically would scavenge sulfur mustard to produce a sulfur mustard-scavenger adduct, which may be excreted as waste or metabolized.

#### *1.4.5.3. Tested Scavengers*

Not much research exist that explore the possibility of using a scavenging model as a post-sulfur mustard exposure counteract method. Among the few, the most promising molecules that have been explored so far include N-acetyl cysteine (NAC), glutathione, and 2,6-dithiopurine.<sup>(62)</sup> NAC and glutathione were tested due to their known antioxidant properties, biological prevalence, and potential scavenging ability. Although NAC and

glutathione offered some relief from sulfur mustard toxicity, several studies concluded their mechanism of action proceeds through pathways disparate to scavenging.<sup>(63)</sup>

2,6-dithiopurine was chosen as a sulfur-containing thiopurine analog to the nitrogenous bases in DNA that are known to create adducts with sulfur mustard. Though this molecule was fairly successful in lessening mutagenesis and other effects involved with sulfur mustard exposure, it was neglected as a potential therapeutic around 2012.<sup>(64)</sup> Recently, methimazole, an antithyroid drug, has proven to be very effective in preventing apoptosis in CEES-affected cell lines. However, research is still ongoing to validate and understand the scavenging ability of this potential antidote.

## **1.5. Methyl isocyanate**

### **1.5.1. Exposure to Methyl isocyanate**

Methyl isocyanate (MIC) is a colorless liquid that has a strong odor (with an odor threshold of 2.1 ppm), a vapor pressure of 348 mm Hg at 20° C, and is highly flammable.<sup>(65)</sup> It is the smallest most reactive, and most toxic member of the isocyanate family.<sup>(66)</sup> Exposure to MIC usually occurs through inhalation or dermal contact<sup>(67)</sup> and the sources of exposure could be either occupational, industrial or accidental.<sup>(68)</sup> MIC is used extensively in the carbamate industry as a chemical intermediate in the production of carbamate insecticides and herbicides. It is also used in the production of polyurethane rubber, plastics, adhesives, lacquers, paints, etc. Occupational exposure could occur for individuals who use MIC containing products in their field of work. For example, farmers who use pesticides like aldicarb and carbofuran are at risk of being exposed.<sup>(69, 70)</sup> Recently, MIC has been found as a component of cigarette smoke (about 4 µg per cigarette), putting primary and second-hand smokers at risk.<sup>(71)</sup> One type of exposure which civilians may be

vulnerable to is accidental exposure. In 1984, one of the world's worst industrial disasters occurred because of an MIC gas leak in Bhopal, India. During the accidental exposure, an acute inhalation exposure to the gas, estimated at 13 to 100 ppm, resulted in the deaths of more than 3,000 people within 5 days and adverse health effects in greater than 170,000 survivors. Within 2-3 hours, about 2,00,000 people were exposed.<sup>(72, 73)</sup>

MIC is considered to have poor warning properties.<sup>(74)</sup> At 2 ppm, no odor is detected but subjects may experience eye, nose, and throat irritation and lachrymation. At 4 ppm, symptoms of irritation are more noticeable and exposure is unbearable at 21 ppm.<sup>(75, 76)</sup>

### **1.5.2. Metabolism of Methyl isocyanate**

The metabolism of MIC is dictated by its high reactivity in biological molecules. MIC spontaneously reacts with proteins under physiological conditions.<sup>(77)</sup> The sites on a protein molecule where binding of methyl isocyanate may take place are N-terminal amino group and sidechains of the following amino acids: lysine (primary amine), cysteine (thiol), histidine (secondary amine in the imidazolyl ring), tyrosine, and serine (hydroxyl). Therefore, biomonitoring of MIC is achieved by analysis of adducts formed between MIC and biological molecules.<sup>(78)</sup> MIC mainly carbamylates the N-terminal amino groups of proteins. MIC was shown to produce N-methylcarbamoyl adduct at the N-terminal valine of globin in vitro and in vivo.<sup>(79)</sup> The adduct is converted using Edman degradation to produce 3-methyl-5-isopropylhydantoin (MIH), which is used as a biomarker to confirm MIC exposure.

The presence of high concentrations of glutathione (GSH) in lung endothelial fluid indicates that inhaled MIC may react chemically with this thiol to form the corresponding

glutathione conjugate, S-(N-methylcarbamoyl) glutathione (SMG). This was confirmed in preliminary *in vivo* studies. When rats were given MIC by intraperitoneal injection, SMG was excreted as a metabolite in bile.<sup>(80)</sup> Hence, the major urinary metabolite of MIC is N-acetyl-S-(N-methylcarbamoyl) cysteine (AMCC), a degradation product of the MIC–S-conjugate with glutathione.<sup>(81, 82)</sup> Under physiological conditions, the S-(N-methylcarbamoyl) conjugates are reversible, transferring the MIC moiety to other nucleophilic groups to produce more stable adducts.<sup>(83)</sup>

### **1.5.3. Toxicity and Mechanism of Action of Methyl Isocyanate**

The high chemical reactivity of MIC is central to its toxicity as well as commercial uses. Since the toxicity of isocyanates is directly related to their volatility and vapor pressure,<sup>[93]</sup> the smaller the isocyanate molecule, the greater its toxicity.<sup>(84, 85)</sup> This makes MIC the most toxic of all isocyanates.<sup>(86)</sup> MIC has both irritant and pulmonary effects. Its direct irritant effect on lungs, eyes, skin, secondary to pulmonary toxicity, allergic response, and nonpulmonary direct effects may contribute to its high toxicity. These effects are instantaneous and proceed even after a lag period of hours.<sup>(76)</sup> Usually, the early effects of acute gaseous exposure to methyl isocyanate are respiratory tract and mucous membrane irritation. With eye exposure, the victim can have intense burning of the eyes, photophobia, blepharospasm, profuse lacrimation, lid edema, and superficial corneal ulceration with a resulting reversible blindness<sup>(87)</sup> In general, deaths following exposure to MIC occur 1 to 2 days later and a second phase of mortality follows after a week or longer.<sup>(88-90)</sup>

Based on known reactions, MIC could plausibly cause injury to exposed tissues by either or both of two mechanisms. The first is through direct addition reactions with tissue macromolecules and the second is simple physical injury by the heat liberated during

hydrolysis.<sup>(91)</sup> For direct addition reaction with tissue macromolecules, MIC and other isocyanates will carbamoylate hydroxyl groups, sulfhydryls, and imidazoles under physiological conditions and, at higher pHs, amines will also react with MIC.<sup>(77)</sup> The modification of these functional groups by MIC has been shown to inhibit certain enzyme activities in vitro, and moreover, isocyanates have for years been used as molecular site probes in the study of enzyme mechanisms.<sup>(92)</sup> In aqueous systems, the reactions of MIC with functional groups compete with the hydrolysis reaction. This is a highly exothermic reaction, and thus the second potential mechanism of tissue destruction is simple physical injury by the heat liberated during hydrolysis.<sup>(91)</sup> Nonetheless, the mechanism(s) by which MIC causes injuries to organs remote from the primary site of exposure still remains unclear and is paradoxical when one considers the chemical reactivity of this isocyanate, whose half-life in aqueous media is estimated to be about 2 min.<sup>(93)</sup> Following inhalation of MIC vapor, one would expect that the isocyanate would undergo rapid hydrolysis and fail to cross the alveolar-blood barrier as the complete species. Yet, two inhalation studies in rats exposed to <sup>14</sup>C-labeled MIC showed that radioactivity was distributed rapidly and extensively throughout the systemic circulation, with the appearance of MIC-derived radioactivity in urine, bile, and tissue proteins shortly after exposure.<sup>(93, 94)</sup> Based on these observations, it was concluded that MIC may be converted in vivo to a “transport” form, perhaps by reaction with the sulfhydryl groups of either hemoglobin or glutathione (GSH) to yield carbamate thioester adducts which could revert spontaneously to free MIC at distant sites.<sup>(77, 94)</sup> Other toxic effects of MIC include sensory irritation<sup>(95, 96)</sup> reproductive toxicity,<sup>(86)</sup> ocular toxicity,<sup>(97, 98)</sup> and neurological toxicity.<sup>(96, 99)</sup> There is also some evidence indicating teratogenic and carcinogenic effects of MIC.<sup>(8, 100-102)</sup>

## **1.6. 2-Mercaptoethane Sulfonate Sodium as a therapeutic for MIC and Sulfur Mustard exposure.**

### **1.6.1. Uses of MESNA**

MESNA, the sodium salt of 2-mercaptoethane sulfonate is a thiol-containing drug and uroprotectant. It is given adjuvant, orally or intravenously with ifosfamide and cyclophosphamide orally due to its ability to increase the levels of free thiol groups in the urinary tract.<sup>(103-106)</sup> It is also an antioxidant used particularly in renal protection and reduces the size of urinary bladder cancer. Numerous studies have shown that MESNA has beneficial effects in ischemic acute renal failure where it scavenges reactive oxygen species (ROS), due to the presence of the thiol group.<sup>(107, 108)</sup> Recent studies indicate that numerous disorders originate from free radical attacks on biological macromolecules such as proteins, lipids and DNA and an effective antioxidant is crucial in combating these free radical effects.<sup>(109)</sup> Coupled with the above, MESNA was proved to be effective in preventing hemorrhagic cystitis induced by high doses of several chemotherapeutic regimens such as cyclophosphamide and ifosfamide. Moreover, recent studies have suggested that it is also effective in reducing intestinal inflammation in colitis.<sup>(110)</sup> Liu et al.<sup>(111)</sup> utilized MESNA as a scavenger of sulfur mustard derivatives, such as 2-chlorethyl ethyl sulfide (CEES) and 2-chlorethyl methyl sulfide scavenger, in a cell-free system. Its efficiency against sulfur mustard in vitro as well as in vivo was also shown by Jost et al.<sup>(112)</sup>

### **1.6.2. Mechanism of action of MESNA**

MESNA is mainly used to inactivate acrolein, the toxic metabolite of anticancer drugs, ifosfamide and cyclophosphamide. Acrolein concentrates in the bladder and causes cell death by upregulation of reactive oxygen species (ROS).<sup>(113)</sup> It also activates inducible

nitric oxide synthase (iNOS) which leads to production of nitric oxide (NO). Both ROS and NO produce products which are detrimental to lipids, proteins, and DNA.<sup>(114)</sup> Furthermore, acrolein may also lead to ulceration of the bladder urothelium. MESNA protects against effects by binding to the toxic metabolites of these drugs.<sup>(115)</sup>

Following oral or intravenous administration, MESNA is quickly reduced to diMESNA in the plasma.<sup>(104)</sup> Just a small portion of the dose remains in the circulation as the physiologically active compound. MESNA and diMESNA are both very hydrophilic, hence they remain in the intravascular compartment where they are rapidly cleared by the kidneys.<sup>(116)</sup> About one-third of the diMESNA is converted back to MESNA in the renal tubular epithelium by glutathione reductase enzymes. The free sulfhydryl groups of MESNA then react directly with the double bond of acrolein or with urotoxic 4-hydroxyoxazaphosphorine metabolites to form stable and nontoxic compounds which are excreted in the urine of patients undergoing the MESNA therapy.<sup>(117, 118)</sup> Because urinary MESNA excretion greatly exceeds plasma MESNA concentrations, regional detoxification of ifosfamide in the urinary system occurs.<sup>(119, 120)</sup> The non-urinary toxic effects of ifosfamide are not reduced by concomitant MESNA and, importantly, MESNA does not interfere with the cytotoxic activity of ifosfamide.<sup>(121)</sup>

### **1.6.3. Metabolism and pharmacokinetics of MESNA**

The main metabolite of MESNA is diMESNA. Early studies have shown that MESNA is metabolized in vivo to its dimer, diMESNA by a complete spontaneous metal catalyzed oxidation.<sup>(122, 123)</sup> Likewise, MESNA can also bind through a disulfide linkage to low-molecular weight endogenous thiols like cysteine (Cys), glutathione (GSH), homocysteine (Hcy), an cysteinyl-glycine.<sup>(107)</sup> MESNA is also moderately protein-bound,



the bulk of which binds covalently through a disulfide with the single non-intramolecular disulfide forming cysteine residue of albumin known as Cys34. This thereby displaces endogenous thiols.<sup>(19, 124)</sup> The disulfide binding of MESNA moieties in the oxidative environment of the plasma is believed to be responsible for MESNA's inability to inactivate circulating chemotherapeutics which is very important in cancer treatment.<sup>(118)</sup>

#### **1.6.4. Toxicity of MESNA**

MESNA has been found to have very low acute and chronic toxicity in a standard preclinical toxicity testing in animals including rats, rabbits, and dogs. It has no teratogenic or mutagenic effects as tested by Ames test.<sup>(103, 125)</sup>

The low toxicity of MESNA is not only found in animals but also in humans. However, the main toxic effect associated with the use of MESNA in humans is vomiting due to its bad taste when given orally. This conundrum could still be overcome by masking the taste by giving MESNA in pleasantly flavored drinks, e.g., as coca cola or orange juice.<sup>(126)</sup> There are a number of other minor side effects associated with MESNA administration intravenously (IV). Such side effects include diarrhoea, headaches, and limb pains.<sup>(103, 127)</sup> Compared to the effects caused by anticancer drugs, the problem of bad taste with MESNA is generally considered insignificant. Nonetheless, patient non-compliance may result, especially in homebased therapy. This in effect may result in hemorrhagic cystitis while a tablet or capsule formulation of MESNA would clearly overcome this problem. In a recent volunteer studies, IV MESNA doses of 60 mg/kg resulted in diarrhea or watery stools.<sup>(103)</sup> Another recorded adverse effect of MESNA is hypersensitivity reactions, including rash and leukopenia. These have ranged from mild dermatologic reactions to severe dermatologic reactions, so it requires close monitoring.<sup>(128)</sup>

## Chapter 2. Identification and Analysis of a Methyl Isocyanate-Adduct for Exposure Verification

### 2.1. Introduction

Methyl isocyanate (MIC) is a highly toxic industrial chemical that is used as an important precursor for the synthesis of carbamate pesticides (aldicarb, methomyl, carbofuran, etc.) and to produce plastics.<sup>(73, 90, 129-131)</sup> It is the smallest, most volatile and toxic member of the isocyanate family.<sup>(85)</sup> MIC has a pungent odor and is extremely irritating to skin and mucous membranes.<sup>(84, 90, 132)</sup> However, the odor does not adequately warn of its presence because the human odor threshold for detection of MIC (>2 ppm)<sup>(10)</sup> and mucous membrane irritation (>0.4 ppm) are much greater than MIC's threshold limit value of 0.02 ppm.<sup>(90, 133)</sup> Hence exposure to MIC can occur at toxic levels without detection of its odor.<sup>(90, 133, 134)</sup>

The devastating effects of MIC exposure were evidenced in one of the world's worst industrial chemical disasters in Bhopal where a total of 200,000 in a city of 800,000 in 1984 were exposed to the gas.<sup>(10, 135, 136)</sup> The exact human death toll during the accidental exposure is still unknown; however, it is estimated that about 5,000 people died within 2 days,<sup>(135, 137)</sup> and the death toll eventually increased to about 20,000.

Due to the high reactivity of MIC, it easily and spontaneously reacts with endogenous nucleophilic sites (e.g., amine moieties in proteins) under physiological conditions.<sup>(138, 139)</sup> As such, direct analysis of MIC to confirm exposure is not possible. MIC specifically carbamylates the N-terminal valine of hemoglobin,<sup>(140-142)</sup> and can react with other amino acids under physiological conditions including the sulfhydryl group of cysteine,<sup>(143, 144)</sup> the hydroxyl groups of tyrosine<sup>(77, 145)</sup> and especially serine,<sup>(145, 146)</sup> the o-amino group of lysine,<sup>(82, 147)</sup> and the imidazole ring of histidine.<sup>(148)</sup> The reactivity and high vapor pressure

of MIC cause it to be highly toxic. Exposure to MIC can cause several detrimental effects. It can affect the respiratory tract, skin, and eyes, and seriously damage the lungs. Chronic exposure to MIC is known to cause chronic respiratory symptoms like asthma, rhinitis and hypersensitivity pneumonitis.<sup>(7, 11, 90, 149-152)</sup> Recent research has also shown that MIC could be a potential carcinogen. A study conducted by Pesatori et al.<sup>(153)</sup> observed twofold excess lung cancer risk in Florida pesticide applicators exposed to carbamate insecticides.

Because MIC reacts strongly with proteins, formation of stable protein adducts offers the possibility for biomonitoring exposure to MIC. Table 1 lists methods for biomonitoring of MIC exposure via analysis of protein adducts. Two major strategies have been employed for analysis of MIC-protein adducts: 1) enzymatic hydrolysis of carbamylated protein adduct and 2) Edman degradation. Protein enzyme hydrolysis is achieved by addition of pronase to globin samples, 24-hr incubation, filtration, and analysis by LC-MS/MS. Aside from enzymatic protein digestion, the main method for confirming exposure to MIC is acid hydrolysis (i.e., Edman degradation) of MIC adducts of hemoglobin to form methyl isopropyl hydantoin (MIH). MIH is formed via hydrolysis of the N-terminal valine adduct of MIC resulting in N-(methylcarbamoyl)valine and subsequent cyclization to form MIH. The MIH is typically extracted via by liquid-liquid extraction and analyzed using gas chromatography (GC) or liquid chromatography (LC) with mass spectrometry (MS). Mráz *et al.*<sup>(154)</sup> reported a simplified sample preparation method for analysis of MIH, but the method involved 20 steps and approximately 9 h which was still lengthy, used up considerable amounts of energy and generated a large amount of organic waste. In another method reported by Wang *et al.*,<sup>(155)</sup> they utilized a 96-well protein precipitation and phospholipid removal plate with similar hydrolysis and MIH formation steps. However, a

sorbent plate was used to isolate the MIH for UHPLC-MS-MS analysis instead of liquid-liquid extraction. This method was rapid, yet it still required many steps (i.e., 18) and specialized equipment for the sample preparation. Recently, a similar rapid, greener, and simpler GC-MS method for analysis of MIH isolated from N-methyl carbamoylated hemoglobin was reported by Logue *et al.*<sup>(130)</sup> but the method still required 14 steps and approximately 5 hours to analyze MIC-exposed samples. Because each of the methods listed in Table 2.1. has major disadvantages, there is a need to develop a simpler and less cumbersome sample preparation method for the analysis of protein adducts of MIC to verify exposure to MIC. The objective of the current study was to develop a simple method to detect MIC-tyrosine adducts utilizing strong base hydrolysis and subsequent liquid chromatography tandem mass spectrometry analysis.

**Table 2. 1** Comparison of methods for analysis of MIC-protein adducts.

Analyte	Protein degradation	Reference	Year	Analysis technique	Approximate time (hr)	Steps	LOD	R <sup>2</sup>	Precision	Accuracy
MIH	Edman degradation	Mráz <i>et al.</i> <sup>(154)</sup>	2002	EI-GC/MS	9	20	0.031 mg/kg	NR	< 10%	NR
MIH	Edman degradation	Logue <i>et al.</i> <sup>(130)</sup>	2018	EI-GC/MS	5	14	0.05 mg/kg	0.993	< 4.5%	100 ± 5.7
MIH	Edman degradation	Wang <i>et al.</i> <sup>(155)</sup>	2014	HPLC-MS/MS	7	18	1.6 mg/kg	0.999	< 1.7%	NR
MIC-Hb adducts	Enzymatic hydrolysis	Mráz <i>et al.</i> <sup>(144)</sup>	2004	HPLC-MS/MS	24.5	5	NR	NR	NR	NR
MLU	Enzymatic hydrolysis	Mráz <i>et al.</i> <sup>(143)</sup>	2006	HPLC-MS/MS	24.5	5	1.015 mg/kg	0.990	NR	NR
MVU	Enzymatic hydrolysis	Mráz <i>et al.</i> <sup>(143)</sup>	2006	HPLC-MS/MS	24.5	5	0.87 mg/kg	0.990	NR	NR
PMC	Base hydrolysis	Current method	2021	HPLC-MS/MS	4	12	0.02 mg/kg	0.998	< 10%	100 ± 9

NR = not reported

MLU = (N-methylcarbamoyl) lysine

MVU = N-methylcarbamoylvaline (MVU)

EI-GC-MS = electron impact ionization- gas chromatography- mass spectrometry

HPLC-MS/MS = high performance liquid chromatography- tandem mass spectrometry

## 2.2. Materials and Methods

### 2.2.1. Materials

All reagents and solvents were at least HPLC grade, unless otherwise stated. Formic acid, acetonitrile, hydrochloric acid (certified ACS), acetone, amino acids (tyrosine, serine, lysine, histidine, and valine) and chloroform were purchased from Fisher Scientific (Fair Lawn, NJ, USA). Sodium hydroxide, phenol and N-methylimidazole were obtained from Sigma-Aldrich (St. Louis, MO). Water used for this study was purified by reverse osmosis and filtered through a Lab Pro polishing unit from Labconco (Kansas City, KS, USA). Methyl isocyanate (MIC) was synthesized for the analytical work in our lab by the method of Kaushik *et al.*<sup>(130)</sup> and Logue *et al.*<sup>(130, 156)</sup> based on Curtius Rearrangement method. The MIC was collected via distillation and the purity was confirmed using <sup>1</sup>H NMR at 95%. MIC for animal inhalation exposures was synthesized by MRIGlobal (Kansas City, MO) through the Curtius Rearrangement method. Purity of this MIC was  $\geq 99.5\%$  as measured by gas chromatography-flame ionization detection. Phenyl methyl carbamate (PMC) and its internal standard (PMC-D<sub>5</sub>) were synthesized in our lab as discussed below. All stock solutions were stored at -30 °C. Working PMC and PMC-D<sub>5</sub> solutions were obtained from stock solutions of PMC (1 mM) or PMC-D<sub>5</sub> (1 mM) via serial dilutions to the desired concentration.

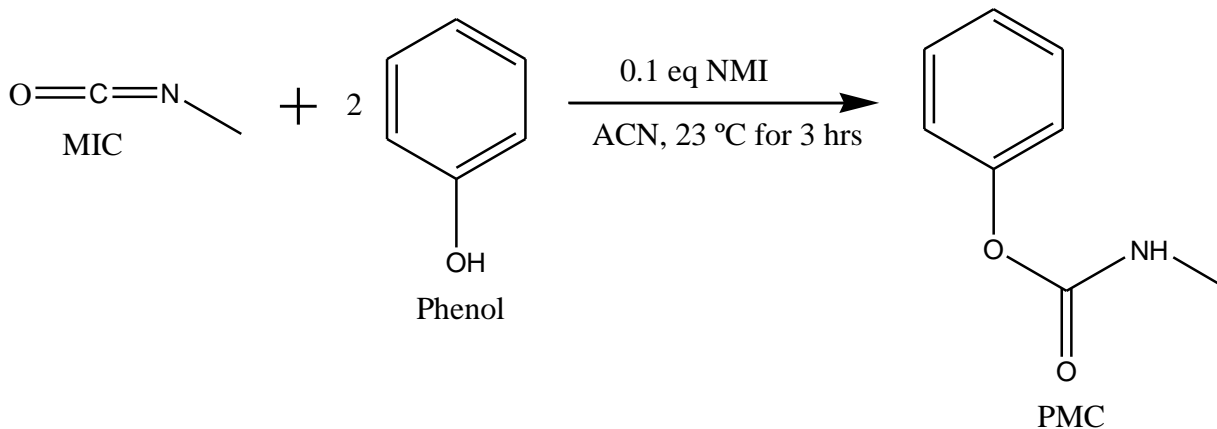


**Figure 2. 1** Scheme for the synthesis of PMC from the reaction of phenol with MIC in acetonitrile (ACN) via Lossen rearrangement using N-methylimidazole (NMI) as a catalyst.<sup>(157)</sup>

## 2.2. Synthesis of PMC and PMC-D<sub>5</sub>

The reaction scheme for the synthesis of PMC is shown in Figure 2.1. The synthesis of PMC and its internal standard were achieved by Lossen's rearrangement modification of the Yoganathan *et al.*<sup>(157)</sup> method for the one pot synthesis of carbamates. Briefly, phenol (0.941 g, 2 eq) and N-methylimidazole (NMI, catalyst) (0.034 g, 0.1 eq) were dissolved in 50 mL acetonitrile with stirring. MIC (2.94 mL, 1 eq) was added dropwise at 23 °C with continuous stirring for 3 hrs. The reaction mixture was left overnight at room temperature and concentrated on a rotary evaporator until a yellowish-white liquid was formed. Normal phase column chromatography was performed using an ethyl acetate:hexane (60:40) mobile phase. Characterization was achieved by 1-H NMR spectroscopy and ESI-MS operated in positive polarity mode. 1-H NMR (600 MHz, CDCl<sub>3</sub>):  $\delta$  2.89 (d, 3H), 7.12 (d, 2H), 7.19 (t, 1H), 7.35 (t, 2H). ESI (+)-MS:  $m/z$  152.40, 77.0, 95. An isotopically labeled standard, PMC-D<sub>5</sub>, was synthesized as described above for PMC, with phenol replaced with phenol-D<sub>5</sub>. ESI (+)-MS:  $m/z$  157.10, 82, 100.

### 2.2.2 Biological samples

For method development and validation, Sprague-Dawley rat red blood cells (RBCs) with K<sub>2</sub>EDTA as anticoagulant, were purchased from Bioreclamation IVT (Westbury, NY, USA) and immediately stored at -80 °C until used. For this experiment, male Sprague-Dawley rats (300-350 g) were obtained from Charles River Laboratories and acclimated at MRIGlobal (AAALAC International accredited) for 5-7 days prior to study, including acclimation to a nose-only inhalation exposure apparatus 30 minutes daily for 3 days prior to exposure. All procedures were approved by the MRIGlobal Institutional Animal Care and Use Committee. For evaluation of the usefulness of PMC as a marker of MIC exposure, rats were exposed to MIC and blood was sampled for PMC analysis. MIC inhalation exposure was performed as previously described by Logue *et al.*<sup>(6)</sup> and Rancourt *et al.*<sup>(158)</sup> Briefly, unanesthetized rats were placed in a flow-directed nose-only inhalation exposure system (CH Technologies, Westwood, NJ) housed in a fume hood connected to a proprietary custom MIC vapor diffusion system (MRIGlobal). The gas constituents delivered through the inner plenum of the exposure system were continuously monitored by Fourier transform infrared spectroscopy, with adjustments made to the amount of MIC delivered so as to limit deviation in the height of the absorption peak for MIC in the atmosphere to less than 1% during the course of exposure. Animals were exposed to 375 or 500 ppm MIC for 30 minutes. After exposure, rats were allowed to recover in their home cages, and for the duration of study, rats were monitored every 2 hours for peripheral blood oxygen saturation levels<sup>(159)</sup>, respiratory distress quality, and physical activity score as previously described Nick *et al.*<sup>(159)</sup>. Upon meeting euthanasia criteria (oxygen saturation <70%, cumulative clinical distress score  $\geq 7$ ), rats were anesthetized by IP injection of a



mixture of ketamine (75 mg/kg), xylazine (7.5 mg/kg), and acepromazine (1.5 mg/kg), and blood was collected from the abdominal aorta into 3.2% trisodium citrate (1:9 citrate: blood). Red blood cells (RBCs) were fractionated by centrifugation of whole blood at 3000 x g for 15 minutes at 4°C. Plasma was removed, and aliquots (0.5-1 mL) of packed RBCs were immediately frozen and stored at -80°C, then shipped on dry ice to South Dakota State University and stored at -80°C until analysis.

### 2.2.3 Sample preparation

Protein precipitation was achieved by adapting the method employed by Logue *et al.*<sup>(130)</sup> RBCs (3 mL) were added to a 15-mL centrifuge tube. Acetone with 1% HCl (v/v) was added to the RBCs with a 3:1 volume ratio of acetone to RBC. The mixture was further vortexed and centrifuged at 800 × g for 10 min at 20 °C. The supernatant was discarded, and the precipitate was washed once by adding 6 mL of acetone and breaking the pellet with a clean spatula. The mixture was vortexed and again centrifuged, as above, and the supernatant was discarded. The precipitate was dried in a centrifugal evaporator (Labconco, Kansas City, USA) equipped with a rotary vacuum pump (Edwards, Glenwillow, USA) at 30 °C until dry. The precipitate was stored at -80 °C until ready for use. A portion of the RBC protein precipitate (100 mg) was added to a clean 15 mL centrifuge tube. For base hydrolysis, aqueous NaOH (1mL of 10 M) was added to the precipitate. The mixture was then vortexed and heated at 70 °C for 2 hr. The sample was then removed from heat and cooled to room temperature. The PMC-D<sub>5</sub> IS (200 µL) was spiked into the mixture and the resulting solution was vortexed 3-4 times. (Note: For method development or calibration, PMC standard was spiked with PMC-D<sub>5</sub>) HCl (1 mL, 18 M) was then added to neutralize the base and chloroform (2.5 mL) was added to extract

PMC. The resulting mixture was capped, vortexed for about 5 min and centrifuged at 2000  $\times$ g for 20 min. Rarely, an emulsion develops in the sample. If an emulsion was visually apparent, the organic layer was transferred into a new tube and centrifuged again at 2000  $\times$ g for 5 min. An aliquot of the organic layer (2 mL) was then transferred into a 4 mL glass screw-top vial and dried under nitrogen for 30 min at room temperature. The dried samples were then reconstituted with 500  $\mu$ L of 80% acetonitrile in water, mixed thoroughly, filtered with a 0.22- $\mu$ m tetrafluoropolyethylene syringe filter, and analyzed using HPLC–MS/MS.

#### 2.2.4 HPLC-MS/MS analysis of PMC

Liquid chromatography analysis was performed on a Shimadzu UFLC with LC-20ADXR controller. The column used for chromatography was an Agilent polymeric reversed-phase column, eclipse Plus C18 (3.0  $\times$  100 mm, 1.8  $\mu$ m, part #:PN 959964-302). The chromatographic separation was achieved using isocratic elution at a flow rate of 0.2  $\mu$ L/min at 90% B held for 5 minutes. Mobile phases A and B were 0.1% formic acid in water and acetonitrile, respectively. The column was equilibrated for 1 min and a volume of 10  $\mu$ L was injected for HPLC-MS/MS analysis. For MS analysis, a tandem mass spectrometer (Sciex Q-Trap 5500 MS) equipped with an electrospray ionization interface in the positive polarity mode was used to detect PMC and PMC-D<sub>5</sub>. Optimization of mass spectrometric conditions was accomplished by direct infusion of a standard solution of PMC and PMC-D<sub>5</sub> into the spectrometer at a flow rate of 10  $\mu$ L/min. After infusion of standard solutions of PMC and PMC-D<sub>5</sub> into the ESI, molecular ions of m/z 152.40 ([M + H]<sup>+</sup>) and m/z 157.10 ([M + H]<sup>+</sup>) respectively, were identified. Multiple reaction monitoring (MRM) parameters for PMC and PMC-D<sub>5</sub> were optimized and are outlined in Table 2.2.

Nitrogen (50 psi) was used as the curtain and nebulization gas. The ion spray voltage was 4,500 V, the source temperature was 500 °C, and both the nebulizer (GS1) and heater (GS2) gas pressures were 90 psi. The collision cell was operated with an entrance potential of 10.0 V and an exit potential of 11.0 V at a “medium” collision gas flow rate. The total mass spectrometry acquisition time was 5 min.

**Table 2. 2** MRM transitions, optimized collision energies (CEs), cell exit potentials (CXPs) and declustering potentials (DPs) for the detection of PMC and PMC-D<sub>5</sub> by MS/MS analysis.

Compounds	Q1 (m/z)	Q3 (m/z)	Time (ms)	CE (V)	CXP(V)	DP (V)
PMC (quantification)	152.40	95	100	23.70	12.88	8.99
PMC (identification)	152.40	77	100	38.28	10.03	39.82
PMC-D <sub>5</sub> (quantification)	157.10	100	100	22.00	45.99	10.35
PMC-D <sub>5</sub> (identification)	157.10	82	100	40.99	14.12	24.02

### 2.2.5 Calibration, quantification, and limit of detection

Validation of the method was achieved by following Food and Drug Administration guidelines.<sup>(160, 161)</sup> To determine the limit of detection (LOD), multiple concentrations of PMC below the LLOQ were analyzed in rat RBC utilizing the sample preparation method described above (Section 2.2.3.) The lowest concentration which reproducibly produced a signal-to-noise ratio of at least 3 was determined as the LOD. Calibrators (0.05, 0.1, 0.2, 0.5, 1, 2, 5, 10, 20, 50, 100 and 200  $\mu\text{M}$ ) and quality-control (QC) standards (0.3, 3, and 30  $\mu\text{M}$ ) were prepared from a stock solution of PMC in 80% acetonitrile:water. Aliquots (200  $\mu\text{L}$  each) of PMC and PMC-D<sub>5</sub> were spiked into rat RBC precipitate to create calibration standards utilizing the sample preparation method described above. Quality-control (QC) standards (0.3, 3, and 30  $\mu\text{M}$ ) were also prepared from the same stock solution. The QC standards were not included in the calibration curve. Each calibration standard was prepared in triplicate and QC standards in quintuplicate. After analysis of the calibration standards, calibration curves were plotted using the average signal ratios of PMC and PMC-D<sub>5</sub> as a function of PMC concentration. Weighted ( $1/x^2$ ) and unweighted calibration curves were created using linear least squares. A weighted  $1/x^2$  fit was chosen as the best model to fit the calibration data. The LLOQ and upper limit of quantification (ULOQ) were established using the inclusion criteria of <15% relative standard deviation (%RSD, as a measure of precision) and a percent error (as a measure of accuracy) of  $100\pm 15\%$ . The percent error was calculated based on the comparison of the PMC concentration back-calculated from the calibration curve to the nominal PMC concentration of the QC standard. The percent residual accuracy (PRA) was used to determine the goodness of-fit of the calibration curves (i.e., PRA values  $\geq 90\%$  are

indicative of a good fit).<sup>(162)</sup> Intraassay precision and accuracy were calculated from each day, and interassay precision and accuracy were calculated by comparing the data gathered over three separate days.

#### *2.2.6 Recovery and matrix effect*

The recovery of PMC was determined by the analyzing five QC replicates (low, medium, and high concentrations) prepared in aqueous solution compared with equivalent QCs in rat RBC precipitate. Recovery was defined as the ratio of the average analyte peak area or signal ratio from spiked rat RBC precipitate which went through the sample preparation procedure to the average peak area or signal ratio of aqueous QC standards containing PMC reconstituted in 80% acetonitrile in water, expressed as a percentage. Calibration curves of PMC from aqueous samples and spiked RBC precipitate were established to evaluate the matrix effect of the RBC precipitate on the analysis of PMC. The ratio of calibration curves slopes, RBC-precipitate to aqueous calibration standards, was used to quantify the matrix effect. A slope ratio (RBC precipitate slope/aqueous slope) equal to one indicates negligible matrix effect, a slope ratio greater than one indicates an enhancement effect and slope ratio less than one indicates suppression of the analyte signal by the RBC precipitate.

#### *2.2.7 Stability*

The stabilities of both the PMC and the MIC-protein adduct were evaluated. The stability of PMC (autosampler, benchtop, and long-term) in RBC precipitate was evaluated by analyzing low and high QCs stored at various temperatures at multiple storage times. Autosampler stability was performed by spiking rat RBC precipitate with low and high QC PMC standards and preparing for analysis. The samples were placed on the auto-sampler

(at ambient temperature) and analyzed at approximately 0, 1, 2, 4, 8, 12, and 24 h following preparation. Internal standard was not used for the autosampler stability experiment, as it would compensate for the loss of PMC during the storage. To evaluate the benchtop stability of the MIC-protein adduct, MIC was initially spiked in RBCs at concentrations which produced PMC signals similar to the low and high QCs, 3.4  $\mu\text{mol/g}$  and 85  $\mu\text{mol/g}$ , respectively. The MIC-spiked rat RBC samples were vortexed for 2 min and shaken overnight in a Benchmark INCU-SHAKER™ 10-L shaking incubator at 300 rpm and room temperature. The samples were then stored on the bench top for 0, 1, 2, 4, 8, 12, and 24 h. They were precipitated, dried, and stored in  $-80\text{ }^{\circ}\text{C}$  freezer until all samples were ready for analysis. During analysis, samples were prepared using the sample preparation steps outlined above and analyzed using the developed HPLC-MS/MS method. For the long-term stability of the MIC-protein adduct, sample preparation was carried out as with the benchtop stability, except that samples were stored at room temperature,  $4\text{ }^{\circ}\text{C}$ ,  $-20\text{ }^{\circ}\text{C}$  and  $-80\text{ }^{\circ}\text{C}$  and  $4\text{ }^{\circ}\text{C}$  for 0, 1, 2, 5, 15, and 30 days. Samples were then prepared and analyzed using the developed method.

## 2.3 Results and Discussion

### 2.3.1 Mechanism of MIC-tyrosine adduct formation

Previous studies of the reaction of MIC with amino acid residues of common proteins showed that MIC reacts under physiological conditions at the N-terminal valine of hemoglobin, the sulfhydryl group of cysteine, the hydroxyl groups of tyrosine and serine, the  $\epsilon$ -amino group of lysine, and the imidazole ring of histidine to form their respective adducts.<sup>(139, 163, 164)</sup> Mraz *et al.*<sup>(139)</sup> in 2004 detected adducts of MIC-histidine, MIC-tyrosine, MIC-lysine and MIC-valine when they reacted 100 molar excess of MIC

with hemoglobin, followed by hydrolysis with pronase HPLC-MS/MS analysis. In this study, we modeled the interaction of MIC with tyrosine, lysine, histidine, serine, and valine residues by reacting MIC with these individual amino acids. We then used a simple base hydrolysis to evaluate the potential for use of resulting hydrolysis products as markers of MIC-protein adducts. Reaction of MIC with these amino acids and rat hemoglobin and subsequent base hydrolysis with heating led to the formation of a novel marker of the MIC-tyrosine adduct, phenyl methyl carbamate (PMC). Figure 2.2 shows the proposed reaction scheme for the reaction of MIC with tyrosine and subsequent base hydrolysis. In summary, the hydroxyl group of tyrosine is proposed to react with the electrophilic carbon of methyl isocyanate to form an MIC-tyrosine adduct which subsequently undergoes base hydrolysis under heat to cleave the phenyl-carbon bond leading to the formation PMC and a serine residue as the by-product. Cleavage by base hydrolysis is supported by the proposed SN2 reaction mechanism outlined in figure 2.3.

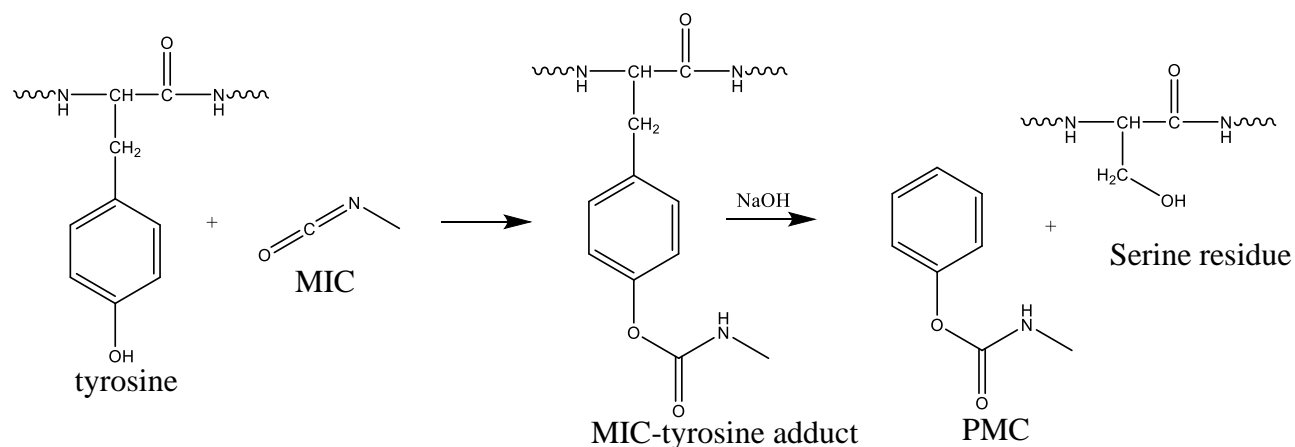


**Figure 2. 2** Reaction pathway for the formation of PMC from the reaction of tyrosine with MIC. Tyrosine is proposed to react with MIC to form an MIC-tyrosine adduct which undergoes base hydrolysis to produce phenyl methyl carbamate (PMC).



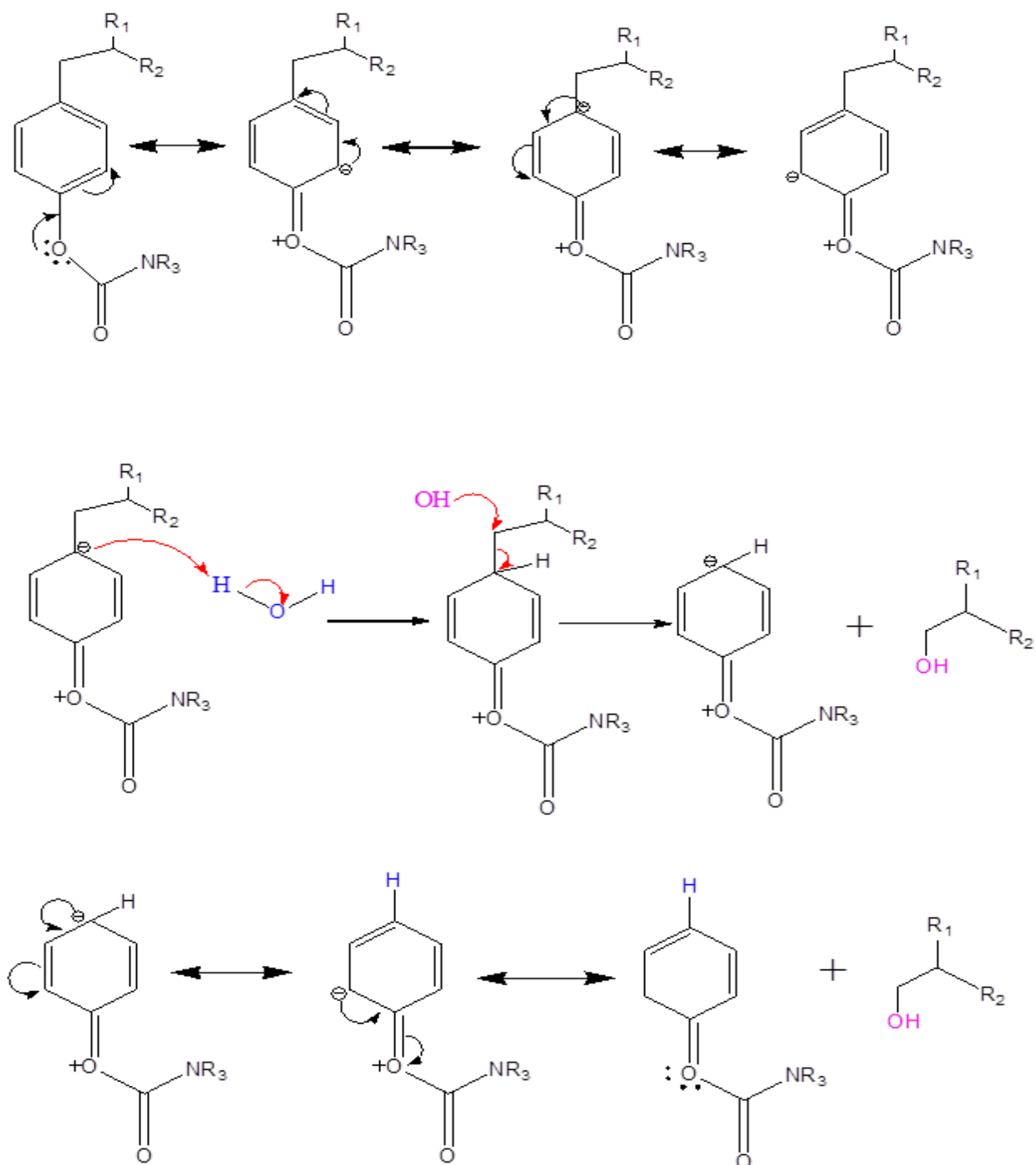
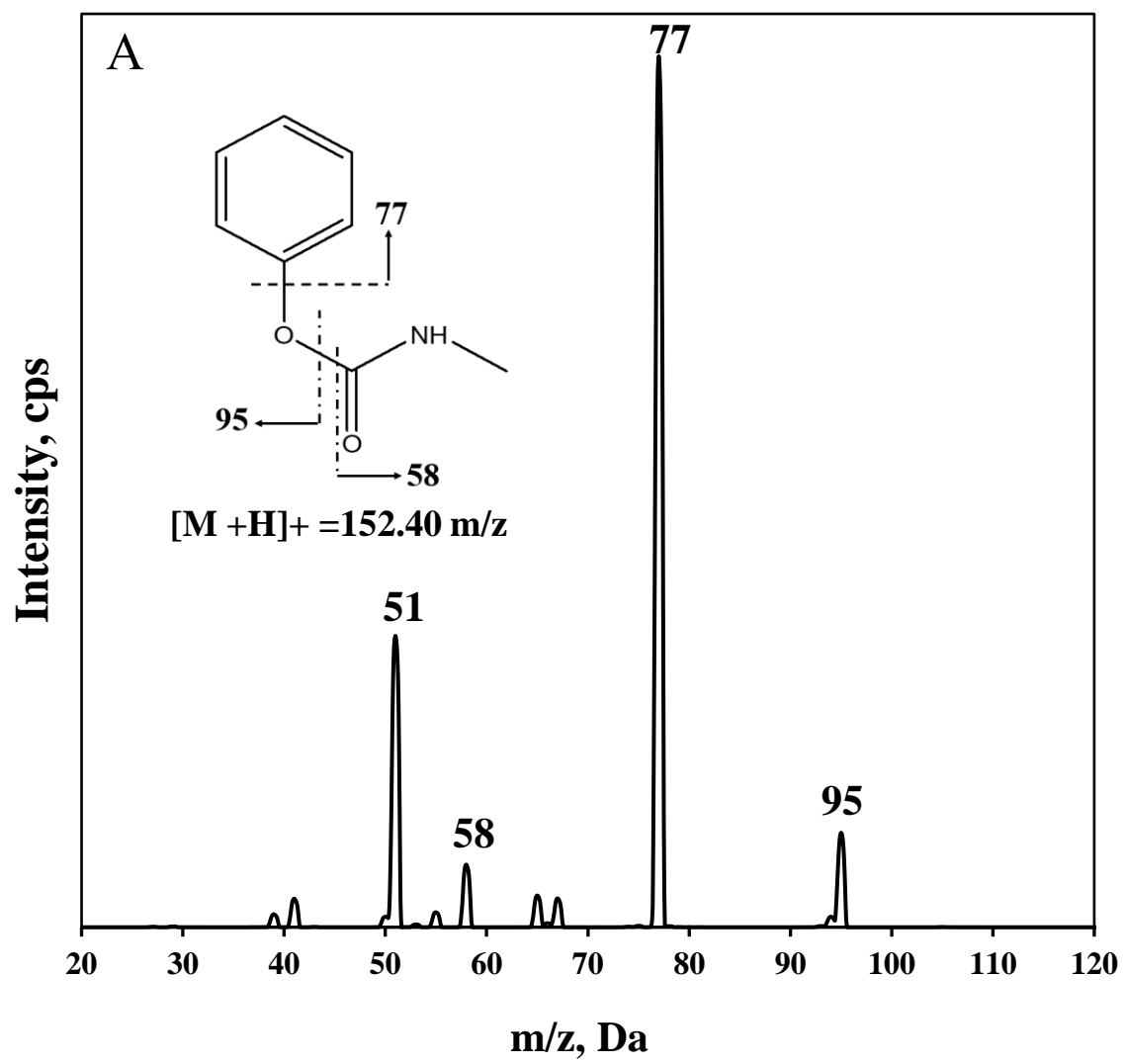


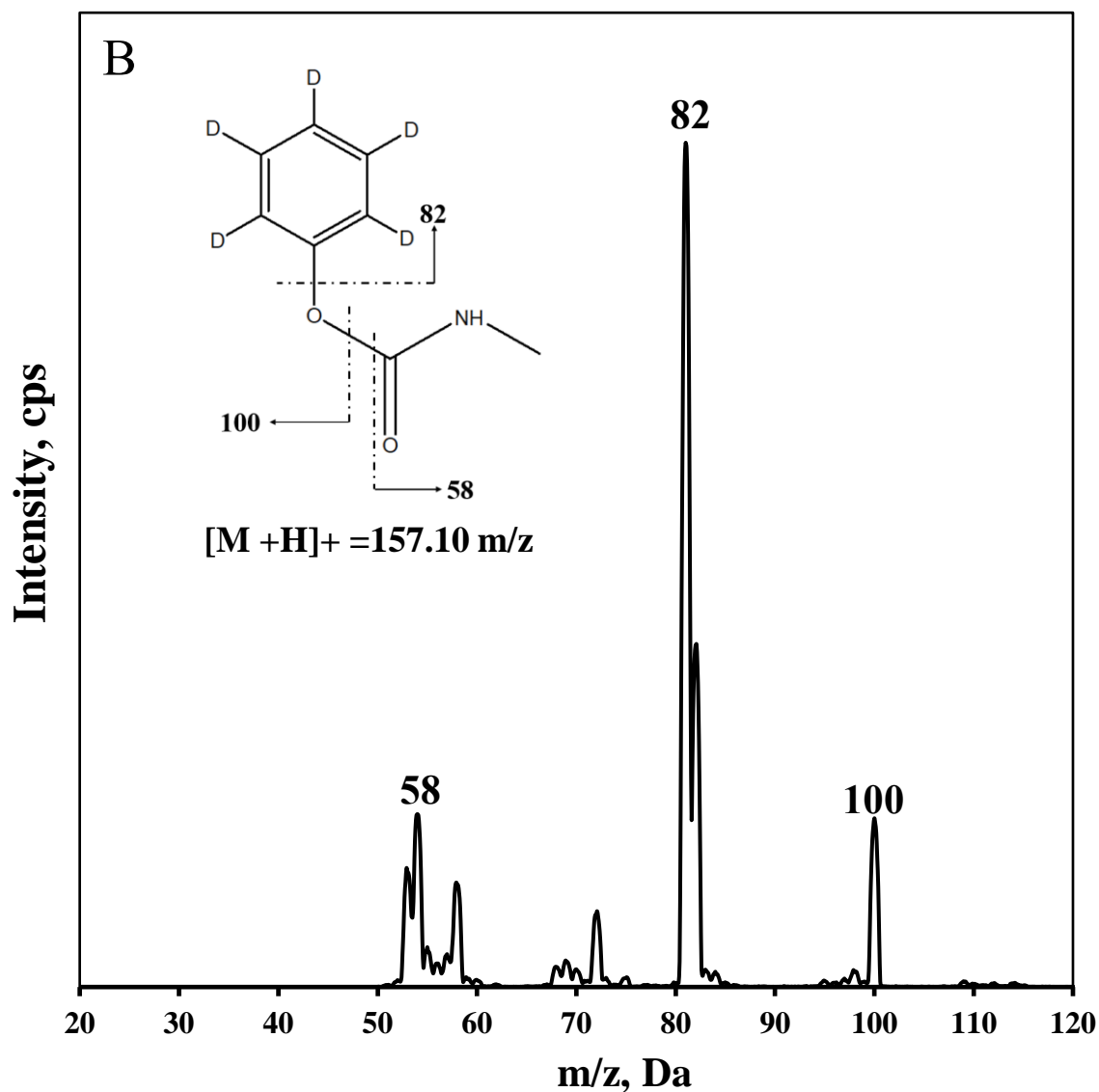
**Figure 2. 3** Proposed reaction mechanism for the formation of PMC. MIC-Tyrosine adduct undergoes an SN2 reaction in the presence of strong aqueous NaOH to cleave PMC at the CH-aromatic bond. R<sub>1</sub>= CHNH, R<sub>2</sub>= NHC=O and R<sub>3</sub>=CH<sub>3</sub>.

### 2.3.2 Phenyl methyl carbamate as a biomarker for MIC exposure.

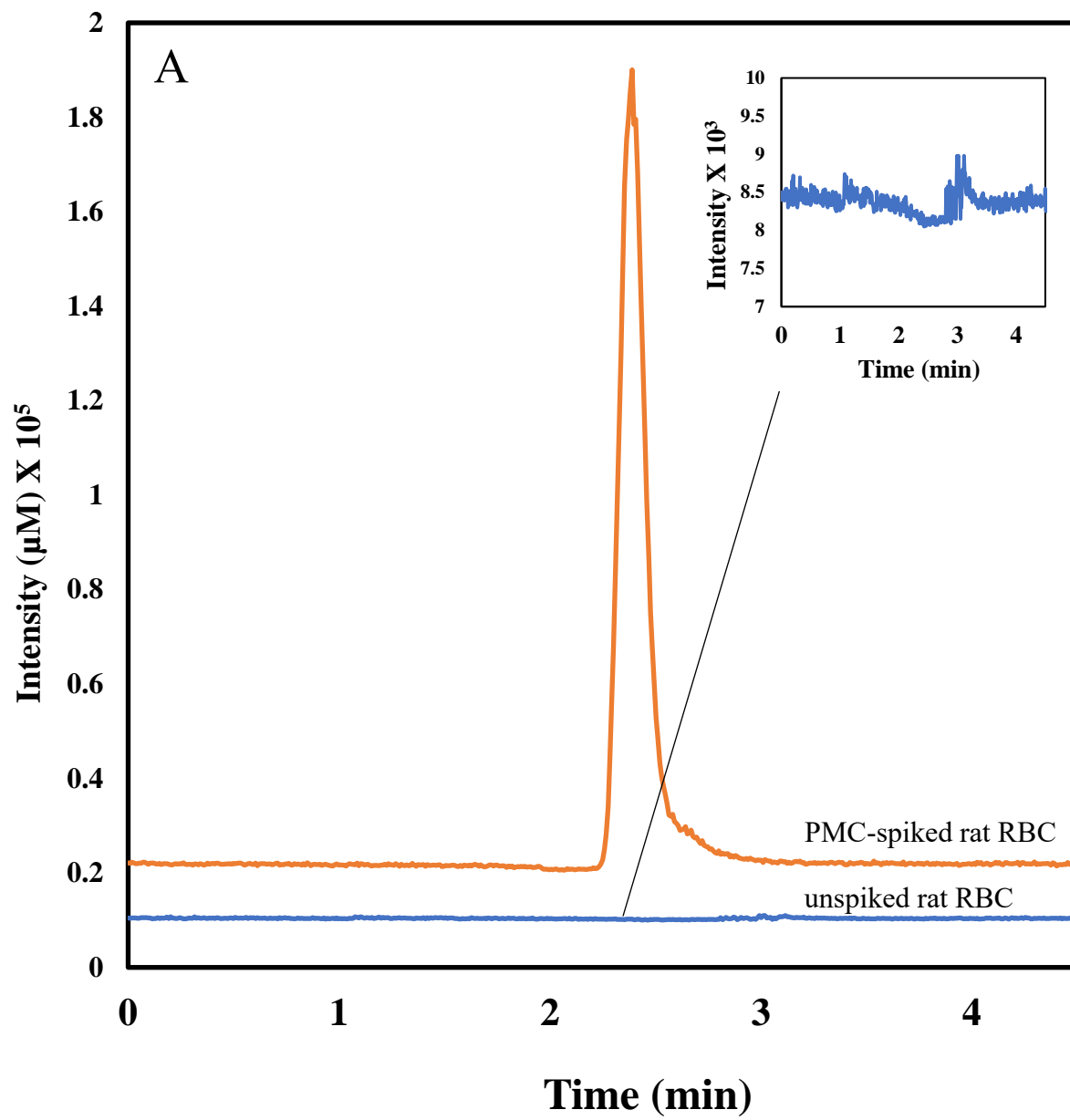
To confirm the formation of PMC from MIC exposure, analytical methods were developed to detect and quantify PMC in the hemoglobin isolated from MIC-exposed rats. The mass spectra of PMC and PMC-D<sub>5</sub> are shown in Figures 2.4A and B respectively, produced by ESI (+)-MS. The molecular ions (M+H)<sup>+</sup>, with abundant ions identified respectively. For PMC, transitions 152.4 → 95 and 152.4 → 77 were used for quantification and identification, respectively. The quantification and identification transitions for PMC-D<sub>5</sub> were 157.1 → 82 and 157.1 → 100, respectively. The optimized MS/MS parameters for the detection of PMC and PMC-D<sub>5</sub> are shown in Table 2.2.

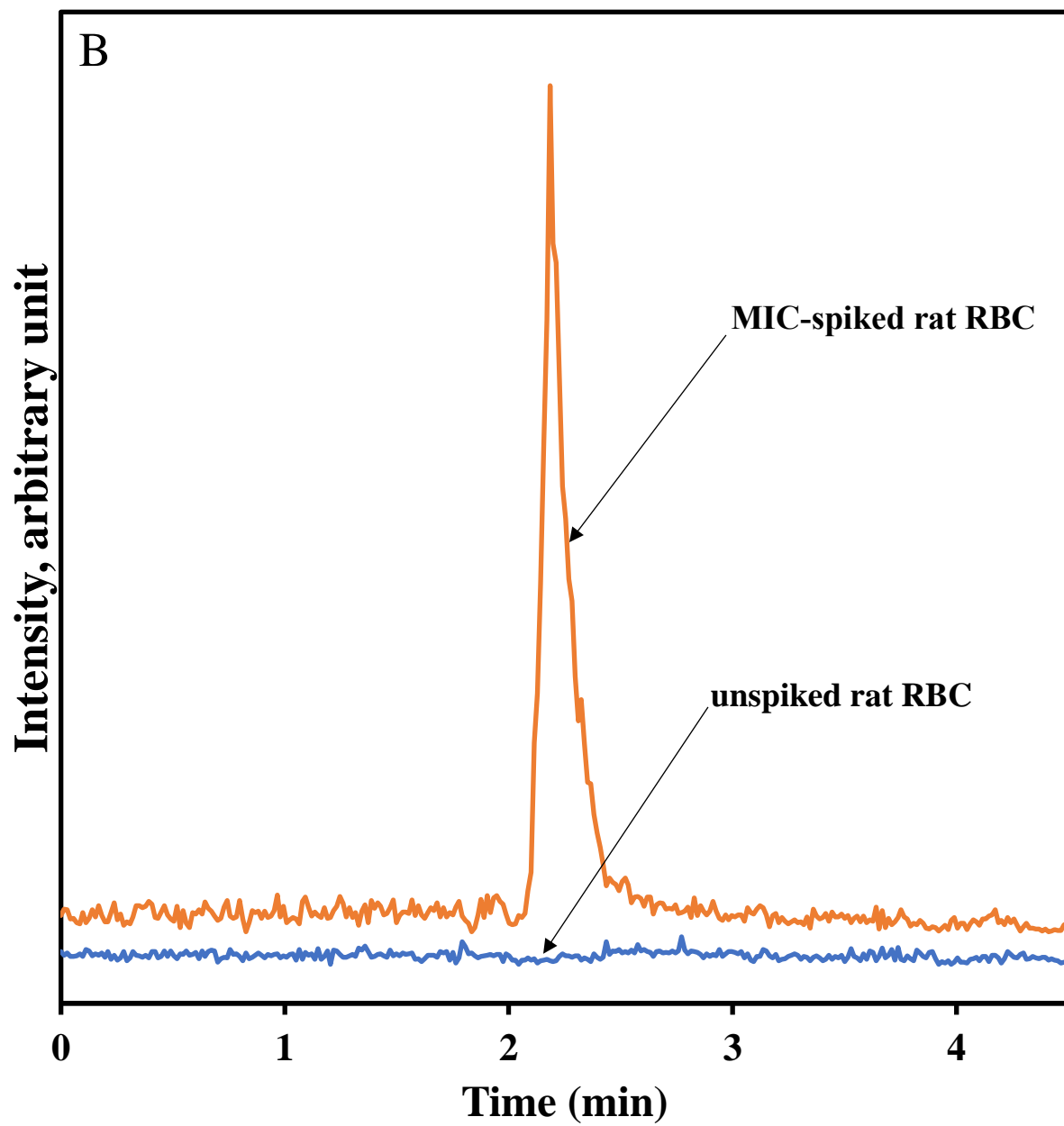
Figure 2.5. shows the HPLC–MS/MS chromatograms of PMC analyzed from spiked rat RBC precipitate (Figure 2.5A), MIC-spiked rat RBC precipitate (Figure 2.5B) and from non-exposed and MIC-exposed rats (Figure 2.5C). PMC was detected from hemoglobin precipitate of both MIC-spiked rat RBC precipitate and MIC-exposed rats, eluting at about 2.4 min. The detection of PMC from both MIC-spiked rat RBC and MIC-exposed rats definitively confirms the formation of PMC from reaction between MIC and tyrosine under strong base hydrolysis. This supports the reaction scheme shown in Figure 2.2 and provides strong evidence of the *in vivo* binding of MIC to tyrosine proteins and its transformation to PMC under strong base hydrolysis.





**Figure 2. 4** ESI (+) product ion mass spectra of PMC (A) and PMC-D5 (B) with identification of the abundant ions. Molecular ions of PMC and PMC-D5  $[M+H]^+$  correspond to 152.40 and 157.10, respectively. Insets, structures of PMC (A) and PMC-D5 (B) with abundant fragments indicated.





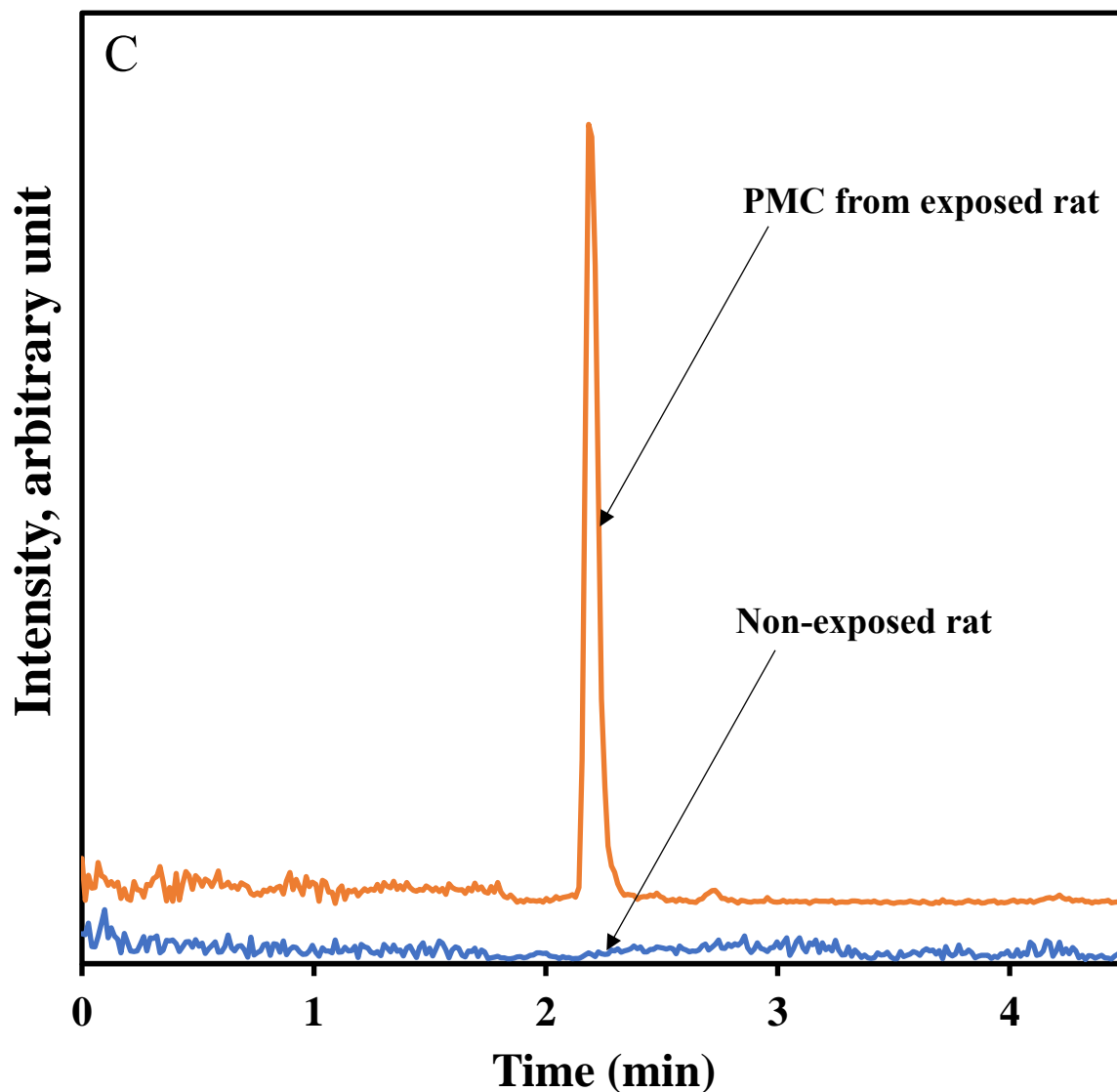


**Figure 2. 5** HPLC–MS/MS chromatograms of (A) PMC-spiked rat RBC (B) PMC from MIC-spiked rat RBC, (C) PMC from RBC of MIC-exposed rat, non-exposed and exposed are presented.

### 2.3.3 Detection of serine as a by-product of base hydrolysis of MIC-tyrosine adducts

Base hydrolysis of the product of MIC with tyrosine according to the proposed reaction scheme (Figure 2.2) should lead to the formation of PMC with a serine residue as the by-product. To confirm this hypothesis, analysis of serine as a by-product of base

hydrolysis of the MIC-tyrosine reaction product was attempted. A high-performance liquid chromatography with fluorescence detection was used to detect serine following O-phthalaldehyde (OPA) derivatization in the presence of a thiol.<sup>(165)</sup> To confirm serine as a by-product, the aqueous layer of a based-hydrolyzed MIC-tyrosine reaction solution was analyzed for serine. Serine was prominently detected from this solution with excellent efficiency and selectivity. The detection of serine from the MIC-tyrosine reaction solution provides strong support for the proposed reaction scheme (Figure 2.2).

#### 2.3.4 HPLC-MS/MS analysis of PMC

The analytical method for PMC presented here involved a simple sample preparation procedure as compared to existing methods used for analysis of MIC-protein. The method consists of RBC precipitation, followed by strong base hydrolysis of MIC-tyrosine adducts from isolated hemoglobin to form PMC, rapid liquid-liquid extraction, and analysis via liquid chromatography tandem-MS analysis. The overall sample preparation and HPLC-MS/MS analysis time was approximately 4 hr, which is far shorter than MIH analysis methods or enzymatic digestion methods for analysis of MIC-protein adducts (Table 1.1). PMC was fully resolved from other components in the RBC matrix and showed excellent efficiency with a peak eluting at approximately 2.3 min.

Calibration curves for PMC were constructed within the concentration range 0.05–100  $\mu\text{M}$ . Using the inclusion criteria of  $100 \pm 15\%$  for accuracy and  $\leq 15\%$  for precision, the 0.05, 0.1 and 100, 200,  $\mu\text{M}$  calibrators fell outside the linear range. Therefore, the linear range was 0.2–50  $\mu\text{M}$  and was best described by a  $1/x^2$  weighted linear regression producing  $R^2 > 0.99$  and percent residual accuracy (PRA) of 96.4. The lower limit of quantification (LLOQ) and upper limit of quantification (ULOQ) were determined to be



0.2 and 50  $\mu\text{M}$ , respectively. The PRA values of all the calibration curves analyzed were  $\geq 90\%$ , indicating excellent fit of the data over the entire linear range (i.e., PRA values  $\geq 90\%$  are indicative of a good fit). The LOD (signal to noise = 3) was 0.02 mg/kg as validated by analysis of multiple lower concentrations of PMC-spiked RBC samples over a 3-day period.

### *2.3.5 Accuracy and precision*

The accuracy and precision of the method were established by quintuplicate analysis of three QC standards: low, medium, and high (0.3, 3, and 30  $\mu\text{M}$ ) on three days within 7 calendar days (Table 2.2). The precision and accuracy for the method was excellent over with interassay accuracies and precisions were within 4% of calibrators. The intraassay accuracies and precisions were also  $\leq 6\%$  and 7% of calibrators, respectively. Calibration curves were constructed on three different days to determine the repeatability of the calibration. As shown in Table 2.3, each of the three calibration curves consistently produced an  $R^2 > 0.999$  and consistent slopes over the 3 days (similar % RSD).

**Table 2. 3** Intra and interassay accuracy and precision of PMC produced by base hydrolysis of MIC-tyrosine adduct.

Nominal concentration ( $\mu\text{M}$ )	Intraassay accuracy (%) <sup>b</sup>			Intraassay precision (%CV) <sup>b</sup>			Interassay accuracy (%) <sup>a</sup>	Interassay precision (%RSD) <sup>a</sup>
	Day 1	Day 2	Day 3	Day 1	Day 2	Day 3		
0.3	100 $\pm$ 1.2	100 $\pm$ 0.6	100 $\pm$ 3.0	3.3	3.3	6.6	100 $\pm$ 1.2	< 3.4
3	100 $\pm$ 0.2	100 $\pm$ 0.3	100 $\pm$ 5.6	3.2	4.4	2.8	100 $\pm$ 0.2	< 3.2
30	100 $\pm$ 3.8	100 $\pm$ 1.7	100 $\pm$ 1.5	2	5.7	4.3	100 $\pm$ 3.8	< 2.0

<sup>a</sup> QC method validation (N = 5).<sup>b</sup> Mean of three different days of QC method validation (N = 15)**Table 2. 4** Calibration equations and coefficients of determination (R<sup>2</sup>) for calibration curves created over 3 days.

Day	Calibration Equation	R <sup>2</sup>	PRA <sup>a</sup>
1	$y = 70.353x + 20.039$	0.9992	96.7
2	$y = 68.883x + 4.683$	0.9996	97.6
3	$y = 64.753x + 14.395$	0.9998	97.2

### 2.3.6 Matrix effect and recovery

The matrix effect was assessed by comparing the slopes of standard curves of PMC in aqueous solution and rat RBC matrix. The value of the slope ratio (RBC matrix slope/aqueous slope) from the calibration curves was 0.85, indicating approximately about 15% suppression of PMC signals in rat RBC matrix. The recoveries for low, medium, and high QCs were 19.69%, 40.58%, and 41.09%, respectively. The loss of PMC during the sample preparation steps may be due to incomplete extraction of PMC from the RBC matrix into the organic layer. Since the % recovery value is the combination of matrix effect and recovery, the minor matrix effect in rat RBC does slightly contribute to recoveries <100%. To investigate the ability of the internal standard to correct for poor recovery, the internal standard was used to correct the signals for the recovery experiment. This correction drastically improved the results, with low (LQC), medium (MQC), and high QC (HQC) samples being 96.38%, 90.60% and 91.10% respectively. It is therefore highly recommended to use internal standard to correct for loss of PMC during sample preparation and matrix effects.

### 2.3.7 Stability of PMC and MIC-tyrosine adduct

To determine the stability of PMC spiked into rat RBC in the autosampler, samples (LQC and HQC) were placed in the autosampler after they went through the sample preparation steps and were analyzed after 0, 1, 2, 4, 8, 12 and 24 hr. PMC signals for both LQC and HQC samples were stable for all times tested. We also investigated the stability of the MIC-tyrosine adduct on the benchtop. This was achieved by spiking MIC directly onto isolated hemoglobin, shaking and storing on the benchtop. Samples were prepared and analyzed after 0, 1, 2, 4, 8, 12 and 24 hr of storage. Both LQC and HQC MIC-tyrosine

adduct were stable for the period tested. For long term stability, MIC-tyrosine adduct was stored at room temperature, 4 °C, -20 °C and -80 °C. Samples were prepared and analyzed after 0, 1, 2, 5, 15 and 30 days. At room temperature and 4 °C, samples were stable up to 5 and 15 days, respectively. However, at the lower temperatures (-20 °C and -80 °C), samples were stable at least 30 days (i.e., the longest time period tested). Based on the results of the stability studies, we suggest that when storage is necessary for more than 2 weeks, MIC-tyrosine samples should be stored at -20 °C or -80 °C.

### *3.8 Analysis of PMC from MIC-exposed animals and its correlation with MIC dose*

Correlation of PMC to MIC dose or exposure was first assessed by analyzing RBCs from rats (N = 44) dosed with different concentrations of MIC (i.e., 375 and 500 ppm) and non-exposed rats (i.e., naïve) to serve as a control group. The developed method for PMC was used to analyze the samples after preparation. PMC was detected in all groups (Figure 2.6). An analysis of variance with Dunn's multiple comparison test to determine significant differences between the groups was performed. Figure 2.6 results shows that there is significant difference between the different groups analyzed. While the actual inhaled dose of MIC cannot be conclusively measured, the relationship shown in Fig. 2.6 is very promising for the potential to use PMC as a biomarker to confirm MIC exposure.

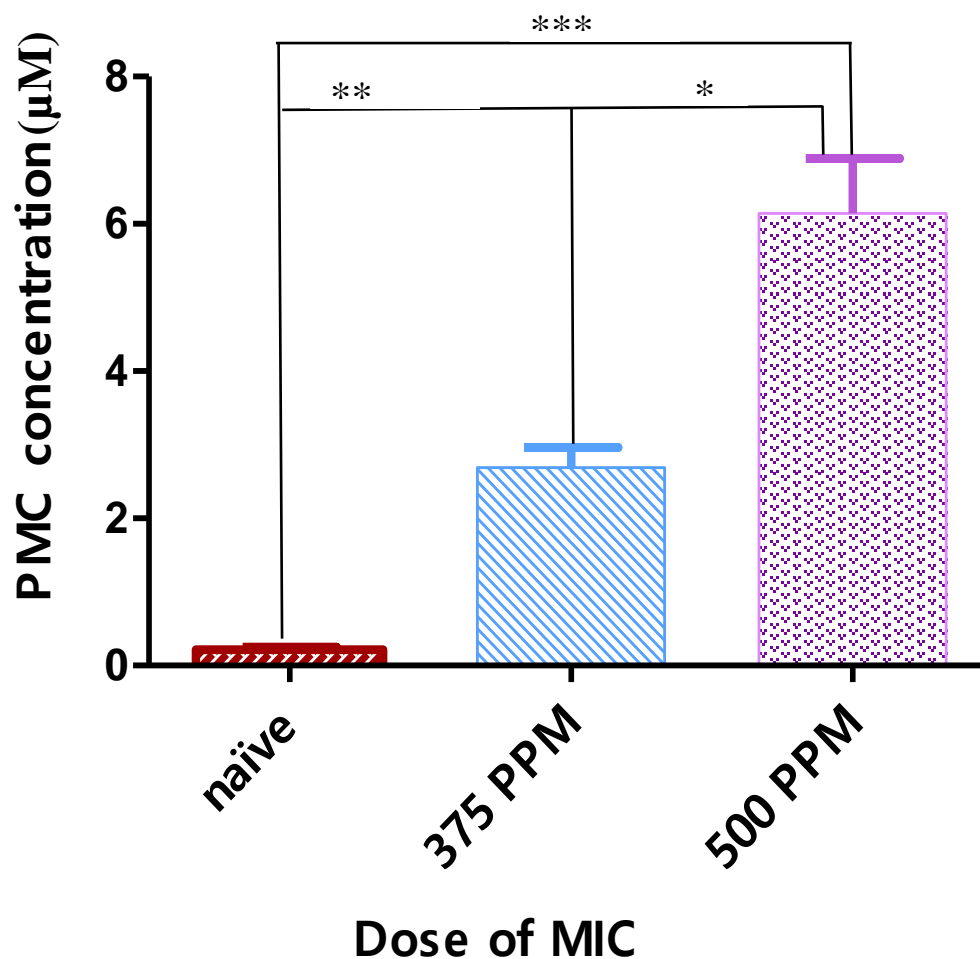


**Figure 2. 6** Correlation of MIC dose to concentration of PMC from exposed rats.

Error bar = standard error mean

\* = significant

\*\* = more significant

\*\*\* = most significant

#### 2.4 Conclusion

A novel MIC biomarker, PMC, was discovered based on the interaction between MIC and tyrosine. Using strong base hydrolysis of tyrosine adducts of MIC, a rapid and simple HPLC–MS/MS with excellent accuracy and precision was successfully developed. This method was able to quantify PMC from base hydrolysis of RBCs from rats exposed

to MIC. The detection of PMC from rats exposed to MIC reveals PMC as a promising biomarker for verification of MIC exposure.

### *2.5 Acknowledgements*

We gratefully acknowledge support from the CounterACT Program, National Institutes of Health Office of the Director, and the National Institute of Environmental Health Sciences (NIEHS), Grant number U54 ES027698 (CWW). The opinions or assertions contained herein are the private views of the authors and are not to be construed as official or as reflecting the views of the National Institutes of Health or the CounterACT Program.

## Chapter 3. Analysis Of Sodium 2-Mercaptoethane Sulfonate in Rat Plasma Using High Performance Liquid Chromatography Tandem-Mass Spectrometry

### 3.1. Introduction

The sodium salt of 2-mercaptoethane sulfonate (MESNA) is a thiol-containing drug used to combat urothelial toxicity in patients treated with antineoplastic drugs (e.g., ifosfamide and cyclophosphamide).<sup>(103, 104, 166-168)</sup> Specifically, some antineoplastic drugs produce toxic side products (e.g., acrolein). MESNA interacts with these metabolites to reduce their toxicity. Because it is important that a chemoprotective agent does not deactivate the potency of anti-cancer drugs, the inability of both MESNA and diMESNA (i.e., oxidized form of MESNA) to passively cross biological lipid membranes due to their hydrophilicity is advantageous since they do not enter cells to disrupt the mechanism of action of anti-cancer drugs.<sup>(103)</sup> Other uses of MESNA in the medical field include prevention of cisplatin-induced nephrotoxicity by locally reacting with cisplatin species in the kidneys<sup>(169-173)</sup> and scavenging reactive oxygen species (ROS) due to the ability of its thiol functional group to act as an antioxidant.<sup>(110, 126, 166, 174)</sup>

Due to the importance of MESNA in the medical field, several methods have been developed over the years for its bioanalysis, including colorimetry and high performance liquid chromatography (HPLC) methods using ultraviolet detection (UV),<sup>[17]</sup> fluorescence detection (FLD),<sup>[4]</sup> and electrochemical detection (ECD).<sup>(109)</sup> However, each of these methods has major limitations. Table 1 lists methods for the analysis of MESNA from biological matrices, along with important analytical characteristics. Ellman in 1959 reported the first analysis of MESNA by non-specific colorimetric assay. However the method was not selective enough to distinguish between MESNA and endogenous thiols

in biological samples, such as cysteine.<sup>(175)</sup> To address this limitation, several HPLC techniques were developed to more selectively analyze MESNA from biological samples.<sup>(175-179)</sup> An HPLC-UV technique using 2-chloro-1-methylquinolinium tetrafluoroborate for precolumn derivatization was reported by Glowacki *et al* in 2001.<sup>(178-180)</sup> The method produced excellent accuracy and precision, but suffered from small linear range. Moreover, the selectivity of the method for practical use was limited, with other thiol containing compounds from the biological sample producing similar retention times as MESNA. Verschraagen *et al.*<sup>(181)</sup> developed a micro-HPLC method using dual ECD with walled-jacked electrodes to selectively analyze MESNA. Although the method worked to selectively analyze MESNA, the recoveries were poor, the linear range was small, and the analysis time was lengthy. The method also produced poor sensitivity relative to other bioanalytical techniques for analysis of MESNA.<sup>(167, 182)</sup> Mare *et al.*<sup>(166)</sup> reported an HPLC-FLD method for analysis of MESNA from plasma and tissues but it requires long sample preparation steps making it inconvenient to analyze large number of samples<sup>(166, 183, 184)</sup>

Due to the drawbacks of the currently available bioanalytical methods, a highly robust and sensitive method for the analysis of MESNA in biological samples is needed. Therefore, the objective of the current study was to develop and validate an HPLC-MS/MS method to analyze MESNA from rat plasma.



**Table 3. 1** Comparison of bioanalytical methods for analysis of MESNA.

Reference	Year	Analytical method	Approximate sample preparation and analysis time (min)	R <sup>2</sup>	Precision (%RSD)	Accuracy (%)	LOD (nM)	Linearity (μM)
Ellman et al. <sup>(175)</sup>	1959	Ellman's free thiol assay	NR	NR	NR	NR	NR	NR
Glowacki et al. <sup>(178)</sup>	2001	HPLC-UV	NR	0.997	< 3%	100 ± 3	40	0.16-30
Verschraagen et al. <sup>(167)</sup>	2003	HPLC-ECD	45	0.999	< 5%	100 ± 6	NR	3–120
Mare et al. <sup>(166)</sup>	2005	HPLC-FLD	40	0.999	< 10%	100 ± 8.7	1.6	0.0025–2.5
Current technique	2021	HPLC-MS/MS	20	0.999	< 10%	100 ± 10	20	0.05–200

NR = not reported, HPLC = high performance liquid chromatography, UV = ultraviolet (detection), ECD = electrochemical detection, FLD = fluorescence detection, MS/MS = tandem mass spectrometry

## 3.2. Materials and Methods

### 3.2.1 Materials

All reagents and solvents were at least HPLC grade, unless otherwise stated. Ammonium formate was purchased from Sigma-Aldrich (St. Louis, MO, USA). Methanol and acetone (LC-MS grade) were obtained from Fisher Scientific (Hanover Park, IL, USA). MESNA (>98% purity) and the internal standard, sodium 3-mercapto-1-propane sulfonate (3-MPS, >90% purity), were purchased from Sigma-Aldrich (St. Louis, MO, USA). Water used for this study was purified by reverse osmosis and filtered through a Lab Pro polishing unit from Labconco (Kansas City, KS, USA). Stock solutions of MESNA and 3-MPS (10 mM) were prepared in water and stored at 4 °C. The stock solutions of MESNA and 3-MPS were freshly diluted to desired working solutions in water or plasma immediately prior to each experiment.

### 3.2.2. Biological Samples

Plasma from Wistar Hannover rats with 3.2% sodium citrate anticoagulant (0.2 µm filtered), was purchased from BioIVT for the analytical method development and validation. The plasma was stored at -80 °C until used. To evaluate the ability of the method to detect MESNA in the plasma of treated animals, plasma samples were obtained from MESNA-treated male Sprague-Dawley rats. For this experiment, male Sprague-Dawley rats were obtained from Charles River Laboratories and acclimated at the University of Colorado Denver-Anschutz Medical Campus (AAALAC International accredited) for at least 7 days prior to study. All procedures were approved by the UCD-AMC Institutional Animal Care and Use Committee. A pharmaceutical grade formulation of MESNA (Baxter Healthcare Corporation, NDC 10019-953-01) was administered to rats at 300 mg/kg by

intraperitoneal (IP) injection. Control animals received an equivalent volume (3 mL/kg) of saline (Hospira) containing 0.25 mg/mL EDTA (Sigma 03690) by IP injection. At various times following treatment (20 min, 1, 3, or 6 hr), rats were anesthetized by IP injection of a mixture of ketamine (75 mg/kg), xylazine (7.5 mg/kg), and acepromazine (1.5 mg/kg) for blood collection. Blood was collected from the abdominal aorta into 3.2% trisodium citrate anticoagulant (1:9 citrate: blood). Plasma was obtained by centrifugation of blood at 2050 x g for 15 minutes at 4 °C and subsequent transfer of plasma to a clean centrifuge tube (2 mL). The plasma was then flash frozen in liquid nitrogen and shipped on dry ice (overnight) to South Dakota State University. Upon receipt, the plasma was stored at -80 °C until analysis was performed.

### *3.2.3. Sample preparation for HPLC-MS/MS analysis*

To plasma samples (150 µL), internal standard (100 µL of 10 µM 3-MPS) was added and the mixture was vigorously stirred. Acetone (750 µL) was then added to the plasma to precipitate proteins. The sample was vortexed 3-4 times, and then cold centrifuged (-5 °C) at 13,000 rpm (12,300 × g) for 7 min. An aliquot (900 µL) of the supernatant was transferred into a 4-mL glass screw-top vial and dried at room temperature under nitrogen flow. After drying, the contents of the glass vial were reconstituted with 200 µL of HPLC mobile phase A (10 mM ammonium formate in water). The solution was thoroughly mixed, filtered with a 0.22-µm tetrafluoropolyethylene membrane syringe filter, and transferred into a 2-mL HPLC vial with glass insert (200-µL) for analysis.

### *3.2.4. HPLC-MS/MS Analysis*

HPLC was performed on a Shimadzu UFLC with model LC-20ADXR controller. The column used for chromatography was an Agilent polymeric reversed- phase column,

Zorbax eclipse-XDB C18 (4.6 × 150 mm, 5.0 μm, part #: PN 993967-902). The chromatographic separation was achieved using isocratic elution at a flow rate of 1 mL/min at 60% B (10 mM ammonium formate in methanol, 5:95) held constant for 5 min. The column was equilibrated for 1 min and 10 μL sample volume was injected for HPLC-MS/MS analysis.

For MS analysis, a tandem mass spectrometer (Sciex Q-Trap 5500 MS) equipped with an electrospray ionization interface in the negative polarity mode was used to detect MESNA. Optimization of MS conditions was accomplished by direct infusion of a standard solution of MESNA into the spectrometer at a flow rate of 10 μL/min. Nitrogen (50 psi) was used as the curtain and nebulization gas. The ion spray voltage was 4,500 V, the source temperature was 500 °C, and both the nebulizer (GS1) and heater (GS2) gas pressures were 90 psi. The collision cell was operated with an entrance potential of 10.0 V and an exit potential of 11.0 V at a “medium” collision gas flow rate. Multiple reaction monitoring mode (MRM) was used for MESNA analysis. Table 3.2 shows the MS/MS MRM operating parameters for the method. Data analysis was completed using the Analyst software program.

**Table 3. 2** MRM transitions, optimized collision energies (CEs), cell exit potentials (CXPs) and declustering potentials (DPs) for the detection of MESNA and 3-MPS by MS/MS analysis.

Compounds	Q1 (m/z)	Q3 (m/z)	Time (ms)	CE (V)	CXP(V)	DP (V)
MESNA (quantification)	140.40	79.9	100	-25.29	-9.27	-24.24
MESNA (identification)	140.40	138.9	100	-21.20	-9.00	-16.11
3-MPS (quantification)	154.70	80.0	100	-43.25	-14.09	-89.93
3-MPS (identification)	154.70	93.9	100	-24.10	-7.20	-51.02

### 3.2.5. Calibration, quantification, and limit of detection

The developed method was validated based on the bioanalytical method development guidelines provided by the Food and Drug Administration (FDA).<sup>(103, 161, 185)</sup> The limit of detection (LOD) of MESNA, which is described as the lowest concentration of MESNA that reproducibly produced a signal-to-noise (S/N) of 3, was obtained by analyzing multiple concentrations of MESNA in plasma below the lower limit of quantification (LLOQ) using the developed HPLC-MS/MS method. The noise was calculated as peak-to-peak noise in the blank samples over the retention time of MESNA.

To define the linear range and estimate the accuracy and precision of the method, stock solution of MESNA (10 mM) in water, was diluted in rat plasma to prepare the calibration standards (0.05, 0.1, 0.2, 0.5, 1, 2, 5, 10, 20, 50, 100 and 200  $\mu\text{M}$ ) and quality-control (QC) standards (3, 30, and 70  $\mu\text{M}$ ). The QC standard concentrations were not included in the calibration range. Each calibration standard was prepared in triplicate and QC standards were prepared in quintuplicate. The calibration curve was plotted using the average peak area signal ratios of MESNA to IS plotted as a function of calibrator concentration. Peak areas of MESNA and IS were obtained by manual integration. To obtain the linearity, accuracy, and precision of the calibration standards, both nonweighted and weighted ( $1/x$  and  $1/x^2$ ) calibration curves were constructed using linear least squares. Since the coefficient of variation ( $R^2$ ) does not accurately quantify goodness-of-fit (GOF) throughout the calibration range,<sup>(186)</sup> Percent Residual Accuracy (PRA) was used together with the coefficient of determination to determine GOF with PRA values  $\geq 90\%$  indicating an excellent fit.<sup>(162, 187)</sup> A weighted  $1/x^2$  fit was chosen as the best model to fit the calibration data based on  $R^2$  and PRA. The LLOQ and upper limit of quantification

(ULOQ) were determined using the inclusion criteria of <15% relative standard deviation (%RSD, as a measure of precision) and a percent error (as a measure of accuracy) of  $100\pm 15\%$ . The percent error was calculated based on the comparison of the MESNA concentration back-calculated from the calibration curve to the nominal MESNA concentration of the QC standard.

To evaluate the intraassay and interassay accuracy and precision of the method, quality control (QC) standards of 3  $\mu\text{M}$  (low QC), 30  $\mu\text{M}$  (medium QC), and 70  $\mu\text{M}$  (high QC) were analyzed over three days (within 5 calendar days). A calibration curve was constructed each day together with the QCs. Intraassay (within same day) precision and accuracy were calculated for each individual day, and interassay precision and accuracy were calculated by comparing the data gathered over three separate days (over 3 days within 5 calendar days).

### *3.2.6. Recovery, matrix effect, and selectivity*

Assay recovery of MESNA was determined by analyzing low, medium, and high QC standards of MESNA from spiked plasma and aqueous samples. Low, medium, and high QC standards were prepared in quintuplicate for both matrices. Recovery was determined as the percentage of the average analyte peak area from spiked plasma which went through the sample preparation procedure to the average peak area or signal ratio of aqueous QC standards containing MESNA reconstituted in mobile phase. Internal standard was not used to calculate recovery. The matrix effect for MESNA analysis was determined by comparing the slopes ( $m$ ) of calibration curves created in both aqueous and plasma matrices. The value of the slope ratio (plasma slope/aqueous slope) from the calibration curves was used to quantify the matrix effect. A slope ratio ( $m_{\text{plasma}}/m_{\text{aq}}$ ) equal to one

indicates the matrix does not affect the analysis. On the other hand,  $m_{\text{plasma}}/m_{\text{aq}}$  greater than one indicates multiplicative enhancement of the analyte in plasma, whereas slope ratio less than one indicates suppression of the analyte signal by plasma matrix. The efficacy of the IS to correct for the matrix effect was evaluated by comparing the ratio of  $m_{\text{plasma}}/m_{\text{aq}}$  of non-IS corrected calibration curves with the IS-corrected calibration curves. To evaluate the selectivity of the method, we confirmed the absence of interfering compounds via evaluation of prominent signals above the baseline in blanks over the retention time of MESNA by comparing several blank rat plasma and MESNA-spiked rat plasma samples.

### 3.2.7. Stability

The short- and long-term storage stability of MESNA were evaluated by analyzing low (LQC) and high QC (HQC) MESNA-spiked plasma samples stored at different temperatures and multiple storage times. The stability of MESNA was determined as a ratio of MESNA signal at time(t) to the signal at time “zero”, expressed as a percentage. MESNA was considered stable in plasma at a specific storage condition if the signal was within 10% of the initial signal. For short-term stability of MESNA, both low and high QCs were assessed over 24-hr, both in the autosampler (at 15 and 5°C) and on the benchtop (at room temperature). The autosampler stability was assessed twice on different days by placing triplicates of low and high QC on the autosampler of the HPLC at 15 and 5°C and analyzing them at approximately 0, 1.5, 2, 4, 8, 12 and 24 hr following preparation. Benchtop stability was evaluated by placing low and high QCs plasma samples on the benchtop (room temperature) for 0, 1, 2, 4, 8, 12 and 24 hr and analyzing them after each time point utilizing the procedure above (Section 3.2.3). The IS was added after storage and prior to sample preparation to correct for the day-to-day instrument signal variation.



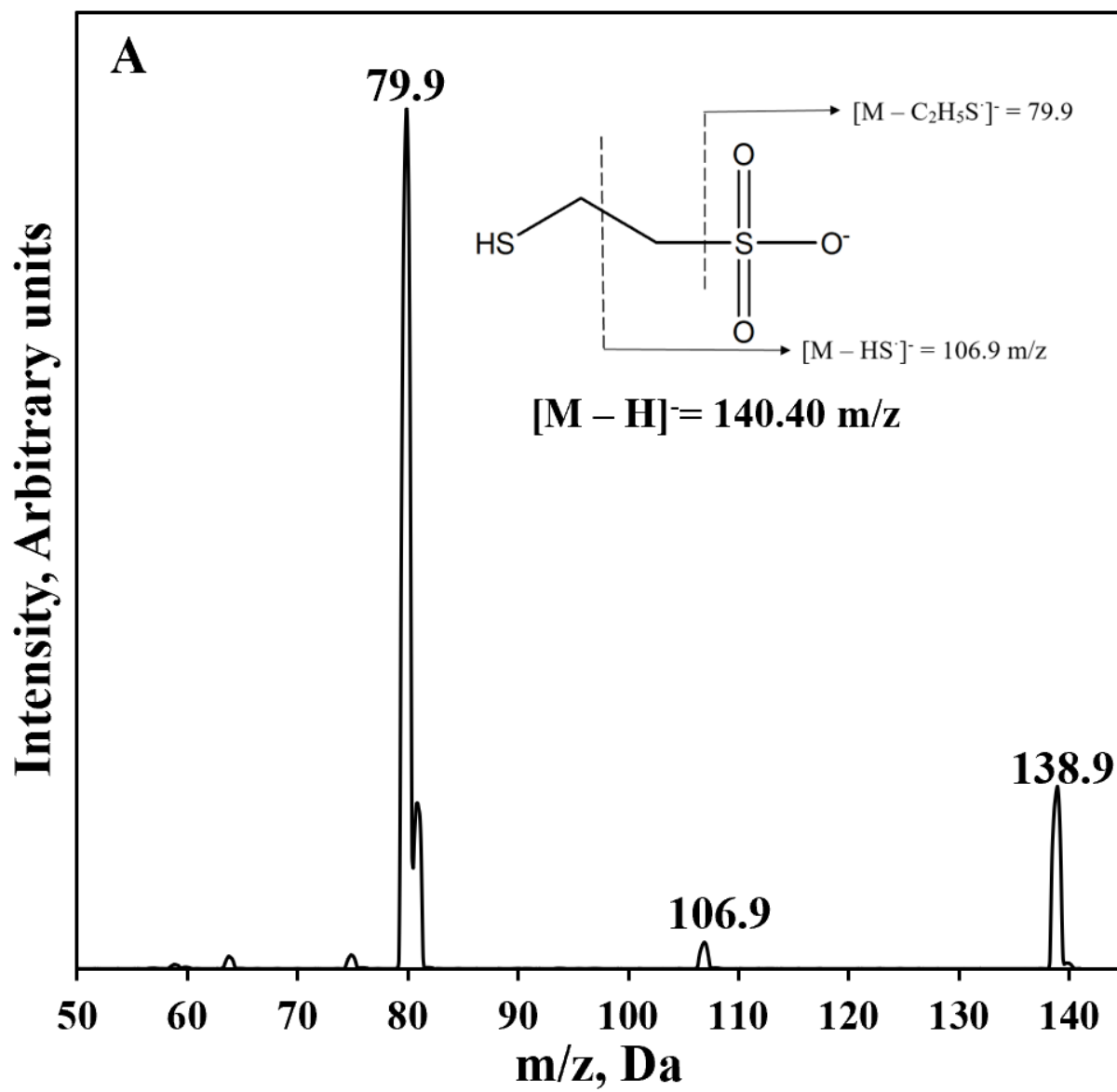
For freeze-thaw (FT) stability, four sets of LQCs and HQCs were prepared in triplicates without IS. One set of both QCs was analyzed in triplicate immediately, while the other sets were stored at -80 °C. For each cycle, all QC standards were thawed unassisted at room temperature. One set of the thawed QCs was analyzed in triplicate after adding IS to evaluate the first cycle FT stability and the remaining two sets of QCs were again stored at -80 °C. This procedure was repeated twice more to evaluate the remaining two freeze-thaw cycles. A total of three freeze-thaw cycles were evaluated. For the long-term stability studies, QC standards were stored at various storage conditions (-80, -20, 4 °C, and room temperature) and analyzed over 30 days (at 0, 1, 5, 10, 15, and 30 days). IS was added to each storage stability standard after storage to correct for day-to-day variation in instrument sensitivity.

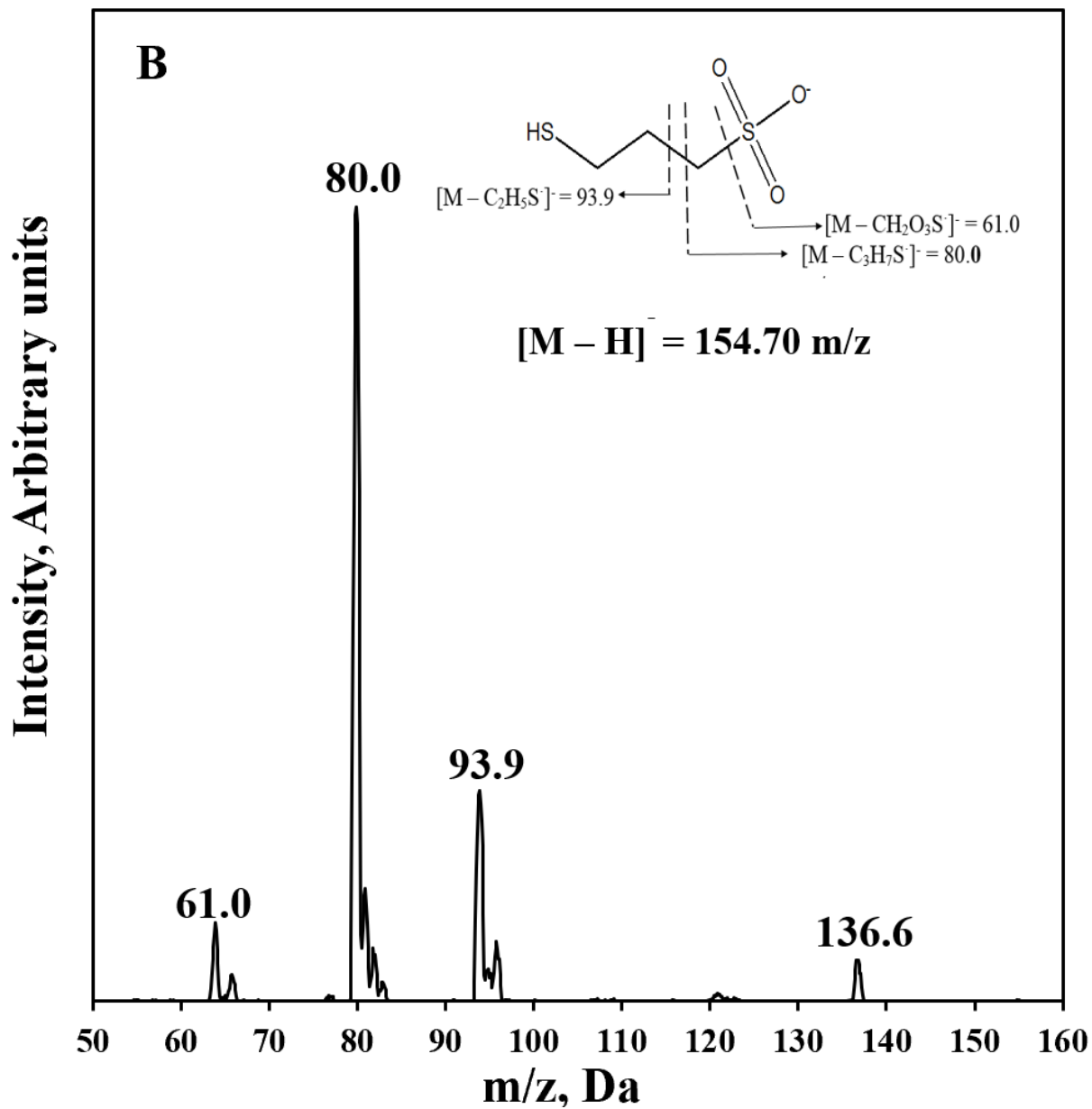
### **3.3. Results and Discussion**

#### *3.3.1. HPLC-MS/MS Analysis of MESNA*

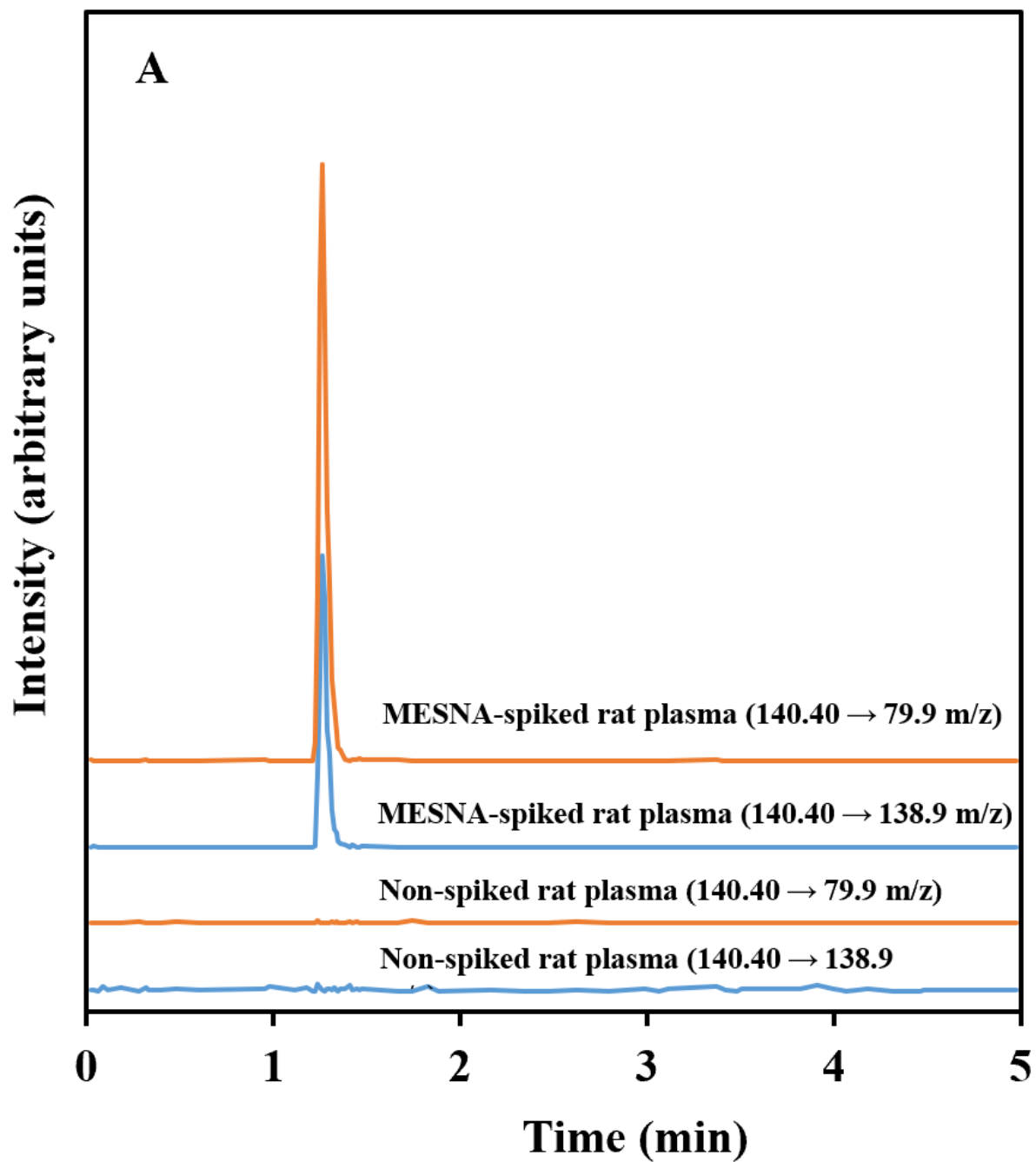
The HPLC-MS/MS method developed for analysis of MESNA from rat plasma features quick and simple sample preparation and analysis. The sample preparation is comprised of 4 simple steps: 1) protein precipitation, 2) centrifugation, 3) transfer and drying of the supernatant, and 4) reconstitution in aqueous mobile phase for HPLC-MS/MS analysis. This quick plasma sample preparation is vital to minimize the potential for conversion of MESNA to diMESNA. The simple sample preparation procedure also allows for analysis of about 90 samples within 24-h period compared to some existing methods. For example, Mare *et al.*<sup>(166)</sup> reports an HPLC-FLD method for MESNA utilizing derivatization with Thioglo TM 3 solution, but requires a 33 min sample preparation procedure and 7 mins analysis time. Verschraagen *et al.*<sup>(181)</sup> also reports an HPLC-ECD

method with sample preparation time of 35 min and chromatographic run time of 12.5 min.<sup>(181)</sup> Conversely, our method utilizes a shorter sample preparation and analysis time of 15 and 5 min respectively. The mass spectra of MESNA and 3-MPS produced by ESI (-)-MS with the most abundant ions identified are shown in Fig. 3.1A and B, respectively. The  $m/z$  ratios of 140.40 and 154.70 correspond to the molecular ions ( $[M-H]^-$ ) of MESNA and 3-MPS, respectively. For MESNA, the 140.40 $\rightarrow$ 79.9 and 140.40 $\rightarrow$ 138.9 transitions were selected as the quantification and identification transitions, respectively. For the internal standard, 3-MPS, the 154.70 $\rightarrow$ 80.0 and 154.70 $\rightarrow$ 138.9 transitions were selected as the quantification and identification transitions, respectively.





**Figure 3. 1** ESI (-) product ion mass spectra of MESNA (A) and 3-MPS (B) with identification of the abundant ions. Molecular ions of MESNA and 3-MPS  $[M-H]^-$  correspond to 140.40 and 154.70 m/z, respectively. Insets, structures of MESNA (A) and 3-MPS (B) with abundant fragments indicated.



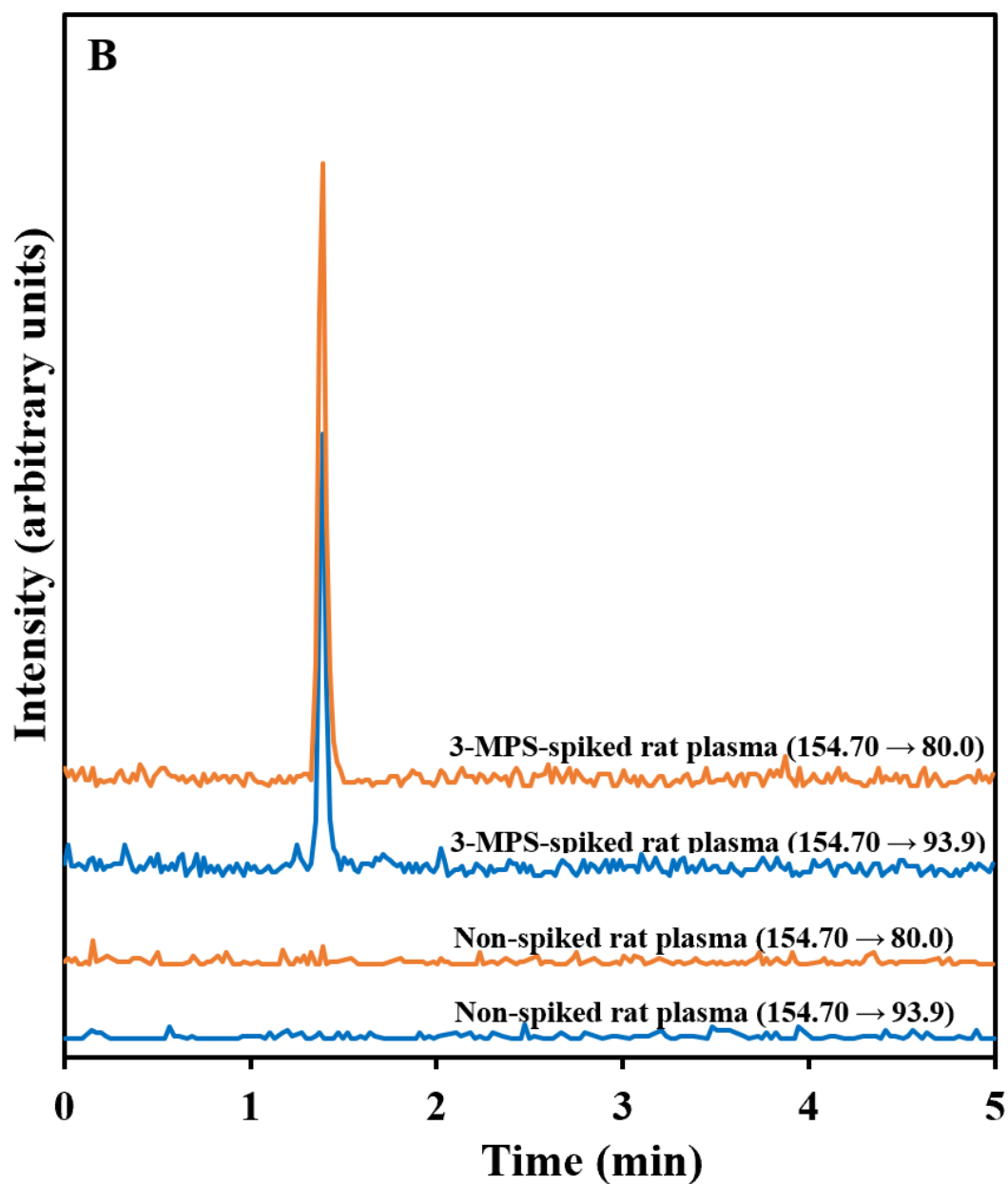


**Figure 3. 2** Representative HPLC-MS/MS chromatograms of spiked (5  $\mu$ M) and non-spiked MESNA and (B) 3-MPS (IS) in rat plasma. The chromatograms show signal response to the MRM transitions of MESNA (140.40  $\rightarrow$  79.9 and 140.40  $\rightarrow$  138.9 m/z) and 3-MPS (150  $\rightarrow$  80.0 and 154.70  $\rightarrow$  93.9 m/z).

HPLC-MS/MS chromatograms of MESNA and its internal standard, 3-MPS, prepared from spiked plasma are shown in Figures 3.2A and B, respectively. Both peaks

eluted at approximately 1.3 min. Our method produced excellent selectivity for both MESNA and 3-MPS with no other prominent peaks present in the chromatograms. The selectivity of the method addresses a disadvantage of multiple methods listed in table.

### *3.3.2. Linear range, calibration, and limit of detection*

The linearity of the method was determined by constructing calibration curves over the initial concentration range of 0.05–200  $\mu\text{M}$ . Based on the linear range inclusion criteria for accuracy and precision, the 0.05, 0.1 and 0.2  $\mu\text{M}$  calibrators were excluded. Thus, the linear range of the method was 0.5  $\mu\text{M}$  (LLOQ) to 200  $\mu\text{M}$  (ULOQ) as best defined by  $1/x^2$  weighted linear regression. All the calibrators within the linear range had individual PRAs >90% indicating an excellent GOF of the calibration equation for each calibrator. This linear range spanned over three orders of magnitude, which is outstanding for bioanalytical methods.<sup>(14, 188)</sup> This wide linear range is very beneficial when it comes to pharmacological studies where analysis of wide range of MESNA concentrations may be necessary. Additionally, the method showed an excellent LOD of 20 nM.

Calibration curves were constructed over a period of three days to determine the consistency of the calibration. As shown in Table 3.3, the  $R^2$  and PRAs were consistent and excellent. PRAs were >90% and  $R^2$  were >0.999 over the period of three days, but the calibration equation varied significantly. Therefore, the calibration curve should be prepared on the day of analysis.

**Table 3. 3** Linear equations, coefficients of determination ( $R^2$ ), and percent residual accuracy (PRA) for calibration curves created over 3 days.

Day	Equation	$R^2$	PRA (%)
1	$y = 10.0428x - 1.345$	0.9932	96
2	$y = 5.8609x - 0.970$	0.9943	93
3	$y = 9.9436x - 0.511$	0.9998	97



### 3.3.3. Accuracy and precision

The accuracy and precision of the method were estimated by quintuplicate analysis of low, medium, and high QCs on three different days within 5 calendar days (Table 3.4). The accuracy and precision of the method were excellent for all the 3 days tested. The intraassay and interassay accuracies were both  $100 \pm 10\%$  of the nominal QC concentrations. The accuracy and precision of the method were remarkable, with all QCs producing %RSDs  $< 10\%$  and accuracies of  $100 \pm 10\%$  while within the FDA-acceptable range for method validation from a biological matrix.<sup>(189-191)</sup>

**Table 3. 4** The intra- and interassay accuracies and precisions of MESNA analysis from spiked rat plasma by HPLC-MS/MS.

Conc ( $\mu$ M)	Intraassay						Interassay	
	Accuracy (%)			Precision (%RSD)			Accuracy (%) <sup>a</sup>	Precision (%RSD) <sup>a</sup>
	Day 1	Day 2	Day 3	Day 1	Day 2	Day 3		
3	100 $\pm$ 0.4	100 $\pm$ 2.0	100 $\pm$ 7.0	8.7	4.6	8.8	100 $\pm$ 7.0	<8.8
30	100 $\pm$ 5.9	100 $\pm$ 5.9	100 $\pm$ 3.2	9.0	8.6	4.2	100 $\pm$ 5.9	<9.0
70	100 $\pm$ 1.9	100 $\pm$ 9.6	100 $\pm$ 0.3	7.8	4.0	6.5	100 $\pm$ 9.6	<7.8

<sup>a</sup>Aggregate of three days of QC method validation (N = 15)

#### 3.3.4. Matrix effect, recovery, and stability

The evaluation of matrix effects reveals the direct or indirect alteration of response owing to the presence of interfering substances in the plasma matrix. To determine the effect of the plasma matrix on the analysis of MESNA, calibration curves were constructed in both plasma and aqueous samples. The slopes of standard curves of MESNA spiked in aqueous solutions and plasma ( $m_{\text{plasma}}/m_{\text{aq}}$ ) were compared to obtain the matrix effect value of 0.96, showing only a minor matrix effect for the analysis of MESNA in plasma. The recoveries for low, medium, and high QCs of MESNA in rat plasma were 90%, 91%, and 99% respectively. Addition of internal standard corrected for incomplete recoveries for low, medium, and high QCs to produce 97%, 95%, and 100% signal accuracy, respectively. Since the percent recovery determined in this manner is a combination of matrix effect and recovery. The minor matrix effect in rat plasma does slightly contribute to recoveries less than 100%.

For the benchtop stability, MESNA was stable in rat plasma for the 24-hr period tested. Conversely, MESNA was unstable in prepared samples after 2 hr in the autosampler at 15 °C. Moreover, while samples were stored on the autosampler at 15 °C, both MESNA and the IS signals were inconsistent, leading to the IS not correcting for the loss of MESNA. In an attempt to stabilize the MESNA and 3-MPS in the autosampler, the autosampler was cooled to 5 °C. At this temperature, the stability of MESNA was greatly improved with MESNA producing stable signals for at least 24 hr. Because the IS is added to samples prior to storage on the autosampler, the loss of MESNA signals in the autosampler at 15 °C may be due to the instability of the IS at higher temperatures or reaction of the IS with MESNA at 15 °C. For freeze-thaw stability, MESNA stability was excellent in plasma (-

80 °C) over the three freeze-thaw cycles evaluated with not more than 10% deviation from the control. The long-term stability of MESNA was evaluated at multiple storage temperatures. For MESNA samples stored at room temperature and 4 °C, stability was within 10% of the initial signals for 5 days and 2 weeks, respectively, and MESNA signals for both high and low QCs decreased rapidly after 15 days of storage for both storage conditions. Conversely, MESNA showed excellent stability (i.e., not more than 10% deviation from the control) in plasma when the sample was frozen (i.e., at both -20 °C and -80 °C) for at least 30 days (longest time period tested). This is consistent with the results obtained by Verschraagen *et al.*<sup>(192)</sup> who showed that MESNA stored at -20°C in deproteinized plasma was stable for at least 35 days. Overall, based on the results of the stability studies, we recommend that when storage is necessary, plasma samples should be stored at either -20 °C or -80 °C and can be thawed and refrozen at least three times for analysis. If samples are to be analyzed within 15 days, they can be stored at 4 °C. Once samples are prepared for the autosampler, they should be kept at 5 °C until analyzed.

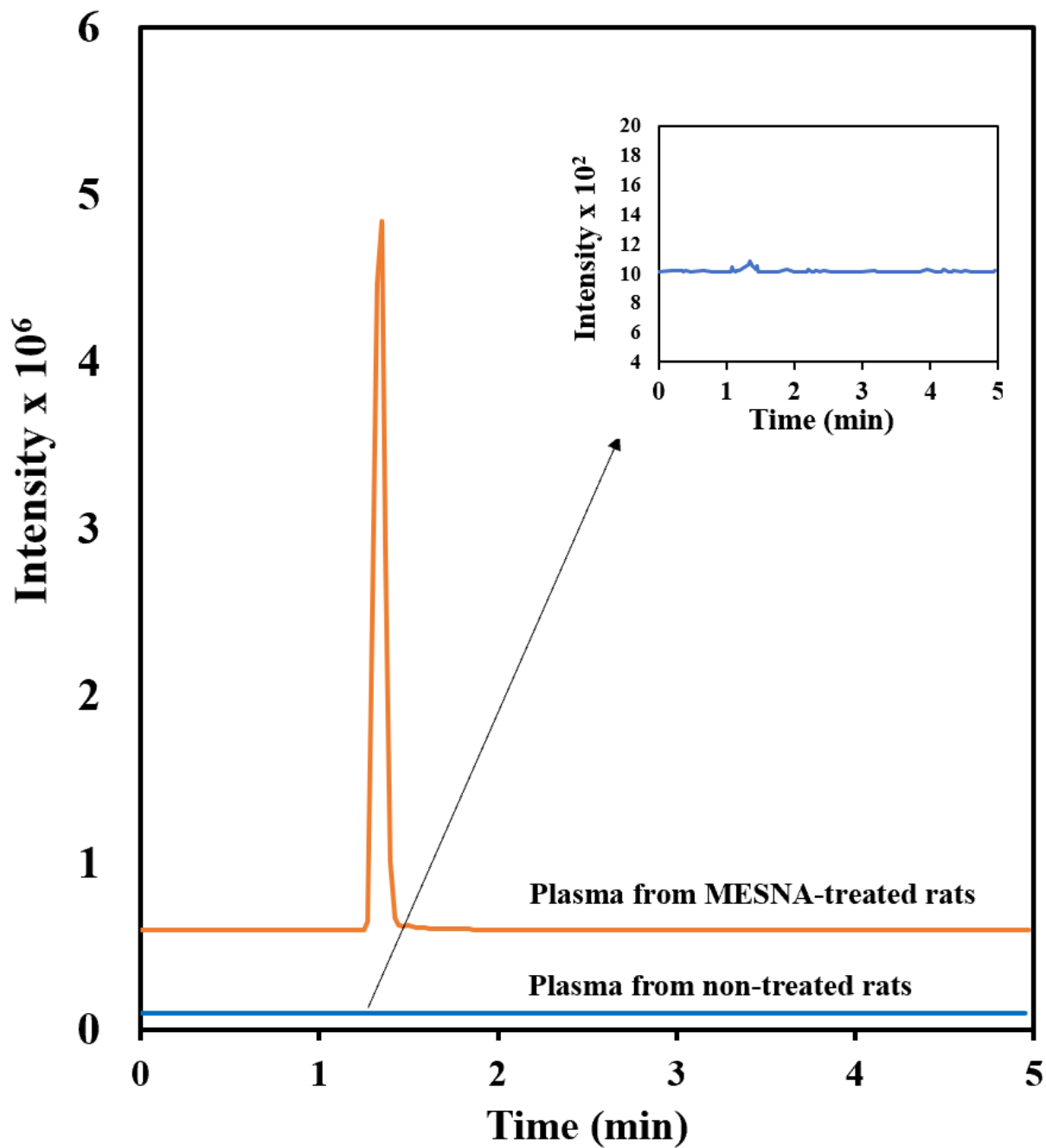


**Figure 3. 3** HPLC-MS/MS chromatogram from the plasma of MESNA-treated rats and rat plasma obtained prior to MESNA treatment. The chromatograms represent signal response to MRM quantification transition of MESNA (140.40  $\rightarrow$  79.9 m/z).

### *3.3.5. Analysis of MESNA in Treated Animals*

The developed method was used to analyze plasma from MESNA-treated rats at different time points. Chromatograms from HPLC-MS/MS analysis of the plasma of rats treated with MESNA and rat plasma obtained prior to treatment are shown in Figure 3.3. In the plasma of treated rats, MESNA was detected as a major peak eluting at 1.30 min. This result shows the applicability of the method for analysis of MESNA-treated animals, and consequently verified the selectivity and usefulness of the method for analysis of MESNA from rat plasma.

### **3.4. Conclusion**

A simple and sensitive HPLC-MS/MS method for the determination of MESNA in plasma was developed. The method presented was accurate and precise and showed the ability to analyze MESNA from plasma of treated animals. This technique will allow for simple and rapid analysis of MESNA for further development of this important therapeutic.

### **3.5. Acknowledgements**

We gratefully acknowledge support from the CounterACT Program, National Institutes of Health Office of the Director, and the National Institute of Environmental Health Sciences (NIEHS), Grant number U54 ES027698 (CWW). The opinions or assertions contained herein are the private views of the authors and are not to be construed as official or as reflecting the views of the National Institutes of Health or the CounterACT Program.

## **Chapter 4. Investigation of the Interaction between Sulfur Mustard Analogue, 2-Chloroethyl Ethyl Sulfide and Methimazole for Possible Reaction Product Formation**

### **4.1. Introduction**

Sulfur mustard (bis (2-chloroethyl) sulfide, (SM)) is a powerful bifunctional alkylating compound and a well-known vesicating (blistering) and warfare agent.<sup>(193-196)</sup> It causes severe damage to skin, eyes, and respiratory tract.<sup>(28, 197, 198)</sup> SM was first used during World War I and has since been used in several conflicts including the Iraq-Iran war in 1988 and Syria in 2019.<sup>(15, 199)</sup> It remains a major threat for use in battlegrounds and terrorist actions against both civilian and military targets because of its easy accessibility, inexpensive manufacture and storage, and lack of effective countermeasures against its toxicity.<sup>(200, 201)</sup> Besides the peril of SM being used in a possible warfare or terrorist attack, there is also a risk of accidental exposure due to the inappropriate disposal of old weaponry containing SM.<sup>(202)</sup>

Exposure to SM causes many devastating effects such as ocular and dermal injury, respiratory tract damage, reproductive and developmental toxicity, and gastrointestinal and hematological damage.<sup>(39)</sup> The vesicating effects of SM lead to inflammation and extensive blistering of the skin, an important primary target organ due its large surface area.<sup>(39, 194)</sup> In addition, SM is known as an efficient carcinogen in humans in relationship to its DNA damaging properties.<sup>(203)</sup> There has also been reports made on induction of internal cancers in humans exposed to SM.<sup>(203, 204)</sup> The toxicity of SM is attributed to its alkylating nature. SM undergoes intramolecular cyclization to form the electrophilic ethylene episulfonium intermediate and liberation of the free chloride ion.<sup>(193)</sup> The cyclic sulfonium ion, in turn,

alkylates many cellular macromolecules, including DNA, RNA, and proteins.<sup>(205)</sup> Also, SM can lead to the depletion of cellular glutathione (GSH) and antioxidant enzymes such as superoxide dismutase, catalase, and glutathione peroxidase, resulting in the accumulation of reactive oxygen species (ROS) followed by lipid peroxidation, protein oxidation, and eventually DNA damage.<sup>(61, 206)</sup> Due to the requirement of containment facilities for SM,<sup>(201, 207, 208)</sup> 2-chloroethyl ethyl sulfide (CEES; a monofunctional SM analog) is extensively used to study the mechanisms of SM-induced toxicity, including both direct and oxidative DNA damage.<sup>(195, 209, 210)</sup> Numerous studies have shown that CEES also alkylates nucleophilic groups in macromolecules and causes an increase in oxidative DNA damage, lipid peroxidation, protein oxidation, and ROS production, in both animal and cell culture<sup>(61, 211, 212)</sup>

Currently, there is no antidote for treating SM poisoning. Despite extensive research efforts, little progress has been made on developing effective treatment regimens, and victims often require extended hospitalization. More researched areas of therapeutics for SM poisoning includes biotherapy and transplantation. Even so, many of these proposed therapies have disadvantages like unwanted toxic effects and counterproductive biological impacts. Hence, strategies to ameliorate the effects of such an attack is critically important.<sup>(35, 213)</sup>

There is increasing evidence that a significant fraction of the SM dose remains biologically active within the victim's body for several days after exposure,<sup>(111, 214, 215)</sup> a window of opportunity exists to administer a "scavenger" to an affected individual instantly and in the days following exposure in hopes of reducing harm by neutralizing unreacted SM. For this strategy to be effectively implemented, it is essential to identify a



candidate compound with excellent affinity towards SM and very low toxicity. N-acetyl cysteine (NAC) and glutathione<sup>(62)</sup> have been tested as scavengers for SM toxicity due to their known antioxidant properties, biological prevalence, and potential scavenging ability but several studies concluded that their mechanism of action proceeds through pathways disparate to scavenging.<sup>(63)</sup>

Methimazole, an antithyroid drug has been use as a scavenger to combat the effects of sulfur mustard poisoning. Recent cell culture studies have shown that methimazole, is able to reduce cell death in CEES-affected cell lines when treated with methimazole. However, there are no studies on the mechanism underlying the scavenging ability of methimazole for CEES in preventing cell death. Due to the nucleophilicity of methimazole, we expect that it will react with CEES to form 2-(2-(ethylthio)ethylthio)-1-methyl-1H-imidazole (ETTMI) which in effect will prevent the action of CEES on affected areas. The aim of this research was to investigate the interactions between methimazole and CEES for a possible formation of 2-(2-(ethylthio)ethylthio)-1-methyl-1H-imidazole.

## **4.2 Materials and Methods**

### *4.2.1 Materials*

All reagents and solvents were at least HPLC grade, unless otherwise stated. Formic acid and acetonitrile were purchased from Fisher Scientific (Fair Lawn, NJ, USA). CEES and methimazole were purchased from Sigma-Aldrich. CEES stock solution (1 M) was prepared in anhydrous ethanol. Stock solution of methimazole (1M) was prepared in PBS buffer. All stock solutions were stored at 4 °C.

#### 4.2.2 Cell culture

Human keratinocyte epithelial HaCaT cells were cultured and used in this study. Briefly, HaCaT cells were grown in Dulbecco's modified Eagle's medium (DMEM) supplemented with 10% (v/v) fetal bovine serum (FBS), 100 U/mL penicillin, 10,000 µg/mL streptomycin and 0.5 µg/ml amphotericin B at 37 °C equilibrated with 5% (v/v) CO<sub>2</sub> in humidified air.

#### 4.2.3 MTT assay

HaCaT cells were seeded in 96-well plates at a density of 1.5-2.5 x 10<sup>4</sup> cells/100 µL cellular media per well. The plates were incubated overnight and treated with CEES (i.e., the SM stimulant), methimazole (i.e., the scavenger candidate) or both at the indicated working concentrations, eight wells per condition. CEES treatments were added within 15 s of mixing the treatment dilution in cell media to keep dosage effects consistent between trials, and methimazole treatments were added 15 s following CEES treatments to mimic a post-exposure response. CEES and methimazole concentration were (1 mM) and (2 mM) respectively following scavenger addition. Analysis was performed following incubation for 4, 8, 24, and 48 hr. To prevent unwanted reactions between the sulfur-containing scavengers and the MTT reagent, PBS (200 µL) was added to wash each well to remove scavenger molecules. The wells were subsequently filled with 100 µL/well of cell media and 20 µL/well of MTT reagent. Plates were incubated for 1.75-2 hr and cell lysates were collected for detection of ETTMI using HPLC-MS/MS.

#### 4.2.4 Sample Preparation

To CEES-methimazole cell lysate (900 µL), acetone (3 mL) was added to precipitate macromolecules. The sample was vortexed 3-4 times right away, and then

centrifuged at 2,000 rpm for 10 min. An aliquot of the supernatant (approximately 3 mL) was then transferred into a 4-mL glass screw-top vial and dried under nitrogen at room temperature. The dried samples were then reconstituted with 500  $\mu$ L of 70% aqueous acetonitrile, mixed thoroughly, filtered with a 0.22- $\mu$ m tetrafluoropolyethylene syringe filter, and analyzed using HPLC–MS/MS.

#### 4.2.5 HPLC-MS/MS analysis of ETTMI

Liquid chromatography analysis was performed on a Shimazu UFLC with LC-20ADXR controller. The column used for chromatography was an Agilent polymeric reversed-phase column, Zorbax eclipse-XDB C18 (4.6  $\times$  150 mm, 5.0  $\mu$ m, part #: PN 993967-902). The chromatographic separation was achieved using isocratic elution at a flow rate of 1 mL/min at 70% B held for 7 min. Mobile Phases A and B were 0.1% formic acid in water and acetonitrile, respectively. The column was equilibrated for 1 min and a sample volume of 10  $\mu$ L was injected for HPLC-MS/MS analysis. For MS analysis, a tandem mass spectrometer (Sciex Q-Trap 5500 MS) equipped with an electrospray ionization interface in the positive polarity mode was used to detect CEES-methimazole adduct. Optimization of mass spectrometric conditions was accomplished by direct infusion of a CEES-methimazole reaction solution into the spectrometer at a flow rate of 10  $\mu$ L/min. After infusion of CEES-methimazole adduct solution into the ESI, molecular ion of  $m/z$  204.30 ( $[M+H]^+$ ) was identified. Multiple reaction monitoring (MRM) parameters for ETTMI was optimized and are outlined in Table 4.1. Nitrogen (50 psi) was used as the curtain and nebulization gas. The ion spray voltage was 4,500 V, the source temperature was 500  $^{\circ}$ C and both the nebulizer (GS1) and heater (GS2) gas pressures were 90 psi. The collision cell was operated with an entrance potential of 10.0 V and an exit

potential of 11.0 V at a “medium” collision gas flow rate. The total mass spectrometry acquisition time was 7 min.

**Table 4. 1** MRM transitions, optimized collision energies (CEs), cell exit potentials (CXPs), and declustering potentials (DPs) for the detection of ETTMI by MS/MS analysis.

Compounds	Q1 (m/z)	Q3 (m/z)	Time (ms)	CE (V)	CXP(V)	DP (V)
ETTMI (quantification)	204.30	89	100	44.11	17.23	12.97
ETTMI (identification)	204.30	61	100	43.65	38.05	29.00

### 4.3. Results and Discussion

#### 4.3.1 Formation of 2-(2-(ethylthio)ethylthio)-1-methyl-1H-imidazole (ETTMI)

2-chloro-ethyl ethyl sulfide (CEES), the monofunctional analog of SM is a strong alkylating agent that alkylates macro molecules, especially DNA. Just like SM, CEES's strong electrophilic character confers on it a high affinity towards various nucleophilic molecules.<sup>(216)</sup> Methimazole is a distinctive scavenger that contains a thiodiamine functional group. Its central carbon is surrounded by two amine groups and a thiol. The thiodiamide functional group has the ability to tautomerize as well as has close proximity of multiple promising nucleophilic functional groups making it an excellent scavenger or molecule to react with CEES.<sup>(217)</sup>

In this study, we investigated the interaction between CEES and methimazole for a possible product formation. Methimazole's reaction with CEES forms ETTMI and prevents the alkylating action of CEES on cell lines which could result in cell death. Figure 4.1 shows the proposed reaction scheme for the reaction of CEES with methimazole to form ETTMI. In summary, the 2-chloroethyl side chain of CEES molecule undergoes intramolecular cyclization where the chlorine act as leaving group and a sulfonium ion is formed. The sulfonium cation then reacts with the nucleophilic sulfur group on methimazole to form ETTMI which prevents further action of CEES on the nucleophilic macromolecules.

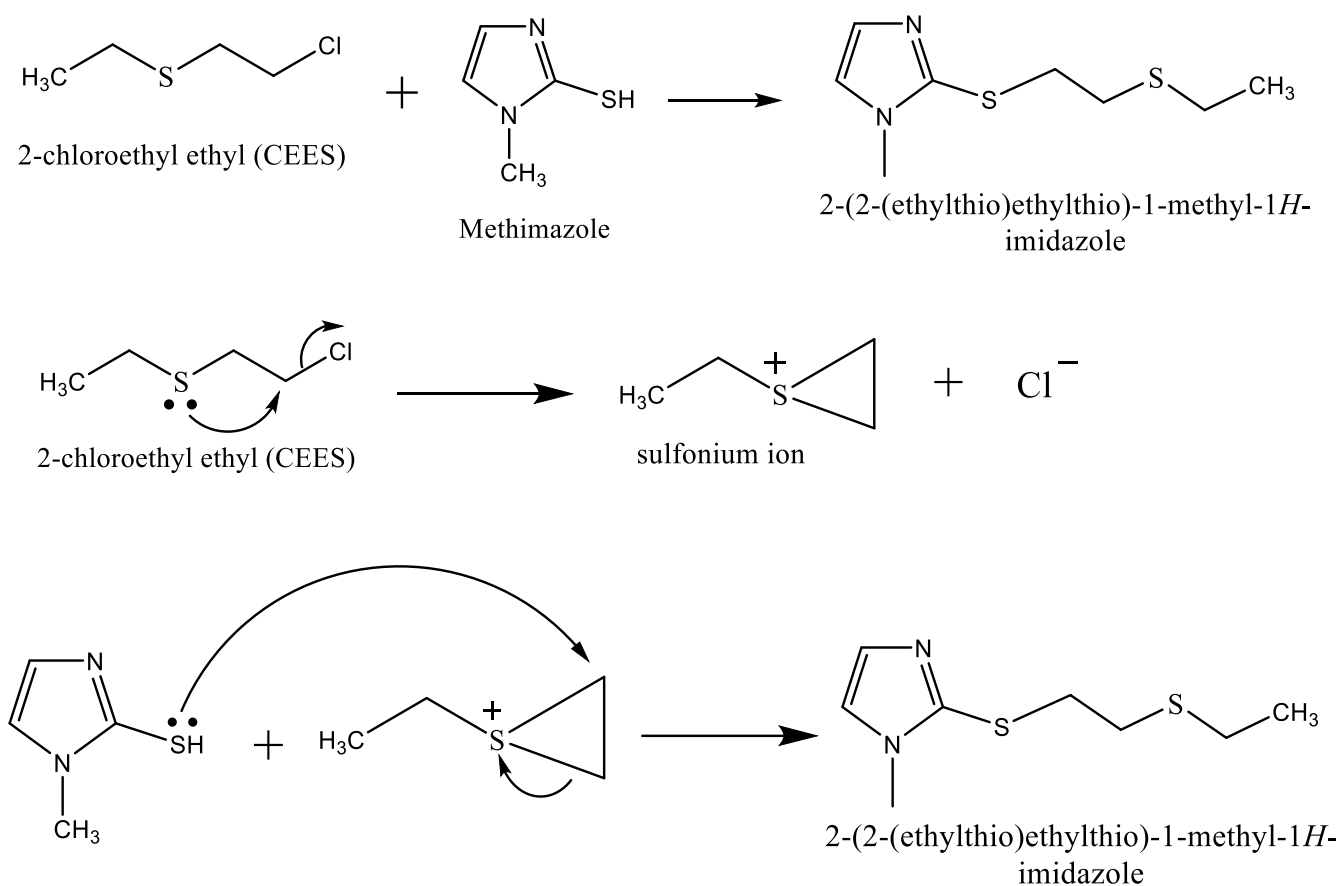


**Figure 4. 1** Reaction pathway for the formation of ETTMI from the reaction CEES with methimazole. CEES is proposed to react with methimazole to form 2-(2-(ethylthio)ethylthio)-1-methyl-1H-imidazole (ETTMI) which prevents the action of CEES on affected cells.

#### 4.3.2 Confirmation of the formation of CEES-methimazole adduct.

To confirm the formation of CEES-methimazole adduct from in-vitro samples, CEES-affected HaCat cell lines were treated with methimazole, and analytical methods were developed to detect the proposed reaction product. The mass spectra of ETTMI as shown in Figure 4.2 is produced by ESI (+)-MS with the molecular ion structure  $((M + H)^+$ ,  $m/z = 204.30$ ) and its abundant fragments identified. The optimized MS/MS parameters for the detection of ETTMI are shown in Table 1. Figure 4.3 shows the HPLC-MS/MS chromatograms of ETTMI analyzed from spiked cell culture media and cell lysate. ETTMI

was detected from both spiked media and cell lysates as shown in the chromatograms at about 1.25 min. Figure 4.4 shows the bar graphs of ETTMI detected from PBS buffer, media, and cell lysates at the different incubation periods. Comparing ETTMI from PBS buffer to media and cell lysates, we saw a greater formation (about 85%) of ETTMI from media and cell lysates indicating that methimazole reacts with CEES preferentially to components in the matrix. This was consistent at the different incubation periods. The detection of ETTMI from both spiked media and cell lysates at the different time points (4, 8, 12, and 24 hr) conclusively confirms the formation of a product from reaction between CEES and methimazole. This supports the reaction scheme shown in Figure 4.1 and confirms the scavenging ability of methimazole for CEES as a possible pathway for reversing the toxic effects of SM.



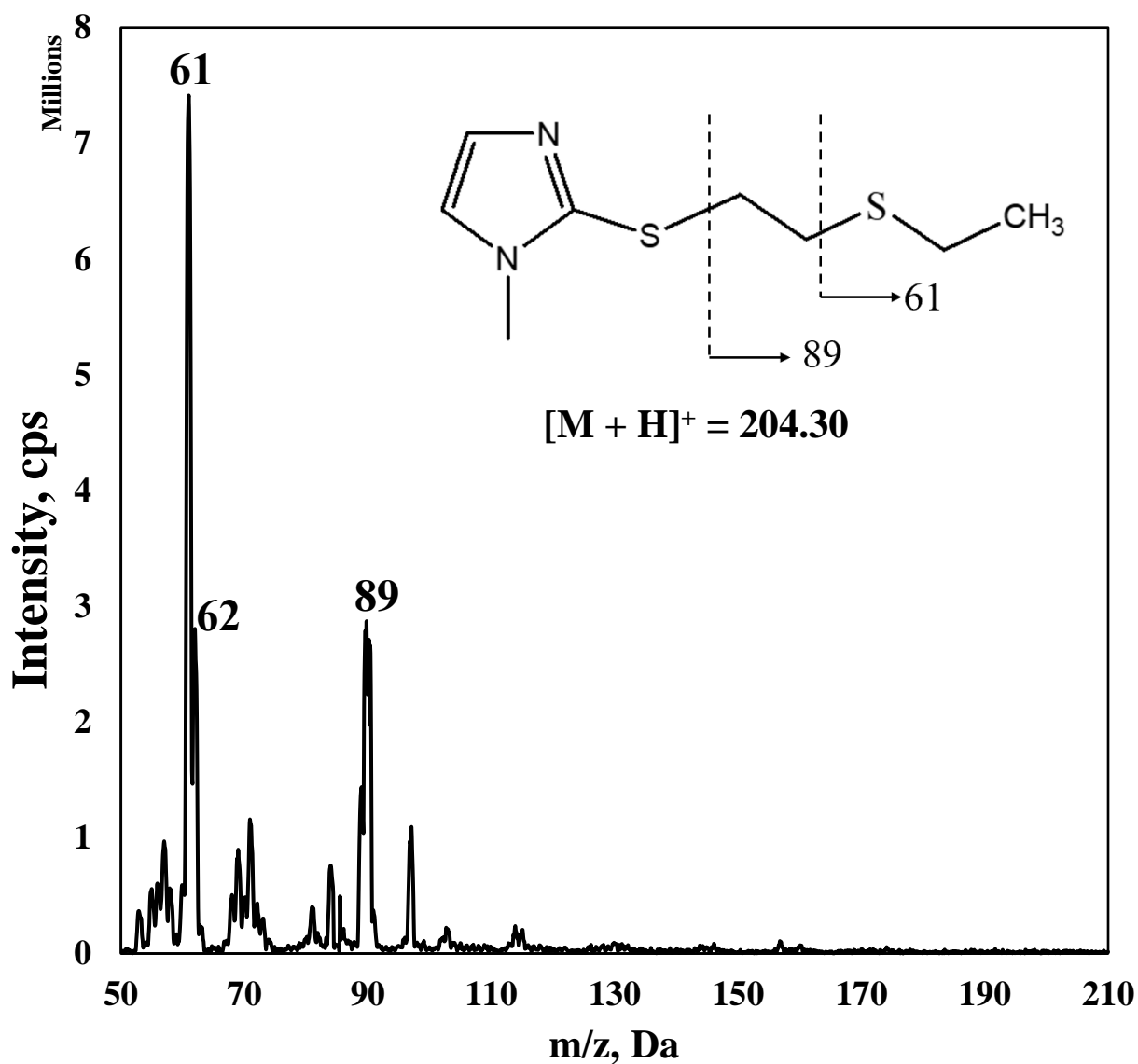


**Figure 4. 2** ESI (+) product ion mass spectra of with identification of the ETTMI abundant ions. Molecular ion of ETTMI [M+H]<sup>+</sup> corresponds to 204.30. Insets, structure of ETTMI with abundant fragments indicated.

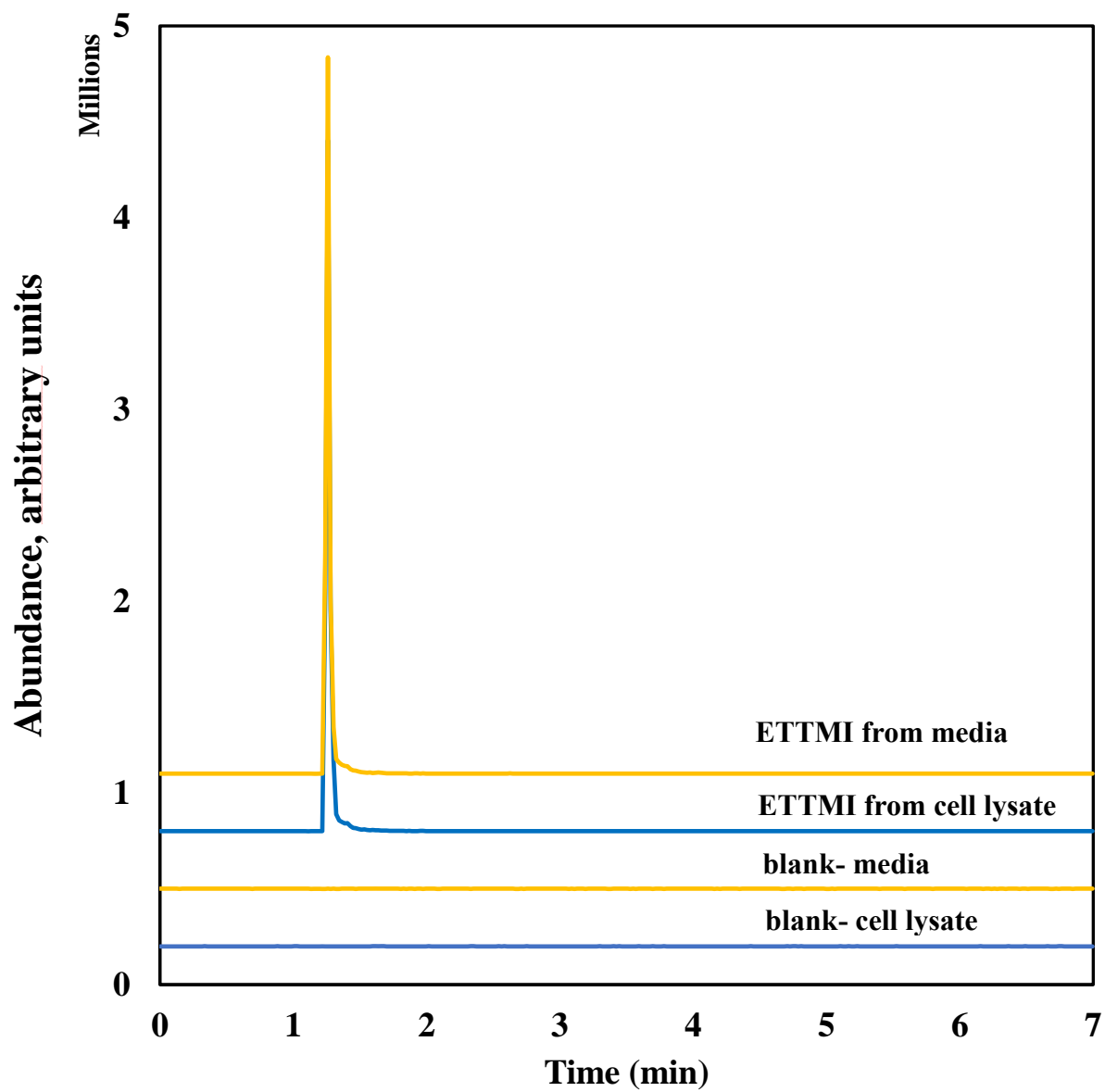


**Figure 4. 3** HPLC–MS–MS chromatograms ETTMI from spiked media and from cell lysates is presented.

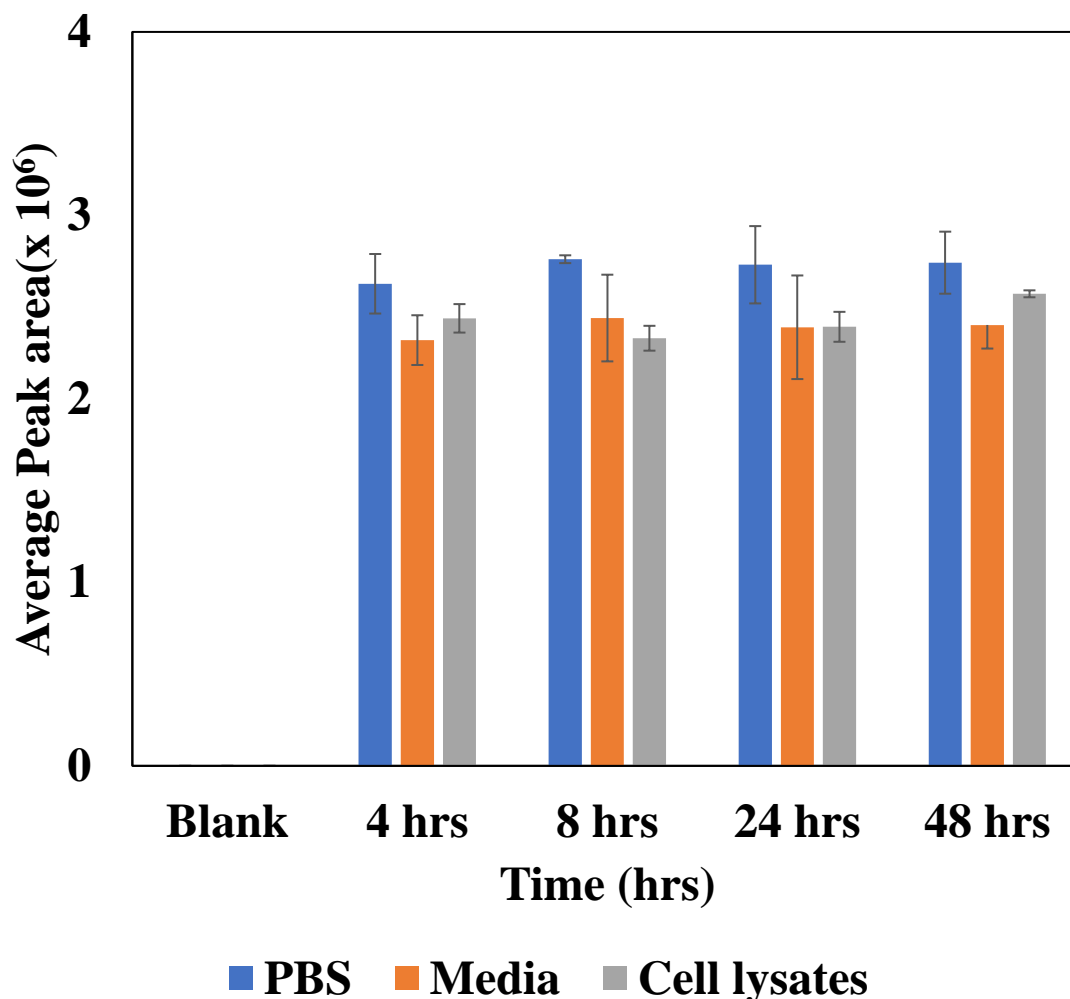


**Figure 4. 4** A bar graph showing the comparison of ETTMI from PBS buffer, media, and from cell lysates is presented.

#### 4.4 Conclusion

A new product formed from the reaction of CEES with methimazole was identified as ETTMI and an HPLC-MS/MS method for the analysis of the compound was developed. ETTMI was successfully detected from CEES-methimazole cell lysates, hence, one of the pathways by which methimazole scavenges CEES is by the formation of the compound, ETTMI thereby prevents CEES from alkylating macromolecules. This prevents the toxic effects posed by CEES in the in-vitro samples.

## **Chapter 5. Conclusions, Broader Impacts, And Future Work**

### **5.1 Conclusions**

A novel MIC-tyrosine adduct, PMC was found based on the interaction of tyrosine and MIC utilizing base hydrolysis and a simple HPLC-MS/MS method was successfully developed and validated to analyze the novel compound, PMC. The detection of PMC in both MIC-spiked rat Hb precipitate and Hb isolated from MIC exposed rats, indicates that PMC is a promising biomarker of MIC exposure. A novel compound ETTMI was identified based on the reaction of methimazole with CEES and an HPLC-MS/MS method was developed for its analysis. The detection ETTMI from invitro samples supports the chemical scavenging ability of methimazole for CEES. A simple and sensitive HPLC-MS/MS method for analysis of MESNA in plasma was successfully developed and validated. This will enhance further pharmacological studies.

### **5.2 Broader impacts**

Exposure to TIAs can cause a spectrum of adverse health effects that range from subclinical to immediately lethal. Hence development of technologies, research into methods to determine their exposure, and development of effective therapeutic agents are vital to combat the effects of TIAs exposure. The detection of the novel compound, PMC formed from strong base hydrolysis of MIC-tyrosine can serve as a promising biomarker of MIC exposure. It will also provide insights into sample preparation methods for MIC-Hb adducts. Additionally, detection of ETTMI from CEES-methimazole invitro samples could be used to characterize the chemical scavenging ability of methimazole as an antidote for sulfur mustard poisoning. Furthermore, the method for the analysis of MESNA showed

here will allow for further development of MESNA as a promising scavenger for MIC and sulfur mustard exposure and will enhance further pharmacological research.

### **5.3. Future work**

Future work should include the application of PMC method to analyze PMC from more animals exposed to MIC by IV and compare to exposure by inhalation. More animal studies should be performed to confirm the effectiveness of PMC as a diagnostic marker. Also, a pure standard of ETTMI should be synthesized for further validation of the developed method. Lastly, the developed method for MESNA should be applied to other matrices like urine, etc.

## References

1. Hayes A, Bakand S. Inhalation toxicology. Molecular, clinical and environmental toxicology. 2010;461-88.
2. Bessac BF, Jordt S-E. Sensory detection and responses to toxic gases: mechanisms, health effects, and countermeasures. Proceedings of the American Thoracic Society. 2010;7(4):269-77.
3. Guidotti TL. An international registry for toxic inhalation and pulmonary edema: notes from work in progress. International archives of occupational and environmental health. 1996;68(6):380-6.
4. Evans RB. Chlorine: state of the art. Lung. 2005;183(3):151-67.
5. Jackson R, Oda RP, Bhandari RK, Mahon SB, Brenner M, Rockwood GA, et al. Development of a fluorescence-based sensor for rapid diagnosis of cyanide exposure. Analytical chemistry. 2014;86(3):1845-52.
6. Logue BA, Zhang Z, Manandhar E, Pay AL, Croutch CR, Peters E, et al. Determination of methyl isopropyl hydantoin from rat erythrocytes by gas-chromatography mass-spectrometry to determine methyl isocyanate dose following inhalation exposure. Journal of Chromatography B. 2018;1093:119-27.
7. Mehta PS, Mehta AS, Mehta SJ, Makhijani AB. Bhopal tragedy's health effects: a review of methyl isocyanate toxicity. Jama. 1990;264(21):2781-7.
8. Goswami H. Cytogenetic effects of methyl isocyanate exposure in Bhopal. Human genetics. 1986;74(1):81-4.
9. Greskevitch M, Kullman G, Bang KM, Mazurek JM. Respiratory disease in agricultural workers: mortality and morbidity statistics. Journal of agromedicine. 2008;12(3):5-10.
10. Broughton E. The Bhopal disaster and its aftermath: a review. Environmental Health. 2005;4(1):1-6.
11. VARMA DF, MULAY S. The Bhopal accident and methyl isocyanate toxicity. Toxicology of Organophosphate & Carbamate Compounds. 2006:79-88.
12. Manandhar E, Pay A, Veress LA, Logue BA. Rapid analysis of sulfur mustard oxide in plasma using gas chromatography-chemical ionization-mass spectrometry for diagnosis of sulfur mustard exposure. Journal of Chromatography A. 2018;1572:106-11.
13. Greenfield RA, Slater LN, Bronze MS, Brown BR, Jackson R, Iandolo JJ, et al. Microbiological, biological, and chemical weapons of warfare and terrorism. The American journal of the medical sciences. 2002;323(6):326-40.
14. Gyamfi OA. Development of Analytical Methods for Toxic Inhaled Hazards (TIH) and Their Metabolites. 2020.
15. Noort D, Benschop H, Black R. Biomonitoring of exposure to chemical warfare agents: a review. Toxicology and applied pharmacology. 2002;184(2):116-26.
16. Urbanetti JS. Toxic inhalational injury. Medical aspects of chemical and biological warfare. 1917;41(2):247.

17. Moritz AR, Henriques Jr FC, McLean R. The effects of inhaled heat on the air passages and lungs: an experimental investigation. *The American journal of pathology*. 1945;21(2):311.
18. Balakrishnan C, Tijunelis A, Gordon D, Prasad J. Burns and inhalation injury caused by steam. *Burns*. 1996;22(4):313-5.
19. Stofer-Vogel B, Cerny T, Borner M, Lauterburg BH. Oral bioavailability of mesna tablets. *Cancer chemotherapy and pharmacology*. 1993;32(1):78-81.
20. Henry CR, Satran D, Lindgren B, Adkinson C, Nicholson CI, Henry TD. Myocardial injury and long-term mortality following moderate to severe carbon monoxide poisoning. *Jama*. 2006;295(4):398-402.
21. HECKERLING PS, LEIKIN JB, MATUREN A, PERKINS JT. Predictors of occult carbon monoxide poisoning in patients with headache and dizziness. *Annals of internal medicine*. 1987;107(2):174-6.
22. Richardson RS, Noyszewski EA, Saltin B, Gonzalez-Alonso J. Effect of mild carboxy-hemoglobin on exercising skeletal muscle: intravascular and intracellular evidence. *American Journal of Physiology-Regulatory, Integrative and Comparative Physiology*. 2002;283(5):R1131-R9.
23. Bessac BF, Sivula M, Von Hehn CA, Escalera J, Cohn L, Jordt S-E. TRPA1 is a major oxidant sensor in murine airway sensory neurons. *The Journal of clinical investigation*. 2008;118(5):1899-910.
24. Alarie Y. Irritating properties of airborne materials to the upper respiratory tract. *Archives of Environmental Health: An International Journal*. 1966;13(4):433-49.
25. Kuwabara Y, Alexeeff GV, Broadwin R, Salmon AG. Evaluation and application of the RD50 for determining acceptable exposure levels of airborne sensory irritants for the general public. *Environmental Health Perspectives*. 2007;115(11):1609-16.
26. Sidell FR, Takafuji ET, Franz DR. Medical aspects of chemical and biological warfare. OFFICE OF THE SURGEON GENERAL (ARMY) FALLS CHURCH VA; 1997.
27. Blewett W. Defense Against Mustard: A P2NBC2 Review and Analysis. Aberdeen Proving Ground, Md: Physical Protection Directorate; 1992.
28. Shohrati M, Davoudi M, Ghanei M, Peyman M, Peyman A. Cutaneous and ocular late complications of sulfur mustard in Iranian veterans. *Cutaneous and ocular toxicology*. 2007;26(2):73-81.
29. Namazi S, Niknahad H, Razmkhah H. Long-term complications of sulphur mustard poisoning in intoxicated Iranian veterans. *Journal of medical toxicology*. 2009;5(4):191.
30. Balalimoud M, Hefazi M. The clinical toxicology of sulfur mustard. 2005.
31. Kehe K, Balszuweit F, Emmeler J, Kreppel H, Jochum M, Thiermann H. Sulfur mustard research—strategies for the development of improved medical therapy. *Eplasty*. 2008;8.
32. Ghabili K, Agutter PS, Ghanei M, Ansarin K, Panahi Y, Shoja MM. Sulfur mustard toxicity: history, chemistry, pharmacokinetics, and pharmacodynamics. *Critical reviews in toxicology*. 2011;41(5):384-403.
33. Manandhar E. Analysis of Novel Cyanide Antidote Dimethyl Trisulfide for Pharmacokinetic Studies, and Sulfur Mustard Metabolites for Identification of Biomarker of Inhaled Dose. 2017.

34. Balali-Mood M, Hefazi M. Comparison of early and late toxic effects of sulfur mustard in Iranian veterans. *Basic & clinical pharmacology & toxicology*. 2006;99(4):273-82.
35. Drasch G, Kretschmer E, Kauert G, Von Meyer L. Concentrations of mustard gas [bis (2-chloroethyl) sulfide] in the tissues of a victim of a vesicant exposure. *Journal of Forensic Science*. 1987;32(6):1788-93.
36. Smith KJ, Hurst CG, Moeller RB, Skelton HG, Sidell FR. Sulfur mustard: its continuing threat as a chemical warfare agent, the cutaneous lesions induced, progress in understanding its mechanism of action, its long-term health effects, and new developments for protection and therapy. *Journal of the American Academy of Dermatology*. 1995;32(5):765-76.
37. Hambrook J, Howells D, Schock C. Biological fate of sulphur mustard (1, 1'-thiobis (2-chloroethane)): uptake, distribution and retention of <sup>35</sup>S in skin and in blood after cutaneous application of <sup>35</sup>S-sulphur mustard in rat and comparison with human blood in vitro. *Xenobiotica*. 1993;23(5):537-61.
38. Cullumbine H. Medical aspects of mustard gas poisoning. *Nature*. 1947;159(4031):151-3.
39. Graham JS, Chilcott RP, Rice P, Milner SM, Hurst CG, Maliner BI. Wound healing of cutaneous sulfur mustard injuries: strategies for the development of improved therapies. *Journal of burns and wounds*. 2005;4.
40. Kehe K, Szinicz L. Medical aspects of sulphur mustard poisoning. *Toxicology*. 2005;214(3):198-209.
41. Sezigen S, Ivelik K, Ortatatli M, Almacioglu M, Demirkasimoglu M, Eyison R, et al. Victims of chemical terrorism, a family of four who were exposed to sulfur mustard. *Toxicology letters*. 2019;303:9-15.
42. Kehe K, Thiermann H, Balszuweit F, Eyer F, Steinritz D, Zilker T. Acute effects of sulfur mustard injury—Munich experiences. *Toxicology*. 2009;263(1):3-8.
43. Meisenberg BR, Melaragno AJ, Monroy RL. Granulocyte colony stimulating factor (G-CSF) for mustard-induced bone marrow suppression. *Military medicine*. 1993;158(7):470-4.
44. Anderson DR, Taylor SL, Fetterer DP, Holmes WW. Evaluation of protease inhibitors and an antioxidant for treatment of sulfur mustard-induced toxic lung injury. *Toxicology*. 2009;263(1):41-6.
45. Pechura CM, Rall DP. Chemistry of sulfur mustard and lewisite. *Veterans at Risk: The Health Effects of Mustard Gas and Lewisite*. 1993.
46. Vogt Jr RF, Dannenberg Jr AM, Schofield BH, Hynes NA, Papirmeister B. Pathogenesis of skin lesions caused by sulfur mustard. *Toxicological Sciences*. 1984;4(2part2):71-83.
47. Papirmeister B, Gross CL, Petrali JP, Meier HL. Pathology produced by sulfur mustard in human skin grafts on athymic nude mice. II. Ultrastructural changes. *Journal of Toxicology: Cutaneous and Ocular Toxicology*. 1984;3(4):393-408.
48. Wheeler GP. Studies related to the mechanisms of action of cytotoxic alkylating agents: a review. *Cancer research*. 1962;22(6):651-88.
49. Xu H, Nie Z, Zhang Y, Li C, Yue L, Yang W, et al. Four sulfur mustard exposure cases: Overall analysis of four types of biomarkers in clinical samples provides positive



implication for early diagnosis and treatment monitoring. *Toxicology reports*. 2014;1:533-43.

50. Black R, Brewster K, Clarke R, Hambrook J, Harrison J, Howells D. Biological fate of sulphur mustard, 1, 1'-thiobis (2-chloroethane): isolation and identification of urinary metabolites following intraperitoneal administration to rat. *Xenobiotica*. 1992;22(4):405-18.
51. Black R, Hambrook J, Howells D, Read R. Biological fate of sulfur mustard, 1, 1'-thiobis (2-chloroethane). Urinary excretion profiles of hydrolysis products and  $\beta$ -lyase metabolites of sulfur mustard after cutaneous application in rats. *Journal of analytical toxicology*. 1992;16(2):79-84.
52. Davison C, Rozman RS, Smith PK. Metabolism of bis- $\beta$ -chloroethyl sulfide (sulfur mustard gas). *Biochemical pharmacology*. 1961;7(1):65-74.
53. Fidler A, Noort D, de Jong AL, Trap HC, de Jong LP, Benschop HP. Monitoring of in vitro and in vivo exposure to sulfur mustard by GC/MS determination of the N-terminal valine adduct in hemoglobin after a modified Edman degradation. *Chemical research in toxicology*. 1996;9(4):788-92.
54. Yue L, Wei Y, Chen J, Shi H, Liu Q, Zhang Y, et al. Abundance of Four Sulfur Mustard-DNA Adducts ex Vivo and in Vivo Revealed by Simultaneous Quantification in Stable Isotope Dilution-Ultrahigh Performance Liquid Chromatography-Tandem Mass Spectrometry. *Chemical research in toxicology*. 2014;27(4):490-500.
55. Sugendran K, Kumar P, Vijayaraghavan R. Treatment for sulphur mustard poisoning-A review. *Defence Science Journal*. 1998;48(2):155.
56. Weibrecht K, Rhyee S, Manuell ME, Longo C, Boyer EW, Brush E. Sulfur mustard exposure presenting to a community emergency department. *Annals of emergency medicine*. 2012;59(1):70-4.
57. Borak J, Sidell FR. Agents of chemical warfare: sulfur mustard. *Annals of emergency medicine*. 1992;21(3):303-8.
58. Houin PR, Veress LA, Rancourt RC, Hendry-Hofer TB, Loader JE, Rioux JS, et al. Intratracheal heparin improves plastic bronchitis due to sulfur mustard analog. *Pediatric pulmonology*. 2015;50(2):118-26.
59. Jacobson AF, Marks MA, Kaplan WD. Increased lung uptake on technetium-99m-sulfur colloid liver-spleen scans in patients with hepatic venoocclusive disease following bone marrow transplantation. *Journal of nuclear medicine: official publication, Society of Nuclear Medicine*. 1990;31(3):372-4.
60. Nejad-Moghaddam A, Panahi Y, Alitappeh MA, Borna H, Shokrgozar MA, Ghanei M. Therapeutic potential of mesenchymal stem cells for the treatment of airway remodeling in pulmonary diseases. *Iranian Journal of Allergy Asthma and Immunology*. 2015;14(6):552-68.
61. Paramov V, Suntres Z, Smith M, Stone WL. Sulfur mustard toxicity following dermal exposure: role of oxidative stress, and antioxidant therapy. *Journal of burns and wounds*. 2007;7.
62. Siegert M, Kranawetvogl A, Thiermann H, John H. N-Acetylcysteine as a chemical scavenger for sulfur mustard: New insights by mass spectrometry. *Drug testing and analysis*. 2018;10(2):243-53.

63. Siegert M, Kranawetvogl A, Thiermann H, John H. Glutathione as an antidote for sulfur mustard poisoning: mass spectrometric investigations of its potency as a chemical scavenger. *Toxicology letters*. 2018;293:31-7.
64. Powell KL, Boulware S, Thames H, Vasquez KM, MacLeod MC. 2, 6-Dithiopurine blocks toxicity and mutagenesis in human skin cells exposed to sulfur mustard analogues, 2-chloroethyl ethyl sulfide and 2-chloroethyl methyl sulfide. *Chemical research in toxicology*. 2010;23(3):497-503.
65. Romano Jr JA, King JM. *Chemical warfare and chemical terrorism: psychological and performance outcomes*: Psychology Press; 2014.
66. Jayaraman K. *Toxic gas: Pesticide plant leak wreaks disaster in India*. Nature Publishing Group; 1984.
67. McConnell EE, Bucher JR, Schwetz BA, Gupta BN, Shelby MD, Luster MI, et al. Toxicity of methyl isocyanate. *Environmental science & technology*. 1987;21(2):188-93.
68. Gupta G, Kaw J, Naqvi SH, Dixit R, Ray P. Inhalation toxicity of methyl isocyanate: biochemical and cytological profile of bronchoalveolar lavage fluid in rats. *Journal of applied toxicology*. 1991;11(3):157-60.
69. Keen C, Coldwell M, McNally K, Baldwin P, McAlinden J, Cocker J. A follow up study of occupational exposure to 4, 4'-methylene-bis (2-chloroaniline)(MbOCA) and isocyanates in polyurethane manufacture in the UK. *Toxicology letters*. 2012;213(1):3-8.
70. Williams M, Todd GD, Pohl HR, Taylor J, Ingerman L, Carlson-Lynch H, et al. *Toxicological profile for toluene diisocyanate and methylenediphenyl diisocyanate*. 2018.
71. Council NR. *The use and storage of methyl isocyanate (MIC) at bayer CropScience*: National Academies Press; 2012.
72. Dhara VR, Kriebel D. *The Bhopal gas disaster: it's not too late for sound epidemiology*. Taylor & Francis; 1993.
73. Senthilkumar CS, Sah NK, Ganesh N. Methyl isocyanate and carcinogenesis: bridgeable gaps in scientific knowledge. *Asian Pacific Journal of Cancer Prevention*. 2012;13(6):2429-35.
74. Vijayan V. Methyl isocyanate (MIC) exposure and its consequences on human health at Bhopal. *International journal of environmental studies*. 2010;67(5):637-53.
75. Quint J, Beckett WS, Campleman SL, Sutton P, Prudhomme J, Flattery J, et al. Primary prevention of occupational asthma: identifying and controlling exposures to asthma-causing agents. *American journal of industrial medicine*. 2008;51(7):477-91.
76. Kimmerle G, Eben A. Toxicity of methylisocyanate and how to determine its quantity in air. *Arch Toxikol*. 1964;20:235-41.
77. Brown WE, Green AH, Cedel TE, Cairns J. Biochemistry of protein-isocyanate interactions: a comparison of the effects of aryl vs. alkyl isocyanates. *Environmental health perspectives*. 1987;72:5-11.
78. Angerer J, GoËen T, KraËmer A, KÄfferlein HU. N-methylcarbamoyl adducts at the N-terminal valine of globin in workers exposed to N, N-dimethylformamide. *Archives of toxicology*. 1998;72(5):309-13.
79. Ramachandran P, Gandhe B, Venkateswaran K, Kaushik M, Vijayaraghavan R, Agarwal G, et al. Gas chromatographic studies of the carbamylation of haemoglobin by methyl isocyanate in rats and rabbits. *Journal of Chromatography B: Biomedical Sciences and Applications*. 1988;426:239-47.

80. Cantin A, North S, Hubbard R, Crystal R. Normal alveolar epithelial lining fluid contains high levels of glutathione. *Journal of applied physiology*. 1987;63(1):152-7.
81. Pearson PG, Slatter JG, Rashed MS, Han D-H, Grillo MP, Baillie TA. S-(N-methylcarbamoyl) glutathione: a reactive S-linked metabolite of methyl isocyanate. *Biochemical and biophysical research communications*. 1990;166(1):245-50.
82. Slatter JG, Rashed MS, Pearson PG, Han DH, Baillie TA. Biotransformation of methyl isocyanate in the rat. Evidence for glutathione conjugation as a major pathway of metabolism and implications for isocyanate-mediated toxicities. *Chemical research in toxicology*. 1991;4(2):157-61.
83. Pearson PG, Slatter JG, Rashed MS, Han DH, Baillie TA. Carbamoylation of peptides and proteins in vitro by S-(N-methylcarbamoyl) glutathione and S-(N-methylcarbamoyl) cysteine, two electrophilic S-linked conjugates of methyl isocyanate. *Chemical research in toxicology*. 1991;4(4):436-44.
84. Brochhagen F. Isocyanates. *Anthropogenic Compounds*: Springer; 1991. p. 1-95.
85. Rye WA. Human responses to isocyanate exposure. *Journal of Occupational and Environmental Medicine*. 1973;15(3):306-7.
86. Varma D, Ferguson J, Alarie Y. Reproductive toxicity of methyl isocyanate in mice. *Journal of Toxicology and Environmental Health, Part A Current Issues*. 1987;21(3):265-75.
87. Padilla RE. Pulmonary toxic agents. *Physician's Guide to Terrorist Attack*: Springer; 2004. p. 253-61.
88. Alarie Y, Ferguson J, Stock M, Weyel D, Schaper M. Sensory and pulmonary irritation of methyl isocyanate in mice and pulmonary irritation and possible cyanidelike effects of methyl isocyanate in guinea pigs. *Environmental health perspectives*. 1987;72:159-67.
89. Boorman G, Brown R, Gupta B, Uraih L, Bucher J. Pathologic changes following acute methyl isocyanate inhalation and recovery in B6C3F1 mice. *Toxicology and applied pharmacology*. 1987;87(3):446-56.
90. Bucher JR. Methyl isocyanate: a review of health effects research since Bhopal. *Fundamental and applied toxicology*. 1987;9(3):367-79.
91. Browning JB. *Union carbide: disaster at Bhopal*: Union Carbide India; 1993.
92. Brown WE. Alkyl isocyanates as active site-specific reagents for serine proteases. Location of alkyl binding site in chymotrypsin by X-ray diffraction. *Biochemistry*. 1975;14(23):5079-84.
93. Ferguson J, Kennedy A, Stock M, Brown W, Alarie Y. Uptake and distribution of <sup>14</sup>C during and following exposure to [<sup>14</sup>C] methyl isocyanate. *Toxicology and applied pharmacology*. 1988;94(1):104-17.
94. Bhattacharya BK, Sharma SK, Jaiswal DK. In vivo binding of [1-<sup>14</sup>C] methylisocyanate to various tissue proteins. *Biochemical pharmacology*. 1988;37(12):2489-93.
95. Ferguson J, Schaper M, Stock M, Weyel D, Alarie Y. Sensory and pulmonary irritation with exposure to methyl isocyanate. *Toxicology and applied pharmacology*. 1986;82(2):329-35.
96. Sethi N, Dayal R, Singh R. Acute and subacute toxicity study of inhaled methyl isocyanate in Charles Foster rats. *Ecotoxicology and environmental safety*. 1989;18(1):68-74.

97. Andersson N, Ajwani M, Mahashabde S, Tiwari M, Muir MK, Mehra V, et al. Delayed eye and other consequences from exposure to methyl isocyanate: 93% follow up of exposed and unexposed cohorts in Bhopal. *Occupational and Environmental Medicine*. 1990;47(8):553-8.
98. Salmon A, Muir MK, Andersson N. Acute toxicity of methyl isocyanate: a preliminary study of the dose response for eye and other effects. *Occupational and Environmental Medicine*. 1985;42(12):795-8.
99. Gupta M, Prabha V. Changes in brain and plasma amino acids of mice intoxicated with methyl isocyanate. *Journal of applied toxicology*. 1996;16(6):469-73.
100. Saxena A, Paul B, Sinha M, Dutta K, Das S, Ray P. A study on the B cell activity in protein deficient rats exposed to methyl isocyanate vapour. *Immunopharmacology and immunotoxicology*. 1991;13(3):413-24.
101. Ghosh BB, Sengupta S, Roy A, Maity S, Ghosh S, Talukder G, et al. Cytogenetic studies in human populations exposed to gas leak at Bhopal, India. *Environmental Health Perspectives*. 1990;86:323-6.
102. Dikshit RP, Kanhere S. Cancer patterns of lung, oropharynx and oral cavity cancer in relation to gas exposure at Bhopal. *Cancer Causes & Control*. 1999;10(6):627-36.
103. Shaw I, Graham M. Mesna—a short review. *Cancer treatment reviews*. 1987;14(2):67-86.
104. Dechant KL, Brogden RN, Pilkington T, Faulds D. Ifosfamide/mesna. *Drugs*. 1991;42(3):428-67.
105. de Vries CR, Freiha FS. Hemorrhagic cystitis: a review. *The Journal of urology*. 1990;143(1):1-9.
106. Skinner R, Sharkey IM, Pearson A, Craft AW. Ifosfamide, mesna, and nephrotoxicity in children. *Journal of Clinical Oncology*. 1993;11(1):173-90.
107. Stofer-Vogel B, Cerny T, Küpfer A, Junker E, Lauterburg B. Depletion of circulating cyst (e) ine by oral and intravenous mesna. *British journal of cancer*. 1993;68(3):590-3.
108. Mashiach E, Sela S, Weinstein T, Cohen HI, Shasha SM, Kristal B. Mesna: a novel renoprotective antioxidant in ischaemic acute renal failure. *Nephrology Dialysis Transplantation*. 2001;16(3):542-51.
109. Mare S, Penugonda S, Ercal N. High performance liquid chromatography analysis of MESNA (2-mercaptoethane sulfonate) in biological samples using fluorescence detection. *Biomedical Chromatography*. 2005;19(1):80-6.
110. Shusterman T, Sela S, Cohen H, Kristal B, Sbeit W, Reshef R. Effect of the antioxidant Mesna (2-mercaptoethane sulfonate) on experimental colitis. *Digestive diseases and sciences*. 2003;48(6):1177-85.
111. Liu J, Powell KL, Thames HD, MacLeod MC. Detoxication of sulfur half-mustards by nucleophilic scavengers: robust activity of thiopurines. *Chemical research in toxicology*. 2010;23(3):488-96.
112. Jost P, Fikrova P, Svobodova H, Pejchal J, Stetina R. Protective potential of different compounds and their combinations with MESNA against sulfur mustard-induced cytotoxicity and genotoxicity. *Toxicology letters*. 2017;275:92-100.

113. Matz EL, Hsieh MH. Review of advances in uroprotective agents for cyclophosphamide-and ifosfamide-induced hemorrhagic cystitis. *Urology*. 2017;100:16-9.
114. Niki E. Do antioxidants impair signaling by reactive oxygen species and lipid oxidation products? *FEBS letters*. 2012;586(21):3767-70.
115. Batista C, Mota J, Souza M, Leitao B, Souza M, Brito G, et al. Amifostine and glutathione prevent ifosfamide-and acrolein-induced hemorrhagic cystitis. *Cancer chemotherapy and pharmacology*. 2007;59(1):71-7.
116. Siu LL, Moore MJ. Use of mesna to prevent ifosfamide-induced urotoxicity. *Supportive care in cancer*. 1998;6(2):144-54.
117. Ansell SM, Alberts AS, Falkson G. Ifosfamide in advanced carcinoma of the esophagus: a phase II trial with severe toxicity. *American journal of clinical oncology*. 1989;12(3):205-7.
118. Brock N, Pohl J, Stekar J, Scheef W. Studies on the urotoxicity of oxazaphosphorine cytostatics and its prevention—III. Profile of action of sodium 2-mercaptoethane sulfonate (mesna). *European Journal of Cancer and Clinical Oncology*. 1982;18(12):1377-87.
119. Shaw I, Weeks M. Excretion of disodium bis-2-mercaptoethanesulphonate (dimesna) in the urine of volunteers after oral dosing. *European Journal of Cancer and Clinical Oncology*. 1987;23(7):933-5.
120. Bryant B, Ford H, Jarman M, Smith I. Prevention of isophosphamide-induced urothelial toxicity with 2-mercaptoethane sulphonate sodium (mesnum) in patients with advanced carcinoma. *The Lancet*. 1980;316(8196):657-9.
121. Hilgard P, Pohl J. Oxazaphosphorine toxicity reduction by mesna. *Cancer treatment reviews*. 1990;17(2):217-20.
122. Cutler MJ. *Pharmacokinetics and Therapeutic Uses of Mesna*. 2010.
123. Brock N, Hilgard P, Pohl J, Ormstad K, Orrenius S. Pharmacokinetics and mechanism of action of detoxifying low-molecular-weight thiols. *Journal of cancer research and clinical oncology*. 1984;108(1):87-97.
124. Urquhart BL, Freeman DJ, Spence JD, House AA. The effect of mesna on plasma total homocysteine concentration in hemodialysis patients. *American journal of kidney diseases*. 2007;49(1):109-17.
125. Carafaro RL. *Lung Cancer: New Research*: Nova Publishers; 2004.
126. Burkert H. Clinical overview of mesna. *Cancer Treatment Reviews*. 1983;10:175-81.
127. Clarke S, Lopez-Vidriero M, Pavia D, Thomson M. The effect of sodium 2-mercapto-ethane sulphonate and hypertonic saline aerosols on bronchial clearance in chronic bronchitis. *British journal of clinical pharmacology*. 1979;7(1):39-44.
128. Robertson L-M, Clark A. Looking beyond the angiotensin receptor blocker: A case of anaphylaxis to mesna. *Annals of Allergy, Asthma & Immunology*. 2016;117(3):324-5.
129. Kafferlein HU, Angerer J. N-methylcarbamoylated valine of hemoglobin in humans after exposure to N, N-dimethylformamide: evidence for the formation of methyl isocyanate? *Chemical research in toxicology*. 2001;14(7):833-40.
130. Logue BA, Zhang Z, Manandhar E, Pay AL, Croutch CR, Peters E, et al. Determination of methyl isopropyl hydantoin from rat erythrocytes by gas-

- chromatography mass-spectrometry to determine methyl isocyanate dose following inhalation exposure. *J Chromatogr B Analyt Technol Biomed Life Sci.* 2018;1093-1094:119-27.
131. Kulkarni G, Naik R, Tandel S, Rajappa S. Contra-thermodynamic transesterification of carbamates by counter-attack strategy: A viable non-phosgene, non-mic route to carbamate pesticides. *Tetrahedron.* 1991;47(7):1249-56.
  132. Löfstedt H, Westberg H, Seldén AI, Lundholm C, Svartengren M. Respiratory symptoms and lung function in foundry workers exposed to low molecular weight isocyanates. *American journal of industrial medicine.* 2009;52(6):455-63.
  133. Kimmerle G, Eben A. Zur Toxizität von Methylisocyanat und dessen quantitativer Bestimmung in der Luft. *Archiv für Toxikologie.* 1964;20(4):235-41.
  134. Yeh H-C, Cuddihy RG, Phalen RF, Chang I-Y. Comparisons of calculated respiratory tract deposition of particles based on the proposed NCRP model and the new ICRP66 model. *Aerosol Science and Technology.* 1996;25(2):134-40.
  135. Varma R, Varma DR. The Bhopal disaster of 1984. *Bulletin of Science, Technology & Society.* 2005;25(1):37-45.
  136. Gupta P. Pesticide exposure—Indian scene. *Toxicology.* 2004;198(1-3):83-90.
  137. Varma D. Anatomy of the methyl isocyanate leak in Bhopal. *Hazard assessment of chemicals.* 1986;5:233-89.
  138. Mraz J, Cimlova J, Stransky V, Nohova H, Kicova R, Simek P. N-Methylcarbamoyl-lysine adduct in globin: a new metabolic product and potential biomarker of N, N-dimethylformamide in humans. *Toxicol Lett.* 2006;162(2-3):211-8.
  139. Mraz J, Simek P, Chvalova D, Nohova H, Smigolova P. Studies on the methyl isocyanate adducts with globin. *Chem Biol Interact.* 2004;148(1-2):1-10.
  140. Shrivastava R. Bhopal gas disaster: Review on health effects of methyl isocyanate. *Research Journal of Environmental Sciences.* 2011;5(2):150.
  141. Segal A, Solomon JJ, Li F. Isolation of methylcarbamoyl-adducts of adenine and cytosine following in vitro reaction of methyl isocyanate with calf thymus DNA. *Chemico-biological interactions.* 1989;69(4):359-72.
  142. Sriramachari S. The Bhopal gas tragedy: An environmental disaster. *Current Science.* 2004;86(7):905-20.
  143. Mráz J, Cimlová J, Stránský V, Nohová H, Kičová R, Šimek P. N-Methylcarbamoyl-lysine adduct in globin: a new metabolic product and potential biomarker of N, N-dimethylformamide in humans. *Toxicology letters.* 2006;162(2-3):211-8.
  144. Mráz J, Šimek P, Chvalová D, Nohová H, Šmigolová P. Studies on the methyl isocyanate adducts with globin. *Chemico-biological interactions.* 2004;148(1-2):1-10.
  145. Nylander-French LA, Wu MC, French JE, Boyer JC, Smeester L, Sanders AP, et al. DNA methylation modifies urine biomarker levels in 1, 6-hexamethylene diisocyanate exposed workers: A pilot study. *Toxicology letters.* 2014;231(2):217-26.
  146. Ehrenberg L, Granath F, Törnqvist M. Macromolecule adducts as biomarkers of exposure to environmental mutagens in human populations. *Environmental health perspectives.* 1996;104(suppl 3):423-8.
  147. Sabbioni G, Hartley R, Schneider S. Synthesis of adducts with amino acids as potential dosimeters for the biomonitoring of humans exposed to toluenediisocyanate. *Chemical research in toxicology.* 2001;14(12):1573-83.

148. Beyerbach A, Farmer PB, Sabbioni G. Biomarkers for isocyanate exposure: Synthesis of isocyanate DNA adducts. *Chemical research in toxicology*. 2006;19(12):1611-8.
149. Vandenas O, Malo J-L, Saetta M, Mapp CE, Fabbri LM. Occupational asthma and extrinsic alveolitis due to isocyanates: current status and perspectives. *British journal of industrial medicine*. 1993;50(3):213.
150. Baur X, Marek W, Ammon J, Czuppon A, Marczynski B, Raulf-Heimsoth M, et al. Respiratory and other hazards of isocyanates. *International archives of occupational and environmental health*. 1994;66(3):141-52.
151. Dhara VR, Dhara R, Acquilla SD, Cullinan P. Personal exposure and long-term health effects in survivors of the union carbide disaster at bhopal. *Environmental health perspectives*. 2002;110(5):487-500.
152. Varadarajan S. Of mechanisms, microscopes and Methyl isocyanate. *Resonance*. 2008;13(3):292-306.
153. Pesatori A, Consonni D, Tironi A, Landi M, Zocchetti C, Bertazzi P. Cancer morbidity in the Seveso area, 1976–1986. *Chemosphere*. 1992;25(1-2):209-12.
154. Mráz J, Dušková Š, Gálová E, Nohová H, Krausová P, Linhart I, et al. Improved gas chromatographic–mass spectrometric determination of the N-methylcarbamoyl adduct at the N-terminal valine of globin, a metabolic product of the solvent N, N-dimethylformamide. *Journal of Chromatography B*. 2002;778(1-2):357-65.
155. Wang C, Liu Q, Jian L, Bo X, Kai M, Cheng J. Rapid Determination of N-Methylcarbamoyl Adduct in Hemoglobin of Workers Exposed to N, N-Dimethylformamide by Ultra High Performance Liquid Chromatography-Mass Spectrometry. *Chinese Journal of Analytical Chemistry*. 2014(9):1326-31.
156. Kaushik M, Sikder A, Jaiswal D. A convenient laboratory synthesis of methyl isocyanate. *Current Science*. 1987;56(19):1008-9.
157. Yoganathan S, Miller SJ. N-Methylimidazole-catalyzed synthesis of carbamates from hydroxamic acids via the Lossen rearrangement. *Organic letters*. 2013;15(3):602-5.
158. Rancourt RC, Rioux JS, Veress LA, Garlick RB, Croutch CR, Peters E, et al. Methyl isocyanate inhalation induces tissue factor-dependent activation of coagulation in rats. *Drug and chemical toxicology*. 2019;42(3):321-7.
159. Nick HJ, Rioux JS, Veress LA, Bratcher PE, Bloomquist LA, Anantharam P, et al. Alleviation of methyl isocyanate– induced airway obstruction and mortality by tissue plasminogen activator. *Annals of the New York Academy of Sciences*. 2020;1479(1):134-47.
160. Bockstaele E, Taverniers I, Loose M. Analytical Method Validation and Quality Assurance. *Pharmaceutical Sciences Encyclopedia: Drug Discovery, Development, and Manufacturing*. 2010.
161. Shah VP, Midha KK, Findlay JW, Hill HM, Hulse JD, McGilveray IJ, et al. Bioanalytical method validation—a revisit with a decade of progress. *Pharmaceutical research*. 2000;17(12):1551-7.
162. Logue BA, Manandhar E. Percent residual accuracy for quantifying goodness-of-fit of linear calibration curves. *Talanta*. 2018;189:527-33.
163. Bhattacharya B, Sharma S, Jaiswal D. Binding of [1-14C] Methyl Isocyanate to Erythrocyte Membrane Proteins. *Journal of applied toxicology*. 1996;16(2):137-8.

164. Sabbioni G, Dongari N, Kumar A. Determination of a new biomarker in subjects exposed to 4,4'-methylenediphenyl diisocyanate. *Biomarkers*. 2010;15(6):508-15.
165. Perucho J, Gonzalo-Gobernado R, Bazan E, Casarejos M, Jiménez-Escrig A, Asensio M, et al. Optimal excitation and emission wavelengths to analyze amino acids and optimize neurotransmitters quantification using precolumn OPA-derivatization by HPLC. *Amino Acids*. 2015;47(5):963-73.
166. Mare S, Penugonda S, Ercal N. High performance liquid chromatography analysis of MESNA (2-mercaptoethane sulfonate) in biological samples using fluorescence detection. *Biomed Chromatogr*. 2005;19(1):80-6.
167. Verschraagen M, Bosma M, Zwiers TU, Torun E, van der Vijgh WJ. Quantification of mesna and total mesna in kidney tissue by high-performance liquid chromatography with electrochemical detection. *Journal of chromatography B*. 2003;783(1):33-42.
168. Laauser C, Habekost G, Habekost A. Mass Spectrometric Detection and Reductive Degradation of the Anti-cancer Drugs Ifosfamide and Cyclophosphamide. *Applied Ecology and Environmental Sciences*. 2018;6(1):15-22.
169. Verschraagen M, Boven E, Zegers I, Hausheer FH, Van der Vijgh WJ. Pharmacokinetics of BNP7787 and its metabolite mesna in plasma and ascites: a case report. *Cancer Chemother Pharmacol*. 2003;51(6):525-9.
170. Bokemeyer C, Schmoll H, Ludwig E, Harstrick A, Dunn T, Casper J. The anti-tumour activity of ifosfamide on heterotransplanted testicular cancer cell lines remains unaltered by the uroprotector mesna. *British journal of cancer*. 1994;69(5):863-7.
171. Ahmed NR. An indirect spectrophotometric determination of mesna in pharmaceuticals and environmental samples. *Iraqi National Journal of Chemistry*. 2011;44:492-500.
172. Takamoto S, Sakura N, Yashiki M, Kojima T. Inactivation of acrolein by sodium 2-mercaptoethanesulfonate using headspace-solid-phase microextraction gas chromatography and mass spectrometry. *Journal of Chromatography B*. 2003;791(1-2):365-9.
173. Haggag RS, Gawad DA, Belal SF, Elbardisy HM. Spectrophotometric and spectrofluorimetric determination of mesna, acetylcysteine and timonacic acid through the reaction with acetoxymercuro fluorescein. *Analytical Methods*. 2016;8(11):2479-93.
174. Şener G, Şehirli Ö, Cetinel Ş, Yeğen BG, Gedik N, Ayanoğlu-Dülger G. Protective effects of MESNA (2-mercaptoethane sulphonate) against acetaminophen-induced hepatorenal oxidative damage in mice. *Journal of Applied Toxicology: An International Journal*. 2005;25(1):20-9.
175. Ellman GL. Tissue sulfhydryl groups. *Archives of biochemistry and biophysics*. 1959;82(1):70-7.
176. El-Yazigi A, Yusuf A, Al-Rawithi S. Liquid chromatographic analysis of mesna and dimesna in plasma and urine of patients treated with mesna. *Therapeutic drug monitoring*. 1995;17(2):153-8.
177. El-Yazigi A, Ernst P, Al-Rawithi S, Legayada E, Raines DA. Pharmacokinetics of mesna and dimesna after simultaneous intravenous bolus and infusion administration in patients undergoing bone marrow transplantation. *The Journal of Clinical Pharmacology*. 1997;37(7):618-24.



178. Głowacki R, Wójcik K, Bald E. Facile and sensitive method for the determination of mesna in plasma by high-performance liquid chromatography with ultraviolet detection. *Journal of chromatography A*. 2001;914(1-2):29-35.
179. Kuśmierk K, Chwatko G, Głowacki R, Kubalczyk P, Bald E. Ultraviolet derivatization of low-molecular-mass thiols for high performance liquid chromatography and capillary electrophoresis analysis. *Journal of Chromatography B*. 2011;879(17-18):1290-307.
180. Kuśmierk K, Chwatko G, Głowacki R, Bald E. Determination of endogenous thiols and thiol drugs in urine by HPLC with ultraviolet detection. *Journal of Chromatography B*. 2009;877(28):3300-8.
181. Verschraagen M, Zwiers TU, Torun E, Donker MG, Reinhoud NJ, Van der Vijgh WJ. Simultaneous determination of BNP7787 and its metabolite mesna in plasma and tissue by micro-HPLC with a dual electrochemical detector. *Journal of pharmaceutical sciences*. 2003;92(5):1040-50.
182. Sidau B, Shaw IC. Determination of sodium 2-mercaptoethanesulphonate by high-performance liquid chromatography using post-column reaction colorimetry or electrochemical detection. *Journal of Chromatography B: Biomedical Sciences and Applications*. 1984;311:234-8.
183. James C, Mant T, Rogers H. Pharmacokinetics of intravenous and oral sodium 2-mercaptoethane sulphonate (mesna) in normal subjects. *British journal of clinical pharmacology*. 1987;23(5):561-8.
184. James C, Rogers H. Estimation of mesna and dimesna in plasma and urine by high-performance liquid chromatography with electrochemical detection. *Journal of Chromatography B: Biomedical Sciences and Applications*. 1986;382:394-8.
185. Health UDo, Services H. Bioanalytical method validation, guidance for industry. <http://www.fda.gov/cder/guidance/4252f1.htm>. 2001.
186. Bhadra S, Zhang Z, Zhou W, Ochieng F, Rockwood GA, Lippner D, et al. Analysis of potential cyanide antidote, dimethyl trisulfide, in whole blood by dynamic headspace gas chromatography–mass spectroscopy. *Journal of Chromatography A*. 2019;1591:71-8.
187. Gyamfi OA, Bortey-Sam N, Donkor AB, White CW, Logue BA. Analysis of TRPA1 antagonist, A-967079, in plasma using high-performance liquid chromatography tandem mass-spectrometry. *Journal of pharmaceutical analysis*. 2020;10(2):157-63.
188. Causon R. Validation of chromatographic methods in biomedical analysis viewpoint and discussion. *Journal of Chromatography B: Biomedical Sciences and Applications*. 1997;689(1):175-80.
189. Braggio S, Barnaby R, Grossi P, Cugola M. A strategy for validation of bioanalytical methods. *Journal of pharmaceutical and biomedical analysis*. 1996;14(4):375-88.
190. Shabir GA. Validation of high-performance liquid chromatography methods for pharmaceutical analysis: Understanding the differences and similarities between validation requirements of the US Food and Drug Administration, the US Pharmacopeia and the International Conference on Harmonization. *Journal of chromatography A*. 2003;987(1-2):57-66.

191. Shabir GA, John Lough W, Arain SA, Bradshaw TK. Evaluation and application of best practice in analytical method validation. *Journal of liquid chromatography & related technologies*. 2007;30(3):311-33.
192. Verschraagen M, Zwieters TU, de Koning PE, Welink J, van der Vijgh WJ. Quantification of BNP7787 (dimesna) and its metabolite mesna in human plasma and urine by high-performance liquid chromatography with electrochemical detection. *Journal of Chromatography B: Biomedical Sciences and Applications*. 2001;753(2):293-302.
193. Wormser U. Toxicology of mustard gas. *Trends in pharmacological sciences*. 1991;12:164-7.
194. Dacre JC, Goldman M. Toxicology and pharmacology of the chemical warfare agent sulfur mustard. *Pharmacological reviews*. 1996;48(2):289-326.
195. Pal A, Tewari-Singh N, Gu M, Agarwal C, Huang J, Day BJ, et al. Sulfur mustard analog induces oxidative stress and activates signaling cascades in the skin of SKH-1 hairless mice. *Free Radical Biology and Medicine*. 2009;47(11):1640-51.
196. Gautam A, Vijayaraghavan R, Sharma M, Ganesan K. Comparative toxicity studies of sulfur mustard (2, 2'-dichloro diethyl sulfide) and monofunctional sulfur mustard (2-chloroethyl ethyl sulfide), administered through various routes in mice. *J Med CBR Def*. 2006;4:1-21.
197. Atkinson WS. Delayed mustard gas keratitis (Dichlorodiethyl Sulfide). A report of two cases. *Transactions of the American Ophthalmological Society*. 1947;45:81.
198. Ghabili K, Agutter PS, Ghanei M, Ansarin K, Shoja MM. Mustard gas toxicity: the acute and chronic pathological effects. *Journal of applied toxicology*. 2010;30(7):627-43.
199. Inturi S, Tewari-Singh N, Gu M, Shrotriya S, Gomez J, Agarwal C, et al. Mechanisms of sulfur mustard analog 2-chloroethyl ethyl sulfide-induced DNA damage in skin epidermal cells and fibroblasts. *Free Radical Biology and Medicine*. 2011;51(12):2272-80.
200. Saladi R, Smith E, Persaud A. Mustard: a potential agent of chemical warfare and terrorism. *Clinical and Experimental Dermatology: Clinical dermatology*. 2006;31(1):1-5.
201. Tewari-Singh N, Rana S, Gu M, Pal A, Orlicky DJ, White CW, et al. Inflammatory Biomarkers of Sulfur Mustard Analog 2-Chloroethyl Ethyl Sulfide-Induced Skin Injury in SKH-1 Hairless Mice. *Toxicological sciences*. 2009;108(1):194-206.
202. Ruhl CM, Park SJ, Danisa O, Morgan RF, Papirnsister B, Sidell FR, et al. A serious skin sulfur mustard burn from an artillery shell. *The Journal of emergency medicine*. 1994;12(2):159-66.
203. Razavi SM, Abdollahi M, Salamati P. Cancer events after acute or chronic exposure to sulfur mustard: a review of the literature. *International journal of preventive medicine*. 2016;7.
204. Batal M, Boudry I, Mouret S, Wartelle J, Emorine S, Bertoni M, et al. Temporal and spatial features of the formation of DNA adducts in sulfur mustard-exposed skin. *Toxicology and applied pharmacology*. 2013;273(3):644-50.
205. Fidder A, Moes GW, Scheffer AG, van der Schans GP, Baan RA, de Jong LP, et al. Synthesis, characterization, and quantitation of the major adducts formed between

- sulfur mustard and DNA of calf thymus and human blood. *Chemical research in toxicology*. 1994;7(2):199-204.
206. Husain K, Dube S, Sugendran K, Singh R, Gupta SD, Somani S. Effect of topically applied sulphur mustard on antioxidant enzymes in blood cells and body tissues of rats. *Journal of Applied Toxicology*. 1996;16(3):245-8.
207. Jowsey PA, Williams FM, Blain PG. DNA damage, signalling and repair after exposure of cells to the sulphur mustard analogue 2-chloroethyl ethyl sulphide. *Toxicology*. 2009;257(3):105-12.
208. Jain AK, Tewari-Singh N, Gu M, Inturi S, White CW, Agarwal R. Sulfur mustard analog, 2-chloroethyl ethyl sulfide-induced skin injury involves DNA damage and induction of inflammatory mediators, in part via oxidative stress, in SKH-1 hairless mouse skin. *Toxicology letters*. 2011;205(3):293-301.
209. Tewari-Singh N, Jain AK, Inturi S, Agarwal C, White CW, Agarwal R. Silibinin attenuates sulfur mustard analog-induced skin injury by targeting multiple pathways connecting oxidative stress and inflammation. *PloS one*. 2012;7(9):e46149.
210. Gould NS, White CW, Day BJ. A role for mitochondrial oxidative stress in sulfur mustard analog 2-chloroethyl ethyl sulfide-induced lung cell injury and antioxidant protection. *Journal of Pharmacology and Experimental Therapeutics*. 2009;328(3):732-9.
211. Laskin JD, Black AT, Jan Y-H, Sinko PJ, Heindel ND, Sunil V, et al. Oxidants and antioxidants in sulfur mustard-induced injury. *Annals of the New York Academy of Sciences*. 2010;1203:92.
212. Tewari-Singh N, Agarwal C, Huang J, Day BJ, White CW, Agarwal R. Efficacy of glutathione in ameliorating sulfur mustard analog-induced toxicity in cultured skin epidermal cells and in SKH-1 mouse skin in vivo. *Journal of Pharmacology and Experimental Therapeutics*. 2011;336(2):450-9.
213. Hattersley I, Jenner J, Dalton C, Chilcott R, Graham J. The skin reservoir of sulphur mustard. *Toxicology in vitro*. 2008;22(6):1539-46.
214. MacLeod MC, Humphrey RM, Bickerstaff T, Daylong A. Inhibition by 6-mercaptopurine of the binding of a benzo (a) pyrene diol-epoxide to DNA in Chinese hamster ovary cells. *Cancer research*. 1990;50(14):4355-9.
215. MacLeod MC, Mann KL, Thai G, Conti CJ, Reiners JJ. Inhibition by 2, 6-dithiopurine and thiopurinol of binding of a benzo (a) pyrene diol epoxide to DNA in mouse epidermis and of the initiation phase of two-stage tumorigenesis. *Cancer research*. 1991;51(18):4859-64.
216. <An indirect spectrophotometric determination of mesna in pharmaceuticals and environmental samples.pdf>.
217. Aboul-Enein HY, Al-Badr A. Methimazole. *Analytical Profiles of Drug Substances*. 8: Elsevier; 1979. p. 351-70.